Role of acto-myosin based force production in cell invasion during development in Caenorhabditis elegans

Rodrigo Cáceres

Université Paris Descartes- Paris 5

Spécialité : Biophysique
Ecole doctorale Frontières du Vivant

THÈSE DE DOCTORAT

Présentée par
Rodrigo Cáceres

"Role of acto-myosin based force production in cell invasion during development in *Caenorhabditis elegans*"

Thèse dirigée par **Julie Plastino**

Date de soutenance le 27 septembre 2017 devant le jury composé de :

Mme. Jody Rosenblatt	Reporter
M. Jeroen van Zon	Reporter
M. René-Marc Mège	Examiner
Mme. Ana-Maria Lennon-Dumenil	Examiner
Mme. Julie Plastino	PhD advisor

Biomimetism of cellular movement, Institut Curie/CNRS UMR168
11, rue Pierre et Marie Curie 75231 Paris cedex 05 FRANCE

TABLE OF CONTENTS

ABBREVIATIONS

Note: All *C. elegans* protein names, consisting of 3 letters and a number, are written first followed by a slash and the vertebrate or Drosophila equivalent. For example the WASP protein is designated WSP-1/WASP.

AC: Anchor Cell

Arp2/3 complex: Actin Related Proteins 2 and 3 complex

BM: Basement Membrane

DIC microscopy: Differential Interference Contrast microscopy

ECM: ExtraCellular Matrix

F-actin: Filamentous-actin

MMP: Matrix MetalloProtease

VPC: Vulval Precursor Cells

VNC: Ventral Nerve Cord

WASP: Wiskott–Aldrich Syndrome Protein

WAVE: WAsp-family VErprolin-homologous protein

PREFACE

Cancer metastasis is the cause of 90% of human cancer deaths. During this process cells from a primary tumor escape and colonize other tissues. To do this the cells must cross extracellular matrix barriers called basement membranes (BM) in a process called invasion. Although complex and multi-step, cell invasion is dependent, at least in part, on the dynamics of the acto-myosin cytoskeleton.

The goal of this thesis was to understand mechanistically how the acto-myosin cytoskeleton contributed to cell invasion. I used an experimental model known as anchor cell (AC) invasion in the nematode *Caenorhabditis elegans*. AC invasion occurs during the normal development of the vulva of *C. elegans*, and is the first step in the formation of an opening between the uterus and worm exterior. AC invasion resembles in many important respects cancer cell invasion, and all major BM and acto-myosin cytoskeleton components are conserved between worms and humans, making results relevant for understanding cancer cell invasion.

This thesis is organized into 6 chapters: the first 2 are introductory chapters, the third is a methods chapter and the last 3 detail the experiments I undertook over the course of my PhD. My published review articles are in the annexes at the end of the document. In the first chapter, cell invasion is introduced, particularly cancer cell invasion, and the main actin structures, actin-binding proteins and their roles in cell shape changes and cancer cell invasion are explained. The second introductory chapter reviews the current state of the art about the experimental model system, AC invasion, used in the thesis. The last 3 chapters focus on the experiments done during the thesis, which are separated into 3 stories concerning 1) the importance of different actin components during AC invasion. 2) super-resolution study of the actin architecture in the AC and 3) the role of acto-myosin contractility during AC invasion in the absence of metalloproteases. Results from the first 2 studies will make up my first author publication, which should be submitted before the defense. I will be a contributing author in the third study that is nearing completion.

CHAPTER 1: CELL INVASION AND THE ACTIN CYTOSKELETON

1.1 OVERVIEW OF INVASION AND INTRODUCTION TO THE MODEL SYSTEM

Cell invasion across extracellular matrix (ECM) barriers such as basement membranes (BMs) occurs in many developmental and pathological contexts. BM is a two-dimensional layer of specialized ECM composed principally of laminin, type IV collagen polymers and glycoproteins that separate epithelia from the underlying tissue (Hohenester and Yurchenco, 2013). Owing to the small pore size of BM, non-permissive to cell passage, cells must enable specific cellular programs to move across BMs.

An example of this process is cancer cell invasion during metastasis. During metastasis, cancer cells leave the primary tumor, cross into the blood stream, are transported to new tissues, and migrate to form new colonies **(Figure 1.1)**. In order to cross the physical barriers imposed by the intervening ECM including BMs, the cancer cell forms actin-rich protrusions called invadopodia, responsible for pulling the cell forward and for digesting and reorganizing the ECM to allow invasion (Rowe and Weiss, 2009).

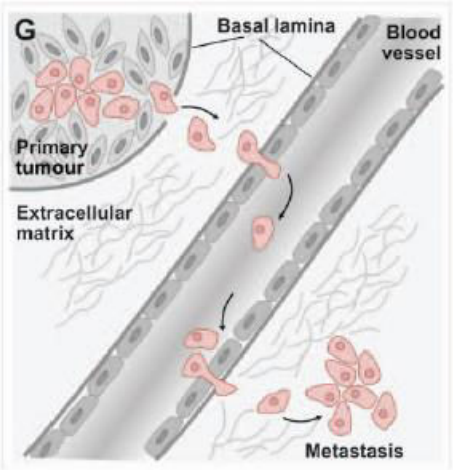

Figure 1.1 Cancer cell invasion. Cells leave the primary tumor by invading through the BM, cross the ECM stroma and invade through the BM of blood vessels. The circulatory system carries the tumor cells to new destinations where the cells invade out of the blood vessel and establish new tumor sites called metastases. From (Nezhad and Geitmann, 2013).

Invasion also occurs in non-pathological contexts, one example being leucocyte transmigration. Leucocytes continually pass back and forth across the BMs of the blood and lymph vessels in order to mount the immune response (Vestweber, 2015). This BM is located beneath the endothelial cells that line the vessels. However a difference with cancer cell

invasion is that this BM possesses low expression regions (LER) of collagen IV and laminins, forming weaker areas that are used by leukocytes to cross (Voisin et al., 2010) and **(Figure 1.2)**. Experiments using microfluidic devices to mimic the transmigration of leucocytes through small gaps show the importance of actin polymerization for leucocyte transmigration (Thiam et al., 2016; Vargas et al., 2016).

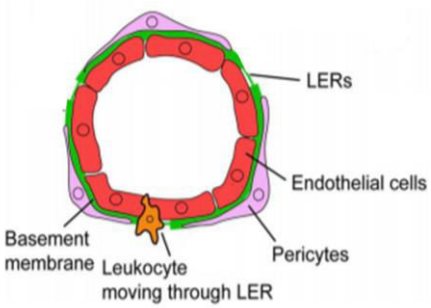

Figure 1.2 Leukocyte transmigration. Representation of a cross-section of an artery lined with endothelial cells on top of a patchy BM showing low expression regions (LERs). Leukocytes invade through the LERs. Adapted from (Kelley et al., 2014).

Angiogenesis, the sprouting and growth of new blood vessels from pre-existing ones, is another non-pathological process involving cell invasion. In response to proangiogenesis signals such as vascular endothelial growth factor (VEGF), endothelial cells lining the vessels become motile, lose contact with their neighbors and invade across the underlying BM (Eilken and Adams, 2010) and **(Figure 1.3).** This process is led by cells displaying actin-filled protrusions.

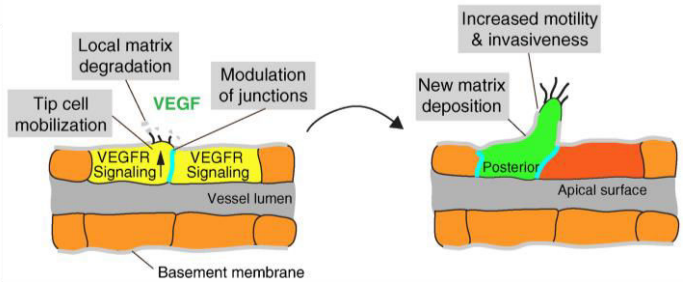

Figure 1.3 Angiogenesis: VEGF induces endothelial cells to breach and remodel the BM, forming a new blood vessel bud. Adapted from (Eilken and Adams, 2010).

Cell invasion also occurs during organ development. One example, which is the focus of this PhD, is anchor cell (AC) invasion during vulval development in *C. elegans*. In immature worms, the uterine and vulva cells are separated by BM, which must be pierced to make a hole that will later become the vulva. A single cell, the AC, is responsible for forming the hole in the BM, and this process is reminiscent of cancer cell invasion through BMs **(Figure 1.4).**

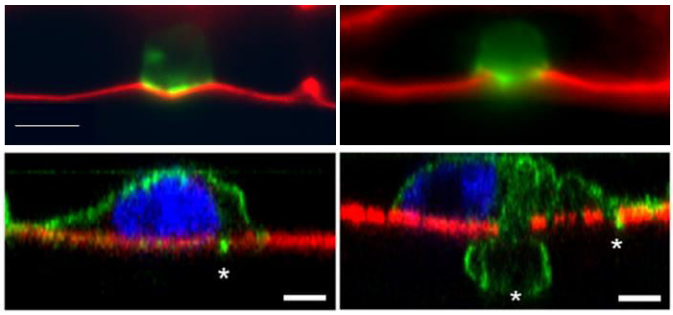

Figure 1.4 Cell invasion through BMs. Top: AC invasion during vulval development: The AC (actin in green) starts out on top of the BM (red), which disintegrates over the course of development due to the invasive activity of the AC to allow the uterine-vulval connection. (R. Cáceres, unpublished, 2016). Bottom: cancer cell invasion of BM--human colon carcinoma cells (actin in green, DNA in blue) invading rat peritoneal BM immunostained for laminin (red). Degradation of the BM and formation of invasive protrusions (invadopodia) allow the infiltration of the cell to the other side of the membrane. Stars indicate sites of penetration. Adapted from (Schoumacher et al., 2010). Scale bars 5 μm.

In the present project AC invasion was used as a model to better understand cell invasion with the goal of determining the combination of actin cytoskeleton components that was necessary for invasion as well as the potential role of myosin in this process. AC invasion allows for the study of invasion in a native 3D environment, without the caveats associated with current 2D and 3D cell culture where the mechanical properties of the native microenvironment are not preserved (Paszek et al., 2005). An additional advantage of working with a *C. elegans* is the ease of imaging in a 3D environment and tractable genetics, while sharing the same highly conserved components of the BM and acto-myosin cytoskeleton that are important for cancer cell invasion.

1.2 ACTIN CYTOSKELETON IN CELL PROTRUSION AND CELL SHAPE CHANGES

Shape changes of cells, including protrusions, are driven in large part by the actin cytoskeleton, a network of actin filaments that continuously elongate (polymerize) and disassemble (depolymerize) inside the cell beneath the membrane. Actin filaments are initially made by a "nucleation" process whereby 3 actin monomers come together to make a nascent filament (Sept and McCammon, 2001). Once the trimer is formed, assembly of actin monomers into filaments occurs in a directional manner due to the polarity of actin filaments that have dynamic (barbed) ends and less dynamic (pointed) ends (Pollard, 1986). In vivo, further polarity of assembly is conferred by the actin monomer-binding protein profilin that inhibits monomer addition to the pointed ends of filaments (Pring et al., 1992). Actin monomers carry a molecule of ATP that is hydrolyzed to ADP once in the filament. This also

contributes to filament polarity by generating an actin-ATP cap at the barbed end while the rest of the filament contains actin-ADP. To enable cell protrusion and movement, actin filaments form different types of structures at different sites in the cell by interacting with different types of actin-binding proteins **(Figure 1.5).**

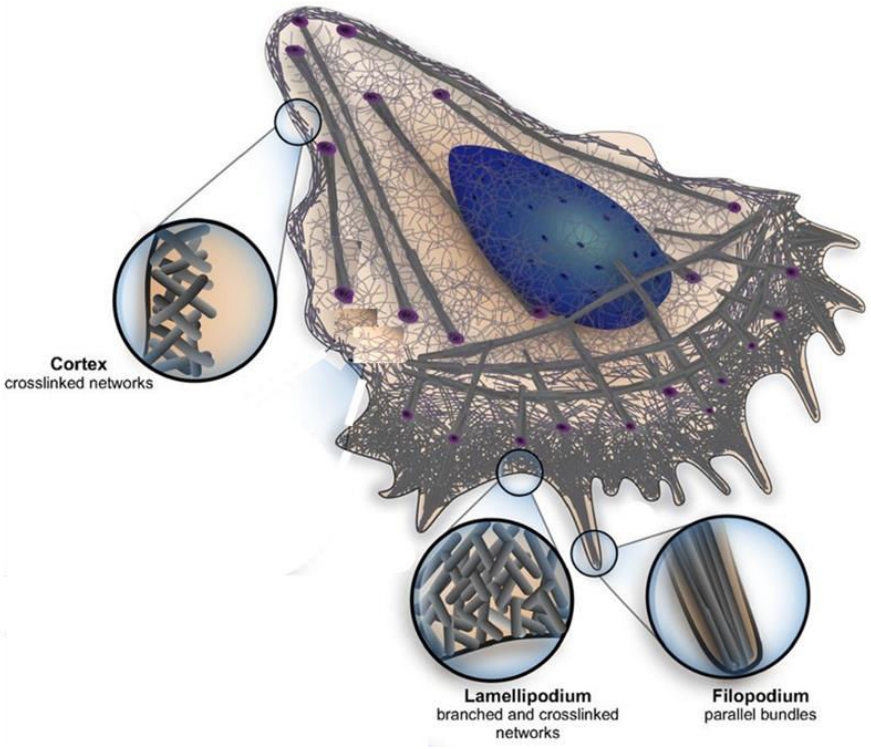

Figure 1.5 Actin structures in a protruding cell: In the cell there are 3 main actin networks, the filopodium, the lamellipodium and the acto-myosin cortex. Actin is represented by gray lines and the cell nucleus in blue. Adapted from (Blanchoin et al., 2014).

In the following sections, I will describe these different networks: branched structures that make up lamellipodia that push out the front of the cell, unbranched filaments that are found in filament bundles like filopodia likewise at the front of the cell and the acto-myosin cortex, a mix of branched and unbranched filaments along with the molecular motor myosin that underlies the cell membrane at the cell rear and can contract to squeeze forward the back of the cell during cell motility and other cell shape changes. I will also devote a section to actin cross-linking proteins since they play roles in the formation and stabilization of actin organization in all 3 architectures in the cell. The actin structures in a protruding cell and their biochemistries are similar to those found in invading cells, allowing them to enact cell shape changes to cross ECM barriers.

1.2.1 BRANCHED ACTIN NETWORKS

Cellular lamellipodia are composed principally of branched actin networks produced by the nucleating activity of the Arp2/3 complex (Pollard and Borisy, 2003; Svitkina and Borisy, 1999) and **(Figure 1.6)**. This complex catalyzes the polymerization of a new actin filament on the side of a preexisting filament, creating a branch at a 70° angle from the side of the mother filament. The daughter filament grows by the barbed end while the pointed end remains attached to the Arp2/3 complex at the branch point (Mullins et al., 1998) and **(Figure 1.6)**.

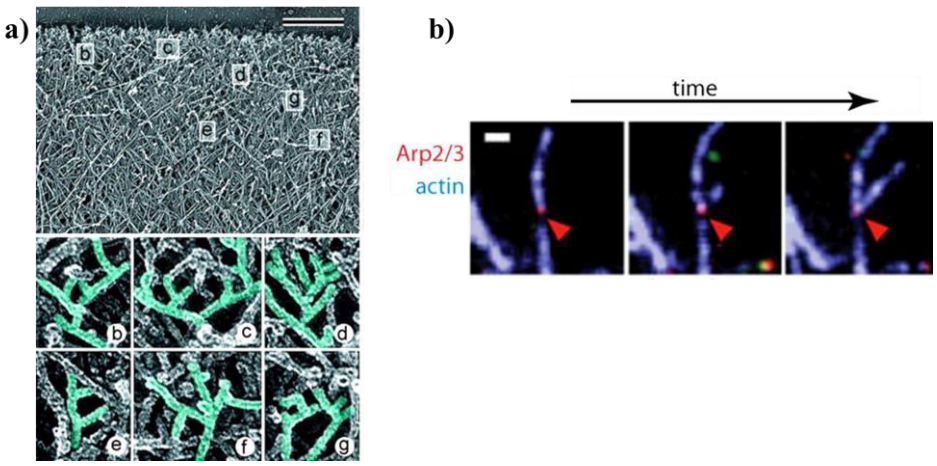

Figure 1.6 Branched filaments created by the Arp2/3 complex. a) Electron microscopy images of a cell lamellipodium. Zoom images show branched structures in various locations in the lamellipodium. Scale bar 0.5 µm. Adapted from (Svitkina and Borisy, 1999) b) Single-molecule time-lapse TIRFM of actin polymerization by the Arp2/3 complex (indicated by a red triangle), forming a branch off the side of a mother filament. Scale bar 1 µm. Adapted from (Smith et al., 2013).

The Arp2/3 complex on its own has very low nucleating capacity and must be activated by a nucleation promoting factor from the WASP (Wiskott–Aldrich Syndrome protein)/WAVE family of proteins (Kurisu and Takenawa, 2009). WASP proteins are composed of several domains, which give it its multifunctional properties. At the N-terminus, WASP has a WH1 (WASP homology) domain, the binding site for WASP-interacting protein (WIP), an adaptor protein involved in endocytosis (Miki and Takenawa, 2003). This domain is followed by a basic region able to interact with the lipid phosphatidylinositol-(4,5)-bisphosphate (PIP2), and a GTPase-binding domain "CRIB/GBD". The C-terminal half of the WASP molecule is composed of a proline rich region that can bind profilin-actin, followed by a verprolin homology domain (V), a cofilin-like region (C) and an acidic domain (A). Collectively, these three domains form what is known as the VCA region. The VCA region binds actin monomers and the Arp2/3 complex via its V and CA domain respectively, thus activating the Arp2/3 complex to nucleate a new filament (Machesky et al., 1999; Marchand et al., 2001). In its resting state, WASP is folded into an auto-inhibited conformation by interaction of the C-

terminus with the "B" and "CRIB" domains, masking the VCA domain. This conformation can be released by interaction of WASP at the cell membrane with PIP2 and the GTPase Cdc42 (Higgs and Pollard, 2000; Rohatgi et al., 1999) and **(Figure 1.7).**

Another member of the WASP/WAVE family of proteins is WAVE, also known as Scar. WAVE is very similar to WASP, with the difference that its interaction with GTPases is indirect because it lacks a CRIB domain, and it preferentially binds phosphatidylinositol-(3,4,5)-bisphosphate (PIP3) instead of PIP2 (Oikawa et al., 2004). As compared to WASP, WAVE is a less efficient activator of the Arp2/3 complex due to its less acidic A domain even though both molecules bind the Arp2/3 complex with similar affinities (Zalevsky et al., 2001a; Zalevsky et al., 2001b). Like WASP, WAVE exists in an inhibited form, but in the case of WAVE, this is because of an inhibitory complex called the WAVE complex (Eden et al., 2002). The WAVE complex is composed of Abi1 (Abelson interacting protein 1), Nap1 (NCK-associated protein 1), Sra1 (specifically Rac-associated protein 1) and HSPC300. The hetero-complex is formed by binding the N- and C-terminal parts in a complex, thus hiding the VCA domain (Ismail et al., 2009). This conformation is released by action of the GTPase Rac along with PIP3 (Miki et al., 1998) and **(Figure 1.7)**.

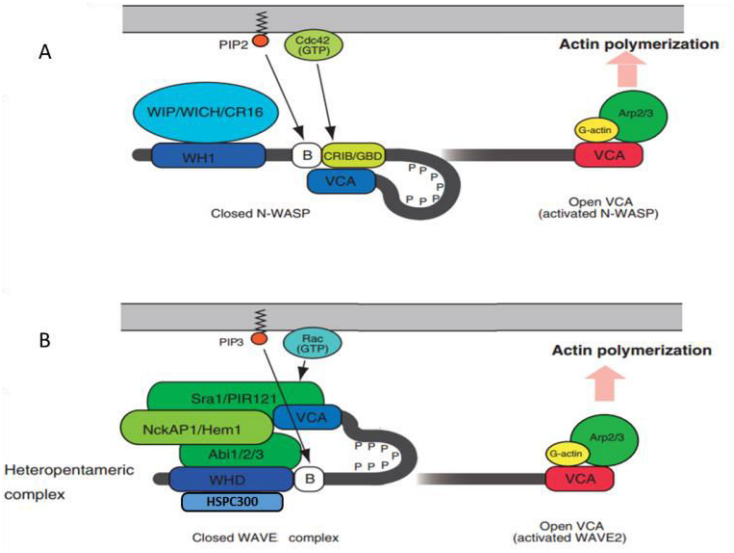

Figure 1.7 Activation mechanism of WASP and WAVE. N-WASP, one form of the WASP protein, has an N-terminal WASP-homology 1 (WH1) domain where WIP can bind. WAVE2, one form of the WAVE protein, has an N-terminal WAVE-/Scar-homology domain (WHD/SHD) that mediates protein complex formation with, Abi1, Nap1, and Sra1. The basic region (B) is common to both N-WASP and WAVE2, where phosphoinositides (PIP2 or PIP3) bind for protein localization or activation of the Arp2/3 complex. N-WASP has the Cdc42-Rac interactive binding region (CRIB) for Cdc42 GTPase binding. WAVE2 binds to Rac GTPase through Sra1. Adapted from (Takenawa, 2010).

Capping protein is another protein that is important for the dynamics of branched networks. Capping protein binds to the barbed ends of actin filaments, stopping their elongation. In so doing capping proteins favor branching over barbed end elongation and thus play a role in the architecture of the branched network by generating short filaments with a high density of branches (Akin and Mullins, 2008; Pollard and Borisy, 2003). This provides mechanical stiffness to generate force via barbed end growth towards the cell membrane **(Figure 1.8)**.

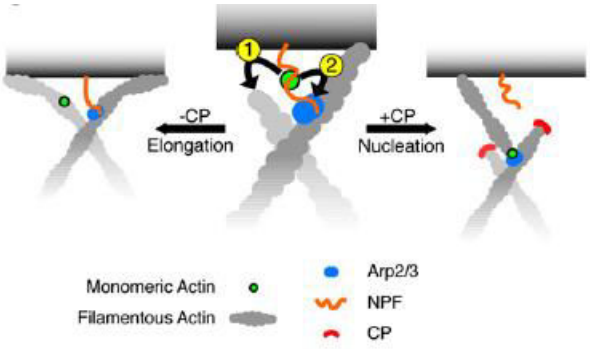

Figure 1.8 How capping protein increases the density of a branched actin network. Capping favors actin monomer participation in branching (right panel) by preventing barbed end elongation (left panel). CP: capping protein. NPF: WASP or WAVE. Adapted from (Akin and Mullins, 2008).

Branched network dynamics are also regulated by the actin filament severing protein ADF/cofilin. This protein has highest affinity for ADP actin subunits in the filament, which accumulate in the older regions, leading to uneven decoration of the filament with ADF/cofilin. ADF/cofilin decoration renders the filament less stiff, and fluctuations create breaking points between stiffer, undecorated and flexible ADF/cofilin-coated parts of the filament (McGough et al., 2003) and **(Figure 1.9)**.

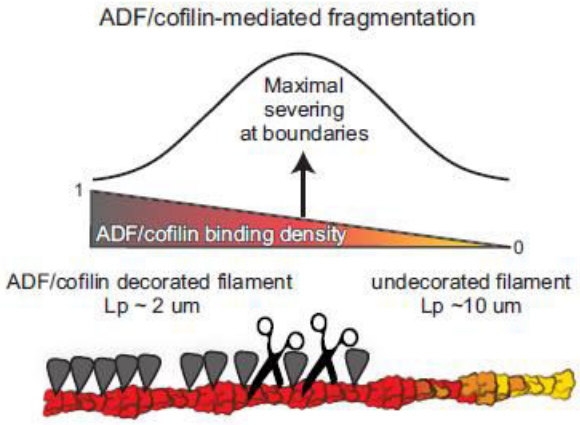

Figure 1.9 Actin filament severing by ADF/cofilin. Cofilin (grey symbols) binds to ADP actin regions of the actin filament (in red) as opposed to ATP or ADP-Pi portions (yellow and orange). This creates a discontinuity in filament stiffness, and breakage (scissor symbol) occurs at frontier regions between decorated and undecorated filament. Adapted from (Blanchoin et al., 2014).

Lamellipodium dynamics can also be regulated by numerous other proteins. Two examples are lamellipodin and Ena/VASP, which both localize to the leading edge of moving cells. Ena/VASP is a barbed end elongation enhancement molecule that is associated with enhanced cell protrusion (Breitsprecher et al., 2008; Breitsprecher et al., 2011; Rottner et al., 1999). Ena/VASP also competes with capping protein for barbed end binding and crosslinks filaments together into parallel bundles (Barzik et al., 2005; Laurent et al., 1999; Suei et al., 2012). Furthermore Ena/VASP may also bind directly to the WAVE molecule or to the Abi1 subunit of the WAVE regulatory complex to enhance WAVE-dependent actin polymerization (Chen et al., 2014; Havrylenko et al., 2015). Lamellipodin is also associated with enhanced motility and binds Ena/VASP. Lamellipodin acts by tethering Ena/VASP to filaments, thus increasing its elongation efficiency (Hansen and Mullins, 2015), and by enhancing the ability of Rac to activate the WAVE complex for Arp2/3-mediated actin polymerization (Carmona et al., 2016; Law et al., 2013).

Branched actin network dynamics in a moving cell is summarized in **(Figure 1.10)**. Extracellular signals activate GTPases in the PIP2 and PIP3-rich plasma membrane. This recruits and activates WASP/WAVE/Scar, which in turn activates the Arp2/3 complex to polymerize branched actin filaments (Pollard and Borisy, 2003). These growing ends are capped by capping protein, preventing their further growth. Hydrolysis of ATP to ADP in the actin filament encourages ADF/cofilin binding and severing. Filaments disassemble from the pointed end, and the released monomers are bound with profilin to enhance exchange of ADP to ATP and to prevent pointed end polymerization, thus funneling growth toward the new barbed ends at the leading edge.

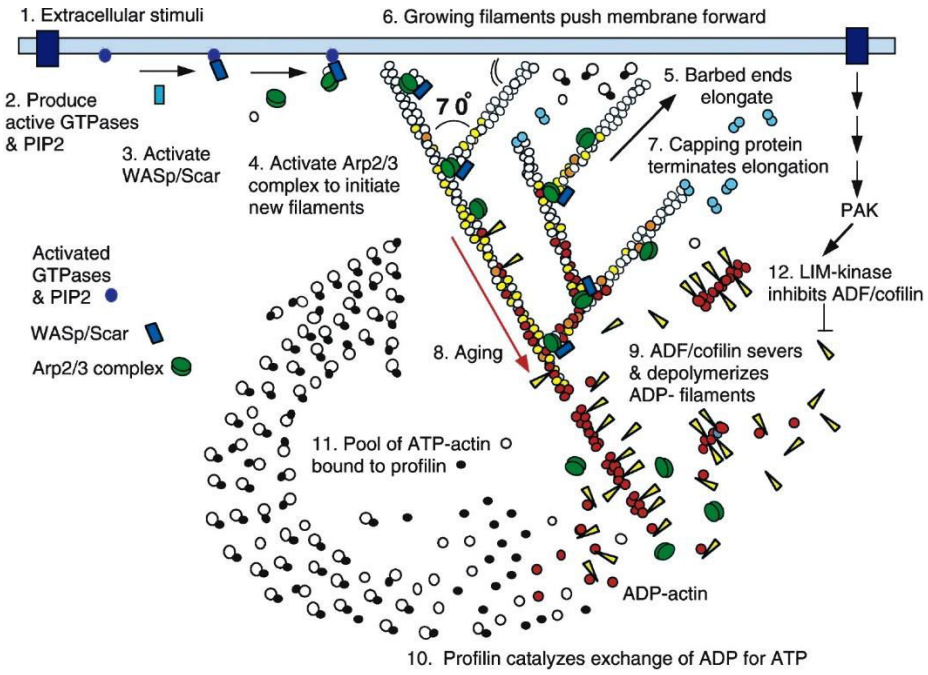

Figure 1.10 Actin dynamics in lamellipodia. Transduction of extracellular signals to nucleation of new actin filaments by the Arp2/3 complex, followed by disassembly via the action of capping protein, ADF/cofilin and ATP hydrolysis to ADP in the actin filament. See text for details. Adapted from (Pollard and Borisy, 2003).

1.2.2 UNBRANCHED FILAMENTS

Although principally composed of branched filaments, the leading edge of protruding cells also contains unbranched filaments. There are several factors that can nucleate unbranched filaments in the cell, the most important being a family of proteins called formins. Formins are dimeric proteins typically composed of a C-terminal region containing a diaphanous autoregulatory domain (DAD) and two formin homology domains (FH1 and FH2) with a diaphanous inhibitory domain (DID) and GTPase-binding (GBD) at the N-terminus (Chesarone et al., 2010) and **(Figure 1.11).** Formins are autoinhibited via an intermolecular interaction between DAD and DIA. GTPase binding disrupts this conformation and opens it up to expose the FH1-FH2 domain, which is the minimal domain for nucleation of actin polymerization (Alberts, 2001; Watanabe et al., 1999). The FH1-FH2 domain acts as a dimer, with the FH2 domains tracking the barbed end as the filament grows, increasing the association of monomeric actin with the barbed end and protecting it from capping proteins (Kovar et al., 2006; Romero et al., 2004; Shemesh et al., 2005). The FH1 domains have multiple sites for binding of profilin-actin, delivering it to the FH2 domains at the growing barbed end (Kovar et al., 2006) and **(Figure 1.11)**.

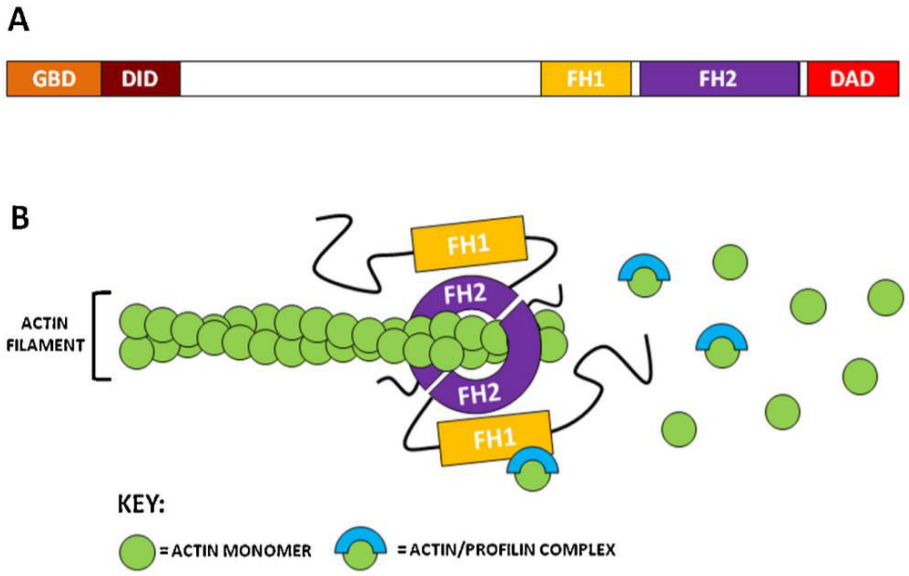

Figure 1.11 Schematic representation of a formin molecule and its mediation of actin filament assembly. (A) The domain arrangement that characterizes a typical formin. GBD, GTPase binding domain; DID, diaphanous inhibitory domain; FH1, formin homology domain 1; FH2, formin homology domain 2; DAD, diaphanous autoregulatory domain. (B) The FH1 domains are thought to pull in monomers via their interaction with profilin-actin, while the FH2 domains are responsible for creating doughnut shaped homodimers in which actin nucleation can occur. Actin monomers are shown in green, profilin in blue, the FH1 domain in yellow and the FH2 domain in purple. From (Randall and Ehler, 2014).

One of the main unbranched actin structures present at the leading edge of a protruding cell is filopodia. There are two models to explain filopodia formation, but both depend on the action of formins to make unbranched filaments. The "convergent elongation model" is based on a reorganization of branched networks at the edge of the lamellipodium via clustering of barbed ends into a "tip complex" composed of formins and anticapping proteins like Ena/VASP, which then elongates (Svitkina et al., 2003) and **(Figure 1.12)**. The second model is known as "tip nucleation" and involves direct actin nucleation at the membrane by clustered formins without need of a previous branched network (Yang and Svitkina, 2011). In both models actin filament cross-linkers are necessary to bundle filaments and give the structure rigidity (Vignjevic et al., 2006). These two models of filopodia initiation are both possible, and it is probable that they co-exist, as has been shown in vitro via reconstitution of filopodia assembly on lipid bilayers (Lee et al., 2010).

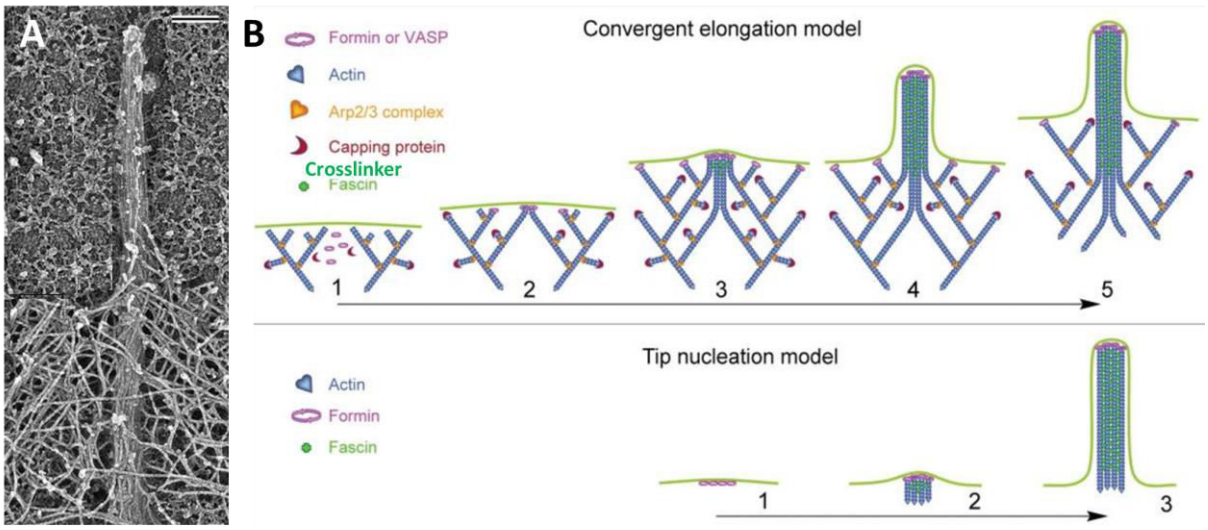

Figure 1.12 A) Filopodia. A) Electron microscopy image of a filopodia formed by bundle of unbranched actin filaments. Scale bar 0.2 µm. Adapted from (Svitkina et al., 2003). B) Mechanistic models of filopodia initiation. Convergent elongation model (top) and tip nucleation model (bottom). See text for details. Adapted from (Yang and Svitkina, 2011).

1.2.3 THE ACTO-MYOSIN CORTEX

Another actin structure important for cell shape changes is the cell cortex, a layer of actin beneath the cell membrane composed of both branched and unbranched filaments (Morone et al., 2006) and **(Figure 1.13)**. Cortical actin is nucleated by both the Arp2/3 complex and formins, thus accounting for its mixed structure (Bovellan et al., 2014). The actin layer also contains minifilaments of the molecular motor non muscle myosin II (Charras et al., 2006). Myosin recognizes the polarity of actin filaments and moves directionally. In the case where actin filaments are in an antiparallel arrangement, the bipolar nature of the myosin minifilament causes the filaments to slide past each other and contract (Aguilar-Cuenca et al., 2014; Levayer and Lecuit, 2012) and **(Figure 1.14)**. Myosin minifilaments are able to interact with unbranched or branched actin filaments, generating high and low contractility respectively.

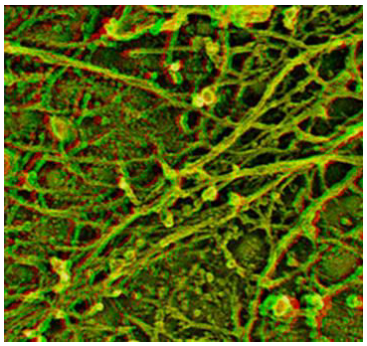

Figure 1.13 Actin cortex. Tomography from a EM of a cell cortex showing the mix of a branched and unbranched network. From (Morone et al., 2006).

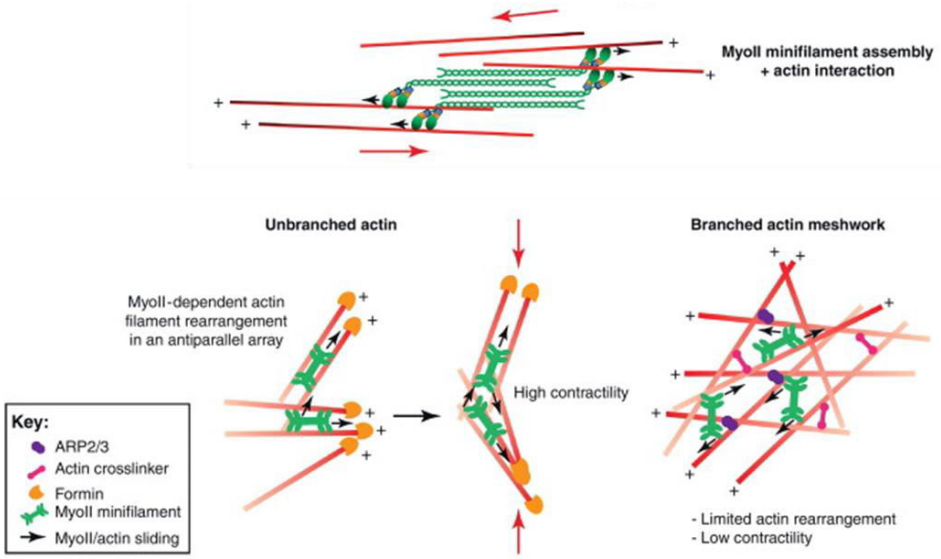

Figure 1.14 Actomyosin contraction. Top: bipolar myosin minifilaments slide antiparallel actin filaments. Bottom panels: myosin minifilaments are also able to generate low or high contraction depending on the geometry of the actin network. Adapted from (Levayer and Lecuit, 2012).

The contractility of the acto-myosin cortex plays an important role in cell rounding for mitosis, contraction of the cytokinetic furrow and squeezing forward the back of the cell during cell crawling (Levayer and Lecuit, 2012). Acto-myosin tension is also what drives the formation of the cellular bleb. A bleb is a bulge of membrane, initially devoid of cytoskeleton, which forms when the link between the cortex and the membrane ruptures (Charras et al., 2006) or when a hole appears in the cortex itself (Paluch et al., 2005) and **(Figure 1.15).** Once the bleb is initiated, its rapid expansion and round shape suggest that the increase in bleb volume is mainly due to hydrostatic pressure created by myosin contractility rather than vesicle trafficking or local unwrinkling of the cell membrane (Charras et al., 2008). These observations also fit theoretical and experimental data that demonstrate the existence of a

critical tension for bleb formation, and an increase in bleb size with increasing tension (Tinevez et al., 2009). Once the bleb has achieved its maximum size, the cortex reforms in the bleb, either leading to stabilization of the protrusion or to retraction of the bleb and reabsorption (Charras et al., 2008).

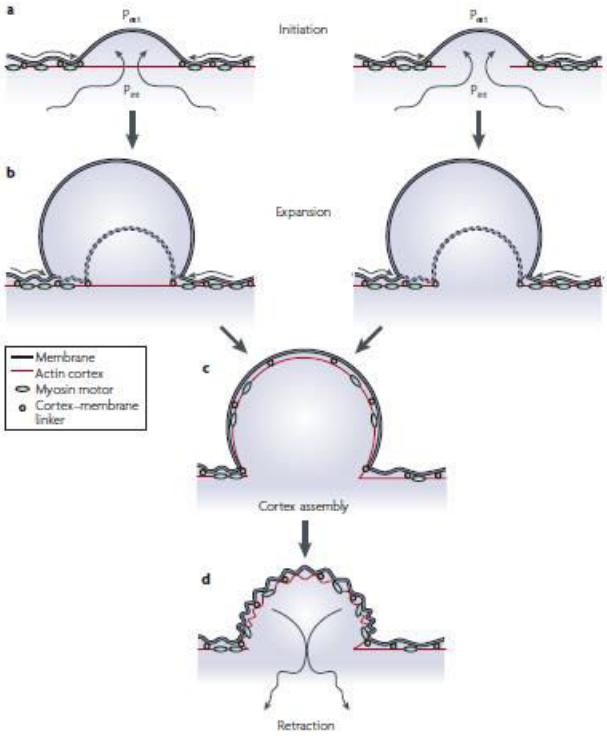

Figure 1.15 Blebbing. The bleb starts by detachment or rupture of the cortex. Cytosol flows into the bleb, expanding it until it achieves a maximum size. Then the cortex reforms to stabilize the protrusion or to generate retraction and reabsorb it. From (Charras and Paluch, 2008).

1.2.4 CROSSLINKED ACTIN STRUCTURES

For all three architectures discussed in the preceding sections (branched structures in lamellipodia, unbranched structures in bundles like filopodia and mixed branched and unbranched networks in the cell cortex), actin cross-linking proteins play key roles in the formation and properties of the different actin arrangements (Revenu et al., 2004; Stevenson et al., 2012). There are many actin crosslinkers in cells, but the best-studied ones are fascin, α-actinin, plastin (also called fimbrin) and filamin (Adams, 2004; Bartles, 2000; Otey and Carpen, 2004; Stossel et al., 2001). Fascin is a monomeric protein able to form small bridges of 8 nm between parallel actin filaments (Jansen et al., 2011) and **(Figure 1.16)**, while α-actinin is a dimeric protein able to form longer filament crosslinks of around 17–24 nm (Goldstein et al., 1979; Luther, 2000) and **(Figure 1.16)**. Due to its flexible amino-terminal F-actin binding domains that rotate freely with respect to each other, α-actinin is able to bind

non-aligned actin filament networks, antiparallel arrangements or parallel bundles (Courson and Rock, 2010). Both fascin and α-actinin are implicated in filopodial structure and function (Fukumoto et al., 2015; Huang et al., 2015; Shao et al., 2014) and have been shown to work synergistically in increasing actin network stiffness (Tseng et al., 2005).

Plastin, like fascin, is a monomeric protein with two actin binding domains able to bundle parallel filaments, but with a distance of about 12 nm, giving a looser bundle than fascin (de Arruda et al., 1990) and **(Figure 1.16)**. Plastin is also found in filopodia, and additionally in filopodial-like structures called microvilli in the intestines (Bretscher and Weber, 1980; Volkmann et al., 2001). Another type of crossslinker is filamin, a dimeric protein with two actin binding domains at the N-terminus, two rigid rod domains, and two flexible hinges, thus conferring the mix of flexibility and stiffness required to tether actin filaments and hold them into an orthogonal arrangement (Gorlin et al., 1990; Hartwig and Stossel, 1981) and **(Figure 1.16)**. Before the discovery of the Arp2/3 complex, it was believed that filamin was responsible for the X, T and Y-shaped junctions visible in the lamellipodium (Flanagan et al., 2001; Hartwig et al., 1989; Schliwa and van Blerkom, 1981). As well as its role in crosslinking, filamins have a role in signaling via interactions with integrin adhesion proteins, and small GTPases, RhoA, Rac1, and Cdc42 (Kiema et al., 2006; Ohta et al., 1999).

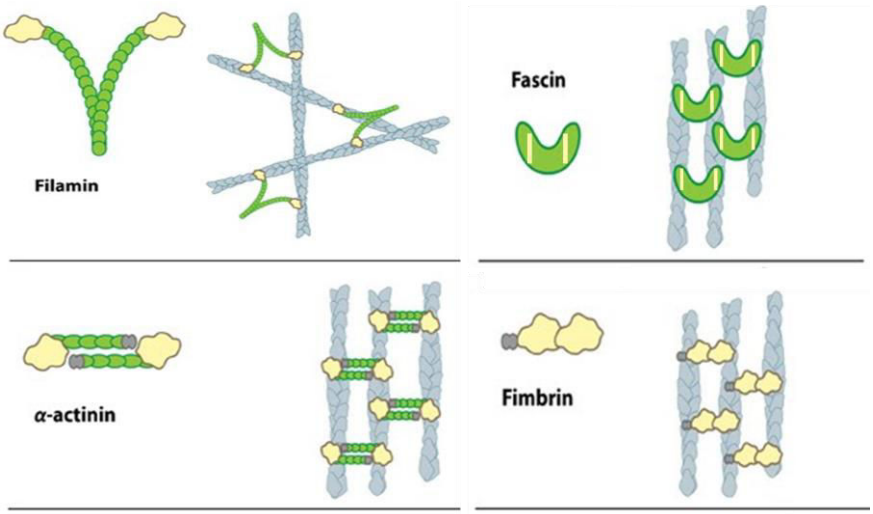

Figure 1.16 Actin crosslinkers. A representation of different actin crosslinkers. Yellow represents the actin binding domains, green the rest of the protein and blue are the actin filaments. Barbed and pointed ends are visible. Adapted from https://www.mechanobio.info/.

Fascin, α-actinin, plastin and filamin are all present in lamellipodial networks (Small et al., 2002; Stossel et al., 2001). All but fascin are also present in the acto-myosin cortex where they presumably crosslink filaments formed by both Arp2/3 complex and formin nucleation

(Charras et al., 2006), and play a role in mediating cortex contractility as has been shown with crosslinked acto-myosin networks in vitro and in vivo via filamin (Alvarado et al., 2013; Ding et al., 2017).

1.2.5 PUTTING IT ALL TOGETHER: ACTIN NETWORKS IN MOTILITY

The branched, unbranched and cortical networks described in the preceding sections work together in many cellular processes including cell motility. The overall picture of cell motility involves the front of the cell being pushed out by the formation of branched lamellipodial networks and bundled filopodial structures (called mesenchymal migration) or by the formation of blebs due to cortical contraction (called bleb-based migration).

During mesenchymal migration, lamellipodia or filopodia can generate adhesions with the substrate/ECM via integrins, transmembrane proteins able to link the ECM with the cytoskeleton (Hanein and Horwitz, 2012; Vicente-Manzanares and Horwitz, 2011) and **(Figure 1.17)**. The adhesion points stabilize the protrusion and exert traction forces to move the whole cell forward. Turnover of adhesions induces detachment and release of the rear part of the cell. Attachment/detachment is regulated by Rho and Rac GTPases. While Rac proteins activate actin polymerization and promote cell adhesion at the leading edge, Rho produces the detaching of integrins (focal adhesions) from ECM proteins and cortex contraction at the back of the cell (Vicente-Manzanares and Horwitz, 2011) and **(Figure 1.17).**

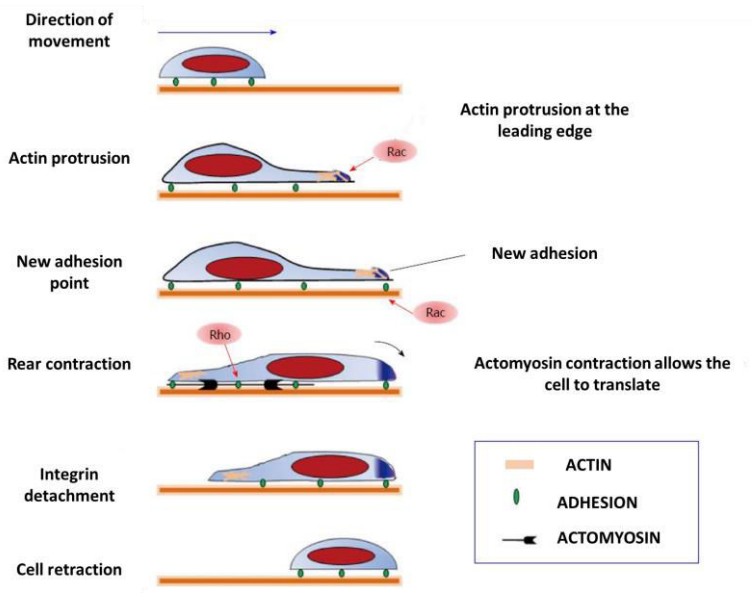

Figure 1.17 Mesenchymal migration. Actin polymerization at the leading edge via Rac GTPase extends the cell membrane to create new adhesion points while the back of the cell contracts via Rho GTPase detaching the integrins from the focal adhesion. Adapted from (Matsuoka and Yashiro, 2014).

On the other hand, in bleb-based migration, cells are minimally adherent. Blebs can intercalate amongst ECM fibers and Rho dependent myosin contraction can force the cell forward (Lämmermann and Sixt, 2009) and **(Figure 1.18)**.

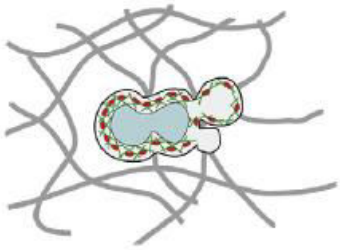

Figure 1.18 Bleb-based migration. Blebs expand amongst ECM fibers, anchoring the cell in place and allowing the back of the cell to be squeezed forward by myosin contractility (myosin in red, actin in green). From (Lämmermann and Sixt, 2009).

Switches between mesenchymal and bleb-based motility are observed in 2D situations, where lamellipodia inhibition by reducing the Arp2/3 complex or reducing cell–substrate adhesion triggers bleb-based motility, while increasing lamellipodial dynamics by activating Rac1 suppresses bleb formation (Bergert et al., 2012). Similar behavior is observed when cancer cells are confined in channels passivated to decrease the level of cell adhesion to the substrate (Liu et al., 2015). Under these conditions, slow-moving mesynchymal-type cells show fast bleb-based locomotion.

1.3 ACTIN CYTOSKELETON IN CANCER CELL INVASION

Cancer cell invasion is a special type of cell motility that involves the movement of cells through the layers of ECM that separate different kinds of tissue. Cancer cell invasion has been observed to proceed by both mesenchymal and bleb-based mechanisms.

1.3.1 MESENCHYMAL-TYPE INVASION

This type of invasion resembles the moving cell described in the previous section. Movement is preceded by a change in the cell properties, termed epithelial-mesenchymal transition whereby epithelial cells lose their apical/baso-lateral polarity and their cell–cell adhesion attributes that make them part of a cohesive tissue and acquire mesenchymal markers including cell-matrix adhesions (Thiery, 2002). They form a protrusion that allows them to move, but also to cross ECM barriers, and in this case the protrusion is called an invadopodium. Invadopodia are actin-filled structures, but they also are equipped with the ability to proteolytically degrade ECM fibers by secreting matrix metalloproteases (MMPs) (Linder et al., 2011; Murphy and Courtneidge, 2011; Revach and Geiger, 2014) and **(Figure**

1.19). The actin network in invadopodia is a mix of a branched network and unbranched bundled filaments, and at later stages, additional cytoskeletal elements like microtubules and intermediate filaments are also observed (Schoumacher et al., 2010) and **(Figure 1.19)**.

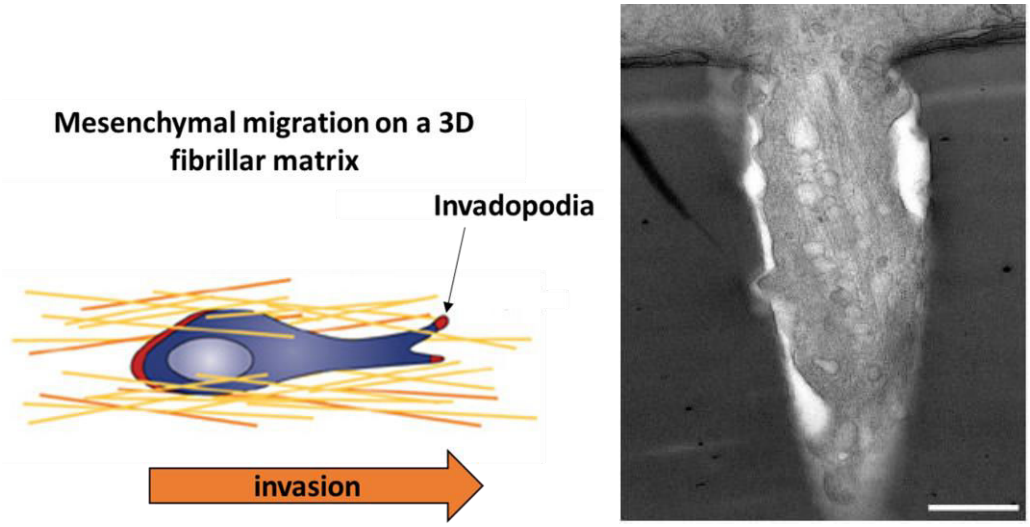

Figure 1.19 Mesenchymal cancer cell invasion. Left panel: representation of a cell invading through a 3D ECM (yellow and orange lines) Arrow indicates the direction of invasion. Adapted from (Friedl and Wolf, 2003). Right panel: electron microscopy image of an invadopodium. Microtubules and intermediate filaments make up the core of the mature invadopodium, while the sides and tip are composed of a dense array of actin filaments, difficult to resolve because of tight packing. Scale bar 0.5 µm. Adapted from (Schoumacher et al., 2010).

The Arp2/3 complex is necessary for invadopodia formation, and the Arp2/3 complex activator N-WASP has been clearly visualized in invadopodia, implying that WASP proteins may be the activators for invadopodial actin nucleation (Nürnberg et al., 2011; Oser et al., 2009; Yamaguchi et al., 2005). However WASP has also been reported to play a role in vesicle trafficking (Benesch et al., 2002; Co et al., 2007; Kovacs et al., 2006), coordinating protease delivery at invadopodia (Nusblat et al., 2011; Yu et al., 2012), so it is possible that WASP's role in invasion relates to trafficking of components to the protrusion and not to actin polymerization to push out the invasive protrusion. The other Arp2/3 complex activator, WAVE, is dim or absent from invadopodia in classical invasion assays (Yamaguchi et al., 2005). However in 3D environments, both WAVE and N-WASP appear to promote invasion (Giri et al., 2013; Takahashi and Suzuki, 2011). Other studies show that inhibition of different forms of WAVE can both upregulate and downregulate cancer cell invasion, depending on the context (Kurisu and Takenawa, 2010). Overall the role of WAVE in invasion is not clear.

Given the mixed architecture of actin in invadopodia, it is not surprising that formins are also linked to cancer invasion and metastasis. Indeed Arp2/3 complex independent invasion, dependent on the formin FHOD3, has been reported (Paul et al., 2015). Upregulation of the

formin FMNL2 was found in metastatic colorectal cancer cell (Zhu et al., 2008). However the same formin was found at lower levels in hepatocellular carcinoma lines (Liang et al., 2011). Similarly for the formin mDia2, some studies show a positive correlation with invasion and others the opposite (Di Vizio et al., 2009; Lizárraga et al., 2009). These observations suggest that the correlation between invasive behavior and the presence of formins depends on the tissue and the type of formin.

Actin crosslinkers have also been implicated in invadopodia formation. High expression levels of fascin are correlated with tumor cell migration and invasion in vitro, and metastasis in vivo (Huang et al., 2015; Vignjevic et al., 2007). Conversely other studies report that loss of filamin enhances ECM degradation, but this seems to be due to filamin's role in regulating proteolytic activity, not its actin crosslinking activity (Baldassarre et al., 2012). Other studies link both filamin upregulation and downregulation with breast cancer progression (Caruso and Stemmer, 2011; Xu et al., 2010). So like formins, it appears that the role of crosslinkers in invasion depends on the cell type and how invasion is evaluated.

1.3.2 BLEB-DRIVEN INVASION

Invasive cancers cells can also display blebbing motility. In particular this is observed when cancer cells migrate in 3D environments in the absence of MMP activity. Because the ECM cannot be digested, cells squeeze through matrix gaps by using the contractile activity of the acto-myosin cortex (Sabeh et al., 2009; Wolf et al., 2003) and **(Figure 1.20)**. Bleb-based invasion in the absence of MMPs is mainly regulated by the phosphorylation of myosin light chain (MLC) by ROCK (Rho kinase) which promotes the interactions between myosin and F-actin to generate contractile force (Wolf et al., 2013).

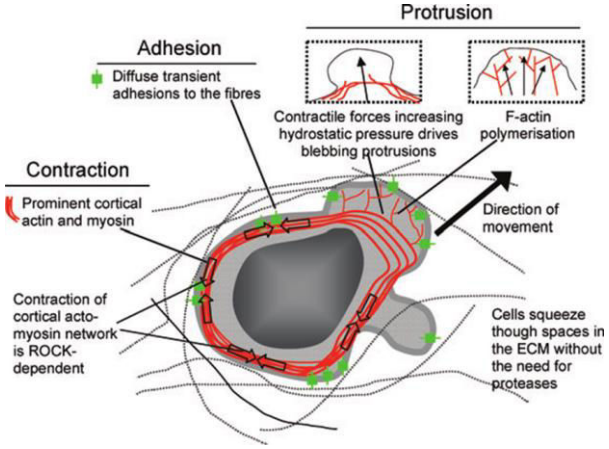

Figure 1.20 Bleb-based cancer cell invasion in a 3D environment. Cells move via membrane blebs that are subsequently stabilized by actin polymerization. In this type of invasion, adhesion is low and ROCK mediates contractile forces to increase the hydrostatic pressure to squeeze the cell forward. Adapted from (Pinner and Sahai, 2008).

As for healthy motile cells, invading cancer cells can switch between mesenchymal and bleb-based modes of invasion depending on the mesh size of the 3D environment, cell-substrate adhesion levels, the presence of proteases and the balance between actin protrusivity via RacGTPase and actomyosin contractility via RhoGTPase-ROCK (Lämmermann and Sixt, 2009; Petrie and Yamada, 2012) and **(Figure 1.21)**.

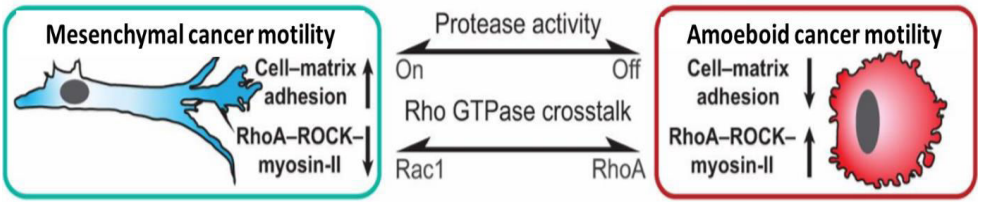

Figure 1.21 Switch between mesenchymal and bleb-based amoeboid cancer migration. Cancer cells switch to the low adhesion, high contractility mode of bleb-based cancer cell migration upon inhibition of protease activity or upon modulation of Rho GTPase crosstalk. Adapted from (Petrie and Yamada, 2012).

CHAPTER 2: ANCHOR CELL INVASION IN *CAENORHABDITIS ELEGANS*

2.1 HOW THE AC OPENS THE HOLE IN THE BM

In early stages, *C. elegans* larvae do not possess a vulva and the uterus is a closed organ, unconnected to the outside of the worm. At the site of the future vulva, the uterine and pre-vulval tissue are separated by a double BM (Morrissey et al., 2014). The role of AC invasion is to pierce the double BM at a specific larval stage, making a hole that will later become the vulva. As briefly introduced in **Chapter 1**, AC invasion looks morphologically similar to the invading cancer cell, since both are dependent on a dynamic actin-filled protrusion to make a hole in a BM. AC invasion generally starts with a unique small hole in the BM at a certain time in development, colocalizing in the AC with actin and with signaling molecules such as PIP2 (Hagedorn et al., 2013) and **(Figure 2.1)**. The protrusion grows and the hole in the BM expands until it reaches the AC border. In later stages, as the vulval tissue begins to invaginate, the hole expands beyond the edges of the AC due to mechanisms that are distinct from the initial invasive process, termed BM sliding (Ihara et al., 2011; Matus et al., 2014; McClatchey et al., 2016).

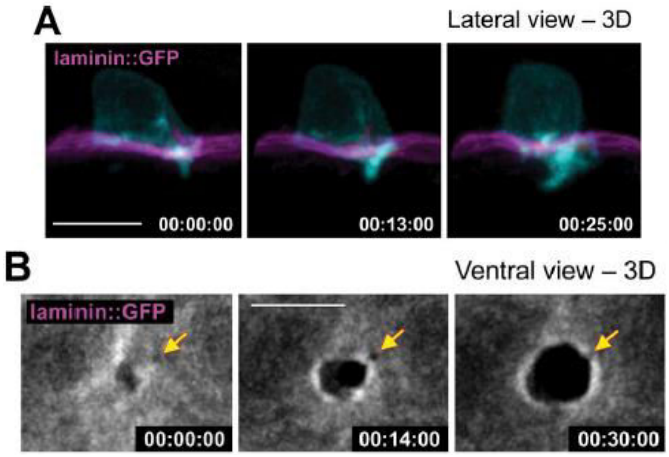

Figure 2.1 AC protrusion growth and BM hole expansion. A) Side view of an AC breaching the BM (magenta) with a PIP2-rich membrane protrusion (blue). B) Ventral view of BM hole expansion to the width of AC. Bar 5 μm. Adapted from (Hagedorn et al., 2013).

It is important to note that, at the time of invasion, the AC is expressing 3 MMPs, the zinc matrix proteases ZMP-1, -3 and -6 (Matus et al., 2015). However there is evidence that BM hole formation and expansion is not all due to matrix digestion. BM accumulates at the perimeter of the gap **(Figure 2.1)** and a photo-conversion experiment using photoconvertible

laminin showed that not all of the BM beneath the AC is digested; some is pushed aside (Hagedorn et al., 2013) and **(Figure 2.2)**. The goal during my PhD was to find the source of these pushing forces, with the long-term objective of relating these results to understanding cancer cell invasion.

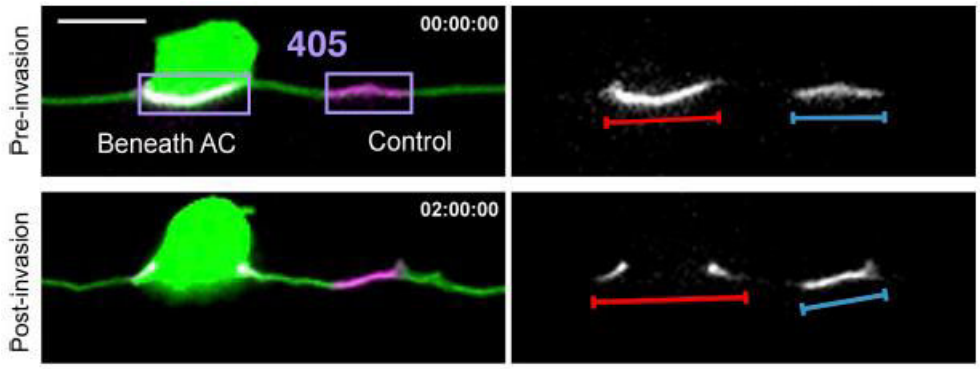

Figure 2.2 BM is displaced as well as being digested. The BM just beneath the AC and a control flanking region are photocoverted just before invasion and imaged after invasion. The control region remains intact, and while much of the photoconverted BM under the AC has disappeared, some remains, pushed to the sides of the AC. Bar 5 μm. AC and BM in green; BM photoconverted to purple. Adapted from (Hagedorn et al., 2013).

2.2 WHY STUDY AC INVASION?

Due to the difficulty of studying cancer cell invasion in living animals, most of what is known about the role of the actin cytoskeleton in cell invasion comes from the study of cultured cancer cells invading artificial BM mimics in 2D assays (Bowden et al., 2006; Linder et al., 2011). However reconstituted extracellular matrices, such as Matrigel, do not retain all of the biochemical properties of in vivo matrices, and the thin 2D geometry of native BM sheets is not respected. Even more importantly, mechanical properties of reconstituted BM do not reflect native membranes: estimates of native BM Young's modulus are in the kPa-100 kPa range, whereas Matrigel has a 10 to 1000-fold lower elasticity, in the 100 Pa range (Paszek et al., 2005; Wood et al., 2010). Since actin dynamics and organization responds to mechanical cues in the environment (Fletcher and Mullins, 2010), it is important to approximate in vivo mechanics as closely as possible in order to acquire biologically relevant information on the actin cytoskeleton in cell invasion. In this context, it is useful to study cell invasion using developmental models where non-pathologic invasion occurs at a specified place and time during organ development, making it easier to detect and image in the living animal. An example of such a process is AC invasion.

2.3 RELEVANCE OF AC INVASION TO CANCER CELL INVASION

Transcriptionally AC invasion is mainly regulated by *fos-1a*, the *C. elegans* ortholog of the transcription factor Fos, which in vertebrates is upregulated in many types of metastatic cancers and regulates MMPs via the AP-1 transcription factor complex (Aoyagi et al., 1998; Hagedorn and Sherwood, 2011; Saez et al., 1995). Adding to this, a whole-genome RNA interference (RNAi) screen identified 99 genes that promote AC invasion, and most of these genes have human orthologs, many of which have been implicated in cell invasion (Matus et al., 2010).

The molecular organization of BMs in *C. elegans* is highly conserved with vertebrates and contains orthologs of the major structural components, including type IV collagen and laminin. The acto-myosin cytoskeleton is also well-conserved in worms, which contain counterparts of the Arp2/3 complex subunits, named ARX1-7 (Sawa et al., 2003), homologs of the activators WASP and WAVE (WSP-1 and WVE-1, respectively) (Miki and Takenawa, 2003; Patel et al., 2008) and a 6-member family of formin proteins: FHOD-1, CYK-1, FRL-1, INFT-2, DAAM-1 and EXC-6 (Mi-Mi et al., 2012; Schönichen and Geyer, 2010). Concerning upstream signaling to the actin cytoskeleton, *C. elegans* has one real Cdc-42, CDC-42, and one true Rac, CED-10, and another Rac, MIG-2, which contains Rac-like and Cdc-42-like motifs (Lundquist et al., 2001; Reiner and Lundquist, 2016; Shakir et al., 2008). As for mammals, CDC-42 is the Rac that is responsible for activating WSP-1 to bind and activate the Arp2/3 complex, with MIG-2 also playing this role, while CED-10 is the upstream activator of WVE-1 (Shakir et al., 2008; Walck-Shannon et al., 2016). *C. elegans* also has most major actin binding regulatory proteins: 2 forms of ADF/cofilin UNC-60A and B (Ono et al., 2003), Ena/VASP, UNC-34 (Withee et al., 2004), 3 profilin isoforms PFN1-3 (Polet et al., 2006) and 2 non-muscle myosin heavy chains NMY-1 and -2 (Piekny et al., 2003). Like in vertebrates, non-muscle myosin activity in *C. elegans* is controlled by kinases and phosphatases: NMYs associate with light chains, for example MLC-4, which need to be phosphorylated by the Rho-binding kinase LET-502/ROCK or MRCK-1 in order to be active (Gally et al., 2009; Piekny et al., 2000; Shelton et al., 1999). In addition MLC-4 is negatively regulated by the phosphatase MEL-11, inhibiting actomyosin contraction (Wissmann et al., 1999). With the notable exception of fascin, the major classes of actin bundling proteins are also present in *C. elegans*: α-actinin, ATN-1 (Francis and Waterston, 1985; Moulder et al., 2010); filamin, FLN-1 (DeMaso et al., 2011) and plastin/fimbrin, PLST-1 (Skop et al., 2004).

Overall acto-myosin biochemistry, BM composition and transcriptional control are similar in the AC as compared to an invading cancer cell, making AC invasion a relevant model for studying the role of actin dynamics during invasion.

2.4 THE PHYSIOLOGICAL CONTEXT OF AC INVASION

Before invasion occurs, the AC communicates with the VPCs so they assume the correct fate for subsequent vulval development, for review (Schmid and Hajnal, 2015). Briefly in the early third larval stage, there are 6 VPCs called P3.p–P8.p arranged along the ventral surface of the worm, with P6.p centered on the AC **(Figure 2.3)**. The AC secretes a LIN-3/Epidermal Growth Factor (EGF) signal, which is received by the VPCs via the receptor tyrosine kinase LET-23/EGFR. P6.p receives the most signal and is induced to adopt the 1° VPC fate, while the two flanking VPCs are induced to the 2° fate. Fate determination is further reinforced by lateral signaling via LIN-12/Notch that confirms the secondary fate of P5.p and P7.p. The other cells adopt non-vulval fates and contribute to the hypodermis.

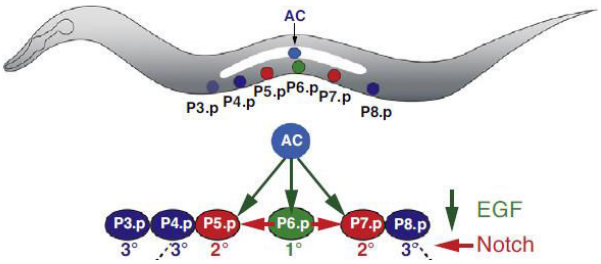

Figure 2.3 VPC arrangement. A representation of a third larval stage worm (L3). AC induces cell fate specification of the VPCs P3.p–P8.p. Adapted from (Schmid and Hajnal, 2015)

Leading up to AC invasion, the 1° and 2° VPCs undergo three rounds of division with precise timing. The progression of AC invasion can be staged by examining whether the central VPC P6.p is at the 2, 4 or 8 cell stage **(Figure 2.4).** In wild type worms, the AC breaches the BM between the 2-cell and 4-cell stage. AC invasion is not a cell-autonomous process. In vulvaless *lin-3* mutant animals or when P6.p is ablated, invasion does not occur (Sherwood and Sternberg, 2003). In addition AC invasion is blocked in mutants where all VPCs adopt 2° fates (Sherwood and Sternberg, 2003). Conversely when P8.p assumes a 1° fate after ablation of P3.p-P7.p, the AC protrusion breaches the BM and elongates in order to reach it, so AC invasion appears to be driven by the 1° VPC independently of its location (Sherwood and Sternberg, 2003). Moreover studies using mutant animals with multiple 1° VPCs, but only one AC, show breaches in the BM only where the AC is located, confirming that the VPCs do not stimulate AC invasion by removing the BM themselves (Sherwood and Sternberg, 2003). On the uterine side of the BM, the gonadal cells adjacent to the AC can be ablated

without affecting invasion, so the direct neighbors of the AC do not appear to play a role in helping the AC to pierce the BM (Sherwood and Sternberg, 2003).

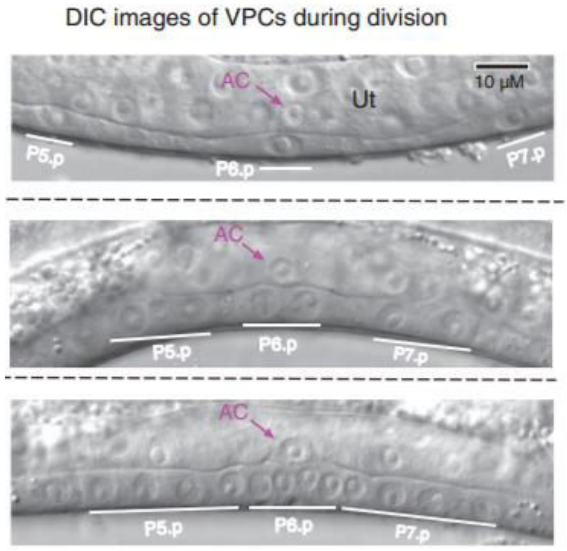

Figure 2.4 VPC division is coordinated with AC invasion. From top to bottom, 1-cell, 2-cell and 4-cell stage, named according to the division of the central VPC P6.p. The AC is indicated with a purple arrow. The BM is observed by differential interference microscopy (DIC) microscopy as a line under the AC which becomes discontinuous upon invasion, which happens between the 2 and 4-cell stage.

Notably although the VPCs divide over the course of AC invasion, the AC itself does not. This is because the AC is arrested at the G1 phase of the cell cycle via transcriptional control (Matus et al., 2015) and **Section 2.6**. When arrest is interfered with and cell division and proliferation of the AC continues, invasive behavior is lost (Matus et al., 2015).

2.5 AC INVASION REGULATION BY SIGNALING

AC invasion is regulated by two main external signals, a diffusible vulva cue from the 1° VPC and another emitted by the ventral nerve cord (VNC) that is adjacent to the vulval cells (Sherwood and Sternberg, 2003; Ziel et al., 2009). The cue from the 1° VPC is unidentified, but it is known that it is diffusible because, as mentioned in the previous section, when P8.p acquires a 1° fate, the AC extends a protrusion to it over a long distance (Sherwood and Sternberg, 2003). The signal from the 1° VPC doesn't completely control the timing of AC invasion however, since in mutant animals where the 1° VPC forms precociously, the AC still invades at or near the normal time of invasion (Sherwood and Sternberg, 2003).

In vulvaless animals there is still 20% successful invasion, and this is believed to be dependent on a UNC-6/netrin signal produced by the VNC (Sherwood and Sternberg, 2003; Ziel et al., 2009). UNC-6/netrin signal is high in the VNC and accumulates in the BM under the AC where is acts via the netrin receptor UNC-40/DCC located at the AC invasive

membrane (Ziel et al., 2009). In neurons, netrin/DCC signaling is known to act on actin regulators, including RacGTPase (Gitai et al., 2003). When UNC-6/netrin is not present, UNC-40/DCC remains active in assembling actin patches, however the actin clusters are mislocalized and dynamic, undergoing an oscillatory behavior of assembly-disassembly (Wang et al., 2014c). UNC-6/netrin is crucial for clustering and stabilizing UNC-40/DCC to form a proper protrusion (Hagedorn et al., 2013; Wang et al., 2014c) and **(Figure 2.5).** Loss of UNC-40/DCC and/or UNC-6/netrin does not inhibit the ability of the AC to create the initial holes in the BM, a process that is apparently not linked to netrin signaling (Hagedorn et al., 2013; Ziel et al., 2009).

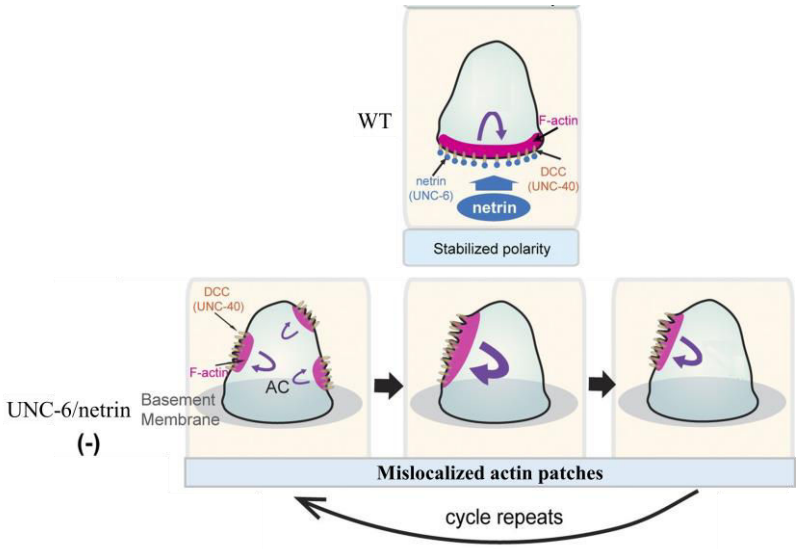

Figure 2.5 Netrins role on actin polarity in the AC. Top panel: in WT animals UNC-6/netrin polarizes the receptor DCC/UNC-40 at the invasive membrane where actin starts to polymerize via DCC/UNC-40 partners. Bottom panel: in the absence of netrin/UNC-6, DCC/UNC-40 is mislocalized at the apical and lateral AC membrane and actin polymerization is not focused at the invasive edge. Adapted from (Wang et al., 2014c)

Instead the formation of initial actin-rich foci that occur before invasion is dependent on integrins (Hagedorn et al., 2013). When integrin is knocked down, foci don't form and furthermore, components of the mature protrusion, UNC-6/netrin, UNC-40/DCC and other actin regulatory proteins are not localized normally at the invasive membrane (Hagedorn et al., 2009; Wang et al., 2014a; Wang et al., 2014c). These results suggest that the integrin and netrin pathways work together to signal to the invasive program (Hagedorn et al., 2009).

2.6 AC INVASION REGULATION BY GENE EXPRESSION

The invasive behavior of the AC is conferred by the specific expression of certain genes in the AC **(Figure 2.6)**. As mentioned briefly above, the transcription factor *fos-1*, the sole *C. elegans* ortholog of the fos bZIP transcription factor family, is specifically expressed in the AC and controls the expression of important target genes (Sherwood et al., 2005). These include *zmp-1*, an MMP, *him-4*, an ECM component involved in adhesion of adjacent BMs and *cdh-3*, a cadherin family protein involved in cell-cell adhesions (Morrissey et al., 2014; Sherwood et al., 2005). Individually mutation of these 3 genes slightly affects AC invasion, however the triple knock-out has a more severe effect, only 75% invasion at the 4-cell stage where wild-type shows 100% (Sherwood et al., 2005). *fos-1a* also positively regulates MIG-10/lamellipodin expression (Wang et al., 2014b).

Another transcription factor found in the AC is *egl-43*, the *C. elegans* ortholog of vertebrate proto oncogene EVI1 (Hwang et al., 2007; Rimann and Hajnal, 2007). *egl-43* acts downstream *fos-1* (Hwang et al., 2007; Matus et al., 2010) and represses the expression of MIG-10 (Wang et al., 2014a; Wang et al., 2014b). The contradictory effects on MIG-10 expression, positively regulated by *fos-1* but negatively regulated by *egl-43*, are believed to tightly control MIG-10 availability since too much MIG-10 is deleterious to invasion (Wang et al., 2014a). EGL-43 is also required for cell fate specification to convert a uterine cell (VU) into the AC (Rimann and Hajnal, 2007).

An RNAi screen for genes that perturb AC invasion yielded numerous candidates from many protein families, such as chaperones, kinases and transcription factors including a histone deacetylase, *hda-1* (Matus et al., 2010). The gene *hda-1* plays a key role in transducing G1 arrest to protrusion formation, downstream of the nuclear hormone receptor *nhr-67* and *cki-1*, a cyclin-dependent kinase inhibitor. In brief, G1 arrest upregulates *hda-1*, which controls the expression of the proinvasive genes *zmp-1*, *cdh-3* and *him-4* both directly and via upregulation of *fos-1*, in addition to directly affecting the expression of the actin regulatory genes *exc-6* (a formin) and *unc-34* (an Ena/VASP protein) (Matus et al., 2010; Matus et al., 2015).

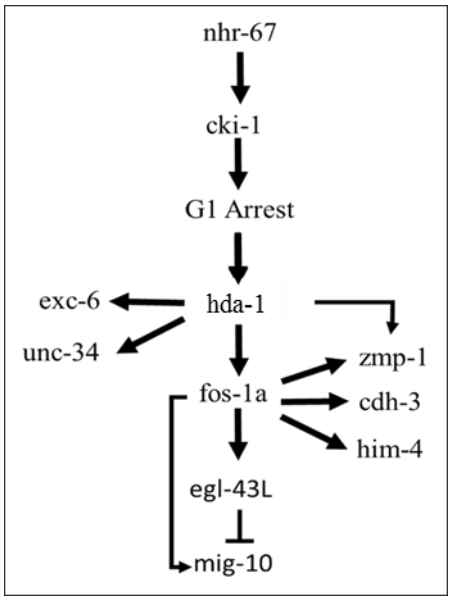

Figure 2.6 A gene expression model of AC invasive differentiation. Summary of how *nhr-67* and *hda-1* affect genes related with AC invasion behavior, including *zmp-1, cdh-3, him-4, unc-34* and *exc-6*. Modified from (Matus et al., 2010; Matus et al., 2015; Sherwood et al., 2005; Wang et al., 2014a)

2.7 ACTIN AND MEMBRANE DYNAMICS FOR AC INVASION

As seen from the preceding sections, the physiology, signaling and transcriptional control of AC invasion is fairly well described. It is equally clear that actin cytoskeleton and membrane components are important for this process. However the molecular players involved in actin and membrane dynamics in the AC are less well understood.

UNC-6/netrin localizes the RacGTPases MIG-2 and CED-10 to the invasive leading edge and their combined loss results in invasion defects (Wang et al., 2014b; Ziel et al., 2009). Since MIG-2 signals to WSP-1 and CED-10 to WVE-1, this suggests the participation of both WSP-1/WASP and WVE-1/WAVE in AC invasion. In addition loss of another GTPase, CDC-42, also upstream of WSP-1/WASP, results in a delay in AC invasion (Lohmer et al., 2016). Active CDC-42 is localized in the F-actin puncta that form prior to the growth of the invasive protrusion, and not in the invasive protrusion itself, indicating that WASP may be important for initial but not later stages of AC invasion (Lohmer et al., 2016).

The implication of both WSP-1/WASP and WVE-1/WAVE in AC invasion indicates that the process may depend on actin polymerization nucleation via the Arp2/3 complex. Nevertheless a formin, EXC-6, is specifically expressed in the AC under control of *hda-1*, but the role of formins during AC invasion is not known (Matus et al., 2015). Two other actin assembly factors important for actin dynamics in lamellipodia, UNC-34/Ena/VASP and MIG-

10/lamellipodin, are also known to contribute to AC invasion, and they do so independently of the UNC-6/netrin pathway (Wang et al., 2014b).

As for lamellipodia, actin disassembly proteins are also important for AC invasion. In animals mutant for the *C. elegans* orthologue of ADF/cofilin, UNC-60, AC invasion is blocked (Hagedorn et al., 2014). Excessive actin accumulates at the invasive membrane, but experiments using a photoconvertible fluorophore coupled to actin show that this actin is non-dynamic, indicating that ADF/UNC-60 is important for actin turnover (Hagedorn et al., 2014). UNC-40/DCC and HIM-4/hemicentin are correctly localized in *unc-60* mutants, but the phospholipid PI(4,5)P2, MIG-2/Rac and CED-10/Rac are not normally polarized when ADF/UNC-60 is disrupted (Hagedorn et al., 2014).

Moreover mispolarization and ectopic accumulation of lysosomal markers in internal compartments after loss of UNC-60 support the idea that UNC-60/ADF promotes membrane recycling from the protrusion via endolysosomes, although it is not clear if there is a direct link or if it's a steric effect created by excess polymerized actin that impedes proper membrane trafficking in the cytosol (Hagedorn et al., 2014). In keeping with a role for membrane dynamics in AC invasion, knocking down GDI-1, a Rab GDP-dissociation inhibitor that is related with vesicle trafficking, reduces AC invasion (Lohmer et al., 2016).

The scheme in **(Figure 2.7)** shows what we knew about membrane and actin dynamics in the AC during invasion at the point when I started my PhD studies. To summarize, in response to an unknown signal from the vulval cells, actin foci form in the AC via the activity of CDC-42 activating WSP-1/WASP, presumably upstream of Arp2/3 complex actin nucleation. The vulval signal also appears to communicate to other assembly factors such as UNC-34/Ena and MIG-10/lamellipodin. Only one or two of these foci will make a hole in the BM and transition into an invasive protrusion, dependent on Racs and presumably WAVE downstream of UNC-6/netrin signaling from the VNC to UNC-40/DCC. As for most force-producing actin structures, actin turnover via UNC-60/ADF is also important and may participate, along with GDI-1, in the trafficking of membrane to the protrusion.

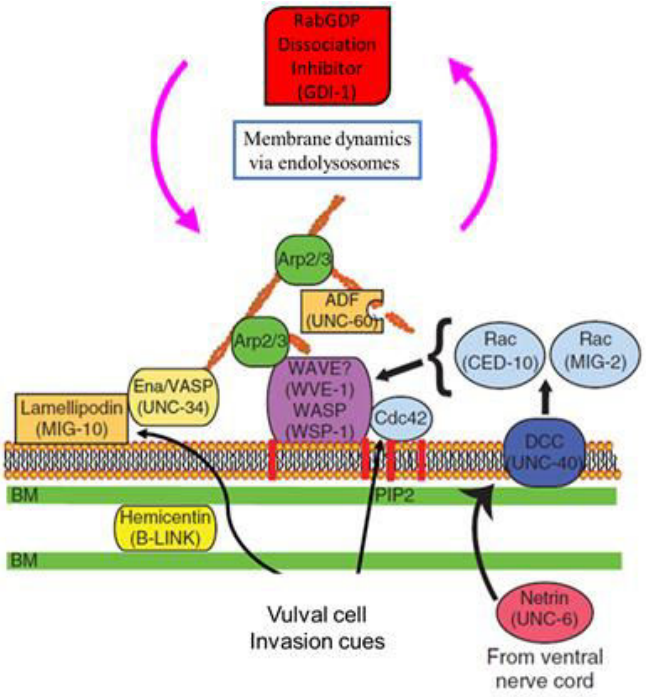

Figure 2.7 Actin-binding proteins and membrane dynamics in AC invasion. Scheme of what was known when I started my PhD. Actin filaments are represented in orange. All other molecules are labeled. Black arrows represent interactions and pink arrows represent membrane recycling. Adapted from (Caceres and Plastino, 2017).

CHAPTER 3: EXPERIMENTAL METHODS

3.1 PROTOCOLS

One of the main techniques of the PhD was RNAi by feeding. **Sections 3.1.1- Section 3.1.3** explain the steps of the procedure.

3.1.1 WORM SYNCHRONIZATION

Worms were synchronized prior to most RNAi treatments so that large numbers of worms in the right stage of invasion could be evaluated.

1. Collect worms from 4 plates full of adult worms (use water) and transfer to a 15 ml Falcon tube.
2. Fill the tube with water and centrifuge at 200 g for 3min.
3. With a Pasteur pipette and a pump, suck off the supernatant (be careful not to touch the pellet). Repeat step 2 and 3 until the liquid is transparent (usually 2 times).
4. Add 100 -150ul of bleach solution (see below), and shake by hand (do not invert the tube or vortex, this makes the worms attach to the walls and not be in contact with the bleach solution).
5. Verify using the stereo microscope that all the worms are disintegrated (around 4-5 minutes after addition of the bleach solution), at this point the solution will have turned yellow.
6. Immediately fill the tube with PBS and mix by inversion 8 times.
7. Centrifuge at 600g at 3 min at room temperature (4°C will kill the eggs).
8. With a Pasteur pipette and a pump, suck off the supernatant (be careful not to touch the pellet).
9. Repeat steps 6-8. After the second wash, leave around 1ml of solution.
10. Verify with a pH strip that the pH is around 7. If it's not, perform another wash.
11. Shake the tube until all the eggs are floating, and pour the solution into a 50 ml Falcon tube (do not use a pipette, all the eggs will attach to the walls).
12. Put the 50 ml Falcon tube on a rotating wheel at room temperature..
13. After 36 hrs most of the worms will be hatched and arrested in L1 larval stage due to lack of food.

Bleach solution in a 15 ml Falcon tube

Bleach* (2.6% active hypochlorite)	3ml
NaOH (35% solution =12.1 M)	333ul
H20	Fill to 5ml

* Do not use bottles that have been opened for more than 2 months.

3.1.2 PREPARING BACTERIA WITH PROBES FOR FEEDING

1. Put 100 ul of HT115 competent cells into a 1.5ml tube.
2. Add 150 ng of DNA, mix very gently by hand (2 taps on the tube). Be sure there are no drops on the walls. DNA is the RNAi probe in the L4440 vector.
3. Incubate 30 minutes on ice.
4. Heat shock at 42°C for 2 minutes in a water bath.
5. Add 1 ml of LB media, mix by inversion and incubate 1h at room temperature.
6. Apply 20 ul and 100 ul to the middle of ampicillin agar plates with tetracycline (see below) and spread with a glass spatula.
7. Centrifuge the rest of the bacteria at 20000g for 2 minutes at room temperature.
8. Remove almost all the supernatant (leave around 100 ul).
9. Resuspend the bacteria and spread it on an Amp/Tet plate as above.
10. Incubate the plates overnight at 37°C.
11. Only work with the big colonies that grow close to the center of the plate.

Ampicillin plates with tetracycline

Add 55 ul of tetracycline (100 mg/ml) to the middle of an ampicillin plate and homogenize with a glass spatula.

3.1.3 RNAI BY FEEDING

1. Pick a single colony with a 10 ul sterile pipette and grow it in 3ml LB medium + 3µl 100 mg/ml ampicillin in a 14ml culture tube at 37°C, 225 rpm agitation.
2. After 3 hours, check the OD using a 100ul of culture+900 LB, after blanking the machine on 900ul LB.
3. When the OD is between 0.6-0.75, spot 100 ul onto 4 NGM-IPTG plates (see below) for each condition. (If the OD is around 0,4 check it again after 20-25 minutes.)
4. Once the bacteria soaks in, invert the plates and incubate at room temperature overnight to induce expression. (For better induction the bacteria need to dry quickly. If 20 min after spotting, the plates are not yet dry, put the plates in the hood with the lids ajar. Keep the windows of the lab closed to avoid contamination at all times.)

5. After induction, apply around 80 arrested L1s (see above, synchronization) to each plate.
6. Evaluate AC invasion after 32-35hrs.

NGM-IPTG plates Make 1.5 L batch and then divide into 3, 500 ml bottles after autoclaving and before adding the salts and the antibiotics. 500 ml bottles can be heated up individually in the microwave, supplemented with salts and antibiotics and poured. 500 ml makes about 50 plates.

	For 1.5 L
NaCl	4.5 g
Bacto Agar	38.25 g
Bacto Peptone	3.75 g
Milli-Q water	1450 ml
Mix, autoclave and Leave it at 55°C on a water bath, After add following the order:	
1M $CaCl_2$	1.5 ml (0.5 ml for 500 ml batch)
1 M $MgSO_4$	1.5 ml (0.5 ml for 500 ml batch)
1 M KPO_4 pH 6.0	37.5 ml (12.5 ml for 500 ml batch)
5 mg/mL cholesterol This solution is in ethanol Avoid the flame.	1.5 ml (0.5 ml for 500 ml batch)

Add IPTG and carbenicillin to 1mM and 25 ug/ml, respectively (1.5ml of IPTG at 1M and 375 uL of carbenicillin at 100 mg/ml for a 1.5 L batch; 500ul and 125 ul for a 500 mL batch).

The plates can be stored at 4°C for up to 3 weeks.

3.1.4 LIVE WORM IMAGING

Sample mounting

1. Put 100 ul of levamisole (0.02%) into the well of a watch glass.
2. Transfer 30-40 worms (minimize bacteria) and incubate until the worms stop moving (15 min approx).
3. Transfer the worms with a mouth pipette onto a 4.5% noble agar pad.

4. Cover the sample with a coverslip and add more drug at the edges of the agar pad to keep it humid.
5. Use VALAP to seal the sample, leaving 2 small windows for oxygen exchange.
6. Use a humid chamber to transport the sample to the microscope room.

Image acquisition (Spinning disk)

Samples are imaged at 20°C with an inverted confocal spinning disk microscope from Nikon or an upright spinning disc from Zeiss, using a 100x NA1.4 OIL DIC N2 PL APO VC objective and a CoolSNAP HQ2 (Photometrics) camera controlled by Metamorph software.

1. Find and center the worms using the 10x objective.
2. Change to the 100X objective and with low laser power (15-20%) and 50 ms of exposure, find the fluorescent AC and select the top and bottom planes.
3. Start time-lapse acquisition using:

   -491nn laser at 30% 150ms exposure time
   -561nn laser at 35% 250ms exposure time (increase over time if necessary, see below*)
   -Transmitted light at max power 350 ms exposure time—only use to check worm morphology, do not use during stack acquisition.
   -0.5 um Z-step
   -Acquire a stack every 45s
4. The worm moves in the z plane because the agar pad dries. Check that the top and bottom plane of the stack still covers the whole AC by changing the stage position by hand when necessary.

* Keep the laser at 0% power during acquisition. Just turn it on at 35% when the AC actin protrusion start to form, when the protrusion expands and at the end (not during the whole acquisition).

RESOLFT microscopy

Point scanning RESOLFT imaging was carried out using a custom setup built by the laboratory of Ilaria Testa. The setup was built around a Leica DMI 6000 microscope with a 63x $STED_{white}$ glycerol objective lens NA 1.4. The correction index collar was used in order to match the refraction index from the worm with the mounting medium. The collar was adjusted for each worm in order to collect the most photons to minimize the expansion of the focal spot along the optical z-axis. RESOLFT requires 3 separate controllable light sources, one for each phase in the RESOLFT scheme: activation (405 nm), off-switching (488 nm) and

read-out (488 nm). The hardware was controlled using a custom designed software based on LabVIEW and National Instrument's FPGA. This allowed us, through a single interface, to control the XYZ scanner, the sequential pulsing scheme of the lasers, and ensured we only collected the photons emitted during the read-out phase.

Image acquisition

1. Once the anchor cell is centered, reduce the scanning window to match as much as possible in the X and Y axes. On the Z axis only take the planes that contain the protrusion (0,5µm steps).
2. Select on the acquisition software the following parameters:

   "Act Time": 20 ms
   "wait1Time":50 ms
   "donutTime":50 ms
   "wait2Time":500 ms
   "readoutTime":100 ms *
   "minDwellTime":0 ms
   "decisionTime From":0 ms
   "decisionTime To":70 ms

   Note: The system is not able to take a time-lapse. It acquires images continuously.
3. The worm moves in the z plane because the agar pad dries. Check that the top and bottom plane of the stack still covers the whole AC by changing the stage position by hand when necessary.

3.1.5 MICROINJECTION

The VCA-BFP, Lifeact-BFP and Lifeact-Dronpa strains were prepared by microinjection, followed by integration (see below) for the VCA and Dronpa strains.

1. Put a drop of halocarbon oil on a dry pad of noble agar 4.5% on a 60x50 mm coverslip.
2. Pick an adult worm into the oil and with a flat platinum filament, smooth the worm down from the middle body to the tail and head to immobilize the worm on the agar.
3. Transfer the sample to the microinjector and center the worm with the 10X objective.
4. Change to the 100X objective and insert the microinjection needle in the gonad arm.
5. Inject the microinjection mix by using the "Injection" button.
6. Remove the needle and transfer the worm to the stereoscope.
7. Put 10 ul of M9 solution onto an NGM plate with food.
8. Transfer the injected worm into the drop and remove all the oil from the worm

Note: This process must be done as quickly and as gently as possible to avoid worm damage.

DNA MIX for injecting

DNA 1Kb ladder	up to 100 ng/ul
Plasmid of interest	30 ng/ul
Co-injection marker (use only one)	
rol-6 same concentration as the plasmid of interest (plasmid pRF4)	30 ng/ul
Pmyo2>mCherry (plasmid pCFJ90)	2.5 ng/ul
Final Volume	50 ul

Centrifuge the DNA MIX at 20000g for 15minutes at 4°C.

Take 15 ul from the top of the solution into a new tube and throw the rest away.

3.1.6 INTEGRATING TRANSGENIC LINES

1. Take an injected line that transmits the transgene well, that is, ones that rescue well for the *unc-119* phenotype (DP38 was the injected strain). Take the best transmitters.
2. Put a drop of water onto an NGM plate without food.
3. Pick 40 young adult DP38 (*unc-119*) worms into the drop to remove bacteria from their bodies.
4. Re-pick the 40 clean worms onto a new NGM plate without food.
5. Irradiate the worms (lid off) in a UV Stratalinker with the "300" energy setting of the machine (corresponds to 30000 microjoules).
6. Transfer the worms onto NGM plates with food (2 worms per plate).
7. After starvation transfer a chunk with approx. 100 worms to a new plate with food.
8. After starvation transfer 8 worms per plate onto new NGM plates (1 worm per plate = 160 NGM plates total).
9. After 3-5 days keep only the plates that have 100% of the selected phenotype, in this case mover, non-*unc*s.
10. From each selected plate, transfer 3 worms onto separate NGM plates.
11. After 3-5 days confirm all 3 plates still have 100% of the selected phenotype.
12. Check the expression levels of your protein of interest and verify normal development and keep the best ones.

3.1.7 SINGLE WORM PCR

This technique was used to verify transgenic worms and to detect alleles during crosses.

1. Put 15 ul of lysis buffer (see below) into each PCR tube of a strip and put on ice.

2. Pick a L4 /young adult into a drop of water on a clean NGM plate.

3. Move the worm around in the drop of water to remove the bacteria.

4. Pick the worm into the PCR tube, confirm the worm is in the lysis buffer and put back on ice (avoid touching the walls of the PCR tube).

5. Centrifuge for 4 s (use the strip centrifuge).

6. Put the PCR strip into the -80ºC for 10 min (until the solution is totally frozen).

7. Put the PCR tube/strip into the thermocycler (verify the tubes are well closed).

8. Once the program is finished, flick the tubes to mix (make sure to mix the condensation from the walls into the rest of the solution) and recentrifuge before using for PCR.

Lysis Buffer—for one reaction of 15 ul, mix in order

H20	12.75 ul
Worm PCR buffer 10X	1.5 ul (made in 2007—recipe unknown)
Proteinase K (NEB)*	0.75 ul

*put the enzyme at the bottom of the solution and clean the tip by pipetting

Worm lysis program

65 ºC 1h
95 ºC 15min
4 ºC Hold

PCR Reaction—for one reaction, mix in order

H20	13.375 ul
10X Taq Buffer	2 ul
Dntp's	0.5 ul
Primer F	0.5 ul
Primer R	0.5 ul
Taq*	0.125 ul
DNA	3 ul from worm lysis

*Only use basic Taq Polymerase. Fancy polymerases don't work. Clean the tip by pipetting.

Mix the solution by flicking. Verify the tubes are well closed. Centrifuge for 4 s (use the strip centrifuge) before putting into the thermocycler.

PCR PROGRAM FOR SINGLE WORM PCR

STEP	TEMP	TIME
Initial Denaturation	95°C	30 seconds
35 Cycles	95°C 57°C 68°C	30 seconds 30 seconds 1minute30sec
Final Extension	68°C	5 minutes
Hold	4°C	

3.2 WORM GENOTYPES

How referred to in the text	STRAIN NAME AND GENOTYPE
CHAPTER 4	
WT	JUP60 (NK696 crossed with NK1073—both from David Sherwood, Duke University) unc-119(ed4) III; qyIs127 [Plam-1::lam-1::mCherry + unc-119(+)]; qyIs242 [Pcdh-3::Lifeact::GFP + unc-119(+)]
WASP-DELETED	JUP75 (NG324 crossed with JUP60. NG324 was from the CGC.) wsp-1(gm324) IV; unc-119(ed4) III; qyIs127 [Plam-1::lam-1::mCherry + unc-119(+)]; qyIs242 [Pcdh-3::Lifeact::GFP + unc-119(+)]
WAVE-DELETED	wve-1(ne350); I/hT2[bli-4(e937) let-?(q782) qIs48](I;III) (from Martha Soto, Rutgers University)
--	DP38 unc-119(ed3) III (from the CGC) This strain was injected to make integrated lines with VCA-BFP and Lifeact-Dronpa.
VCA-BFP	JUP64 unc-119(ed3) III; curIs20 [Pzmp-1-pes10::TagBFP:: VCA(WASP) + unc-119(+)]
VCA+ Lifeact-GFP	JUP84 (JUP64 injected with Lifeact-GFP) unc-119(ed3) III; curIs20 [Pzmp-1-pes10::TagBFP:: VCA(WASP) + unc-119(+)]; curEx21 [Pcdh-3 ::Lifeact::GFP + Pmyo2::mCherry]
Endogenous WSP-1-GFP; WVE-1-RFP	GOU2062 (from Guangshuo Ou) cas762[TagRFP::wve-1a knock-in] I; cas723[GFP::wsp-1a knock-in] IV
Endogenous WSP-1-GFP and WVE-1-RFP + Lifeact-BFP	GOU2062 injected with Lifeact-BFP cas762[TagRFP::wve-1a knock-in] I; cas723[GFP::wsp-1a knock-in] IV; curEx22 [Pcdh-3::Lifeact::tagBFP] + Pmyo-2::mCherry]
mig-2	CF162 (from the CGC) mig-2(mu28) X
ced-10	LE1012 (from the CGC) ced-10(tm597)/dpy-13(e184) IV
cdc-42	VC898 (from the CGC) cdc-42(gk388)/mIn1 [mIs14 dpy-10(e128)] II

frl-1	RB696 (from the CGC) Y48G9A.4(ok460) III
fhod-1	fhod-1(tm2363) (from National BioResource Project)
cyk-1	VC1895 (from the CGC) cyk-1(ok2300)/mT1 [dpy-10(e128)] III
daam-1	daam-1(tm2133) (from National BioResource Project)
inft-2	RB1280 (from the CGC) F15B9.4(ok1296) V/nT1 [qIs51] (IV;V)
exc-6 (a.k.a. inft-1)	NJ833 (from the CGC) exc-6(rh103) III
Triple formin mutant cyk-1, inft-2, exc-6	GS7960 (from Daniel Shaye, Univeristy of Illinois) cyk-1(or596ts) exc-6(gk386); inft-2(ok1296); arIs198
α-actinin mutant	RB1812 (from the CGC) atn-1(ok84) V
plastin mutant	plst-1(tm4255) IV (from National BioResource Project)
filamin mutant	fln-1 (tm545) IV (from National BioResource Project)
double mutant	JUP80 (RB1812 crossed with plst-1 (tm4255)) atn-1(ok84) V ; plst-1(tm4255) IV
UNC-40-GFP	NK389 (from David Sherwood, Duke University) qyIs67 [Pcdh-3::UNC-40::GFP + unc-119(+)]
PIP2-mCherry	NK1588 (from David Sherwood, Duke University) qyIs108 [Plam-1::lam-1::dendra + unc-119(+)]; qyIs23[Pcdh-3::mCherry:: PLCδ^{PH} + unc-119(+)]
ZMP-1-GFP	NK1123 (from David Sherwood, Duke University) qyEx260 [Pzmp-1::GFP::ZMP-1-GPI]
CHAPTER 5	
Lifeact-DRONPA	JUP72 unc-119(ed3) III; curIs23 [Pcdh-3::Lifeact::Dronpa-M159T + unc-119(+)]
CHAPTER 6	
MMP- strain used for RNAi	NK1267 (from David Sherwood, Duke University) zmp-1(cg115); zmp-3(tm3482); zmp-4(tm3078); zmp-6(tm3073); zmp-5(tm3209); qyls108 [Plam-1::lam-1::dendra + unc-119(+)]; qyIs23[Pcdh-3 ::mCherry:: PLCδ^{PH} + unc-119(+)]
WT control for MMP- RNAi experiments	NK1588 (from David Sherwood, Duke University) qyls108 [Plam-1::lam-1::dendra + unc-119(+)]; qyIs23[Pcdh-3 ::mCherry:: PLCδ^{PH} + unc-119(+)]
(MMP-) + LifeACT-BFP, cortex measurements	JUP63 (NK1267 injected with Lifeact-BFP) zmp-1(cg115); zmp-3(tm3482); zmp-4(tm3078); zmp-6(tm3073); zmp-5(tm3209); qyls108 [Plam-1::lam-1::dendra + unc-119(+)]; qyIs23[Pcdh-3 ::mCherry:: PLCδ^{PH} + unc-119(+)]; curEx24 [Pcdh-3::Lifeact::tagBFP + Pmyo2::mCherry]
WT control for MMP- cortex measurements	JUP62 (NK1588 injected with Lifeact-BFP) qyls108 [Plam-1::lam-1::dendra + unc-119(+)]; qyIs23[Pcdh-3 ::mCherry:: PLCδ^{PH} + unc-119(+)]; curEx25 [Pcdh-3::Lifeact::tagBFP + rol-6(su1006) + Pmyo2::mCherry]
MRCK-GFP	ML1602 (from Michel Labouesse, UPMC) mrck-1(ok586) unc-42(e270); mcEx551[Pmrck::MRCK-1::GFP + pCFJ90 (Pmyo-2-mCherry)

3.3 CONSTRUCTS

pCFJ150-Pzmp-1-pes10::tagBFP::VCA(WASP)

tagBFP was from plasmid pBS Plam-1::BFP-3'UTR; unc-119 from David Sherwood.

VCA was amplified from a cDNA clone of *C. elegans* WASP starting at Gly1477 and going to the stop codon. BFP was fused with VCA as an N-terminal tag and then recombined into Gateway cloning vector pDONR221. The promoter sequence Pzmp-1 and the enchancer element pes-10 were amplified from pBS-zmp-1p-pes-10-spGFP1-10 from David Sherwood as done in (Hagedorn et al., 2009), and introduced into Gateway cloning vector pDONR[P4-P1R]. The entry vectors were recombined along with the unc-54 3′UTR (gift of G. Seydoux; Addgene plasmid #17253: pCM5.37) into the destination vector pCFJ150 - pDESTttTi5605[R4-R3] (gift from Erik Jorgensen Addgene plasmid # 19329).

pCFJ150-Pcdh-3::Lifeact::GFP

The cdh-3 promoter was amplified as in (Ziel et al., 2009) and introduced into Gateway cloning vector pDONR[P4-P1R]. Lifeact::GFP was from (Havrylenko et al., 2015). The fragments were recombined as above with unc-54 UTR and pCFJ150.

pCFJ150-Pcdh-3::Lifeact::tagBFP

As above except Lifeact was fused to tagBFP.

pCFJ150-Pcdh-3::Lifeact::Dronpa-M159T

Lifeact and linker as in (Havrylenko et al., 2015) was synthesized in frame with DronpaM159T. The Dronpa sequence was obtained by taking the mammalian sequence and adapting it for *C. elegans* codon usage and by putting in syntrons using the website http://worm-srv3.mpi-cbg.de/codons/cgi-bin/optimize.py. The gene was the synthesized by Eurofins Genomics.

CHAPTER 4: THE ROLE OF ACTIN POLYMERIZATION NUCLEATORS AND CROSSLINKERS IN ANCHOR CELL INVASION

4.1 GOAL OF THE STUDY

As described in the previous chapters, most studies on cell invasion are performed in vitro using cancer cells plated on or seeded in BM mimics where native mechanical and geometrical properties of the BM are not entirely respected. These are important factors for most cell biology questions: for example a 10-fold difference in substrate elasticity is enough to change the fate of a mesenchymal stem cell from a brain cell to a muscle cell (Engler et al., 2006). However lack of preservation of the mechanical microenvironment is particularly problematic for actin cytoskeleton studies where changes in ECM properties and geometry have been shown to change the dynamics and biochemistry of actin-based structures (Fraley et al., 2010; Geraldo et al., 2012; Petrie et al., 2012). Using AC invasion as a model allows us to study the role of the actin cytoskeleton in an invasive process in a native 3D environment. Specifically during this part of my PhD, I sought to address the role of the Arp2/3 complex and the relative contributions of its two activators, WAVE and WASP, in an invasive process, if formins played a role and if the invasive protrusion required actin cross-linkers to increase its mechanical stability. In all this my overall hypothesis was that actin polymerization creates forces that help break open the BM and push it aside, and does not just play a structural or trafficking role as has been suggested by some studies (Yu et al., 2012).

4.2 THE ARP2/3 COMPLEX AND ITS ACTIVATORS DURING AC INVASION

As mentioned in **Chapter 2**, WSP-1/WASP plays a role during AC invasion, along with its upstream effector CDC-42/Cdc-42 (Lohmer et al., 2016). Also the Rac GTPases CED-10 and MIG-2 are found at the invasive front of the AC (Ziel et al., 2009), suggesting the involvement of WAV-1/WAVE and WSP-1/WASP. The involvement of its activators pointed toward the Arp2/3 complex as a nucleator for actin polymerization in AC invasion, but this had not been proven. Likewise how the loss of WSP-1/WASP and WAV-1/WAVE affected the formation of the invasive protrusion had not been quantified.

4.2.1 THE EFFECT OF REDUCTION OF ARP2/3 COMPLEX AND WASP ON AC INVASION

The components of the Arp2/3 complex are essential genes, so worms completely lacking Arp2/3 complex function are not available. I therefore used RNAi knockdown followed by scoring of invasion to evaluate the role of the Arp2/3 complex in AC invasion. This is an approach that I used extensively during this and other sections, and involves performing RNAi by feeding (see **Chapter 3**) and then evaluating invasion at the 4-cell stage (see **Chapter 2, Section 2.4**). At this stage in WT worms, 100% of ACs had cleared a large opening in the BM. At the 4-cell stage, I grouped my observations into 3 categories: 1) the hole in the BM was as wide as the AC, this was "full invasion"; 2) a defect in the BM was detectable, but the hole was not as wide as the AC, this was "partial invasion"; 3) there was no break in the BM, this was "no invasion". **Figure 4.1** gives an example of the 3 categories with coupled DIC and fluorescent images of BM and AC actin. This shows that BM openings can be seen by DIC microscopy, and in fact, all of the scoring after RNAi treatments in this and other sections was performed using DIC images**.**

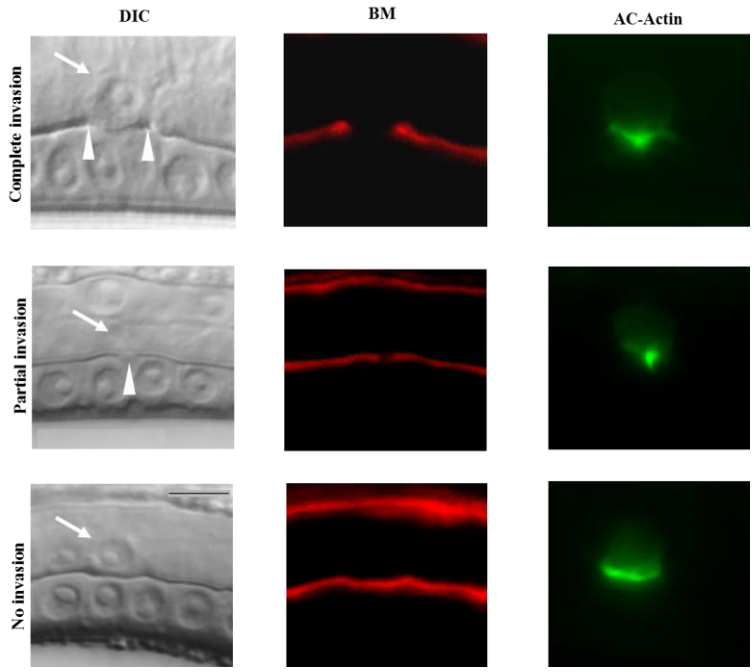

Figure 4.1 Images of complete, partial and no invasion at the 4-cell stage. The 4 nuclei are visible in the cells directly beneath the AC, indicated by a white arrow. Invasion was evaluated by examining DIC images (left), where a break in the contrasted line of the BM indicated invasion (marked by white arrowheads). Corresponding epifluorescent images are of laminin::mCherry under the native promoter to visualize BM in the entire worm and Lifeact::GFP under an AC-specific promoter to visualize actin filaments in the AC only. Alleles *qyIs242* and *qyIs127*; see **Chapter 3**. Fluorescent images are shown for illustration, but scoring was done only on DIC images. Scale bar 5 µm.

When *arx-2*, the equivalent of the Arp2 subunit of the Arp2/3 complex, was knocked down, 30% of the worms showed a complete lack of a hole in the BM under the AC at the 4-cell stage **(Table 4.1)**. This indicated a role for the Arp2/3 complex in AC invasion, despite the known resistance of the Arp2/3 complex to RNAi due to its long-term stability (Wu et al., 2012; Zhu et al., 2016). This was in keeping with the reported role for WASP in AC invasion, a result that I reproduced, finding that only 23% of ACs had invaded at the 4-cell stage **(Table 4.1).** For this and in the following, I used a mutant worm that is a functional null for the sole copy of *C. elegans* WASP (Withee et al., 2004), strain NG324, genotype *wsp-1(gm324)*. This allele will be referred to as "WASP-deleted". WASP-deleted worms have low brood size, but are otherwise viable and fertile.

Table 4.1 The effect of Arp2/3 complex knock-down and WASP deletion on AC invasion.

	No invasion	Partial invasion	Full invasion
arx-2 RNAi[a]	30%	23%	47%
WASP-deleted worm[a]	64%	13%	23%
WASP-deleted worm (Lohmer et al., 2016)	54%	28%	18%

[a] N>30 worms were observed for each condition.

4.2.2 ACTIN DYNAMICS IN THE AC IN THE ABSENCE OF WASP

In order to characterize the effect of WASP deletion on actin dynamics during AC invasion, a worm strain was constructed that carried the *wsp-1(gm324)* and additionally expressed LifeAct::GFP under an AC-specific promoter and laminin::mCherry to visualize BM, as for **(Figure 4.1).** Typical still images of F-actin and BM in WT and WASP-deleted worms at the 2-cell, 4-cell and invagination stages are shown in **Figure 4.2**. The defect in invasion quantified in **Table 4.1** by DIC is clearly visible by fluorescence: at the 4-cell stage where the WT AC has invaded, the WASP-deleted AC has not. This is not a complete block, however, and by the invagination stage, WT and WASP-deleted ACs look fairly similar.

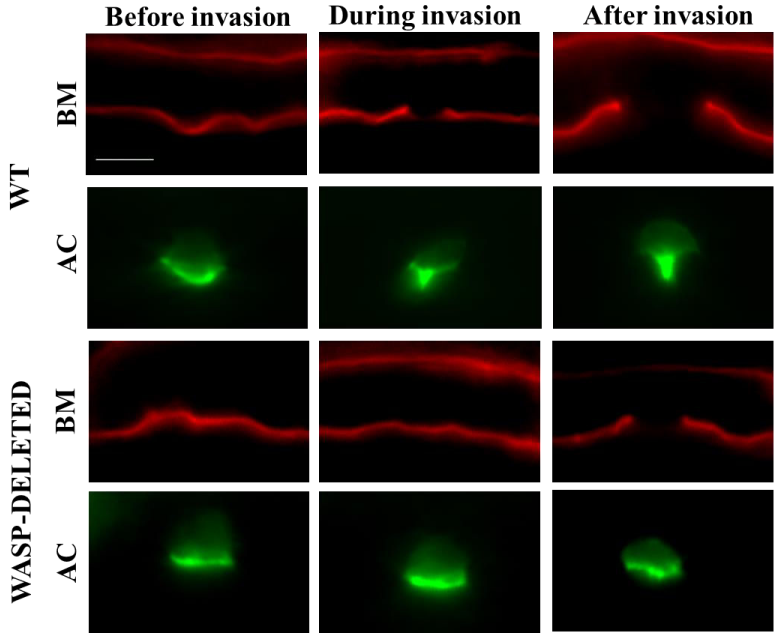

Figure 4.2 WT and WASP-deleted AC invasion. Representative epifluorescence images of the AC (Lifeact::GFP) and BM (laminin::mCherry) before, during and after invasion in WT and WASP-deleted worm. Alleles *wsp-1(gm324)*, *qyIs242* and *qyIs127*; see **Chapter 3**. Scale bar 5 µm.

Already from these still images by epifluorescence microscopy, differences in protrusion morphology were evident, so I decided to quantify this further by time-lapse spinning disk microscopy. F-actin dynamics in the AC were imaged over time, generally from the late 2-cell stage to the late 4-cell stage for WT, fully covering the invasive process, and from the 4-cell stage when invasion should have occurred until invagination started for WASP-deleted worms. **Figure 4.3** shows a representative series of maximum intensity projections of F-actin images from the time-lapse acquisition for WT and WASP-deleted worms. This is an extract and does not represent an entire acquisition.

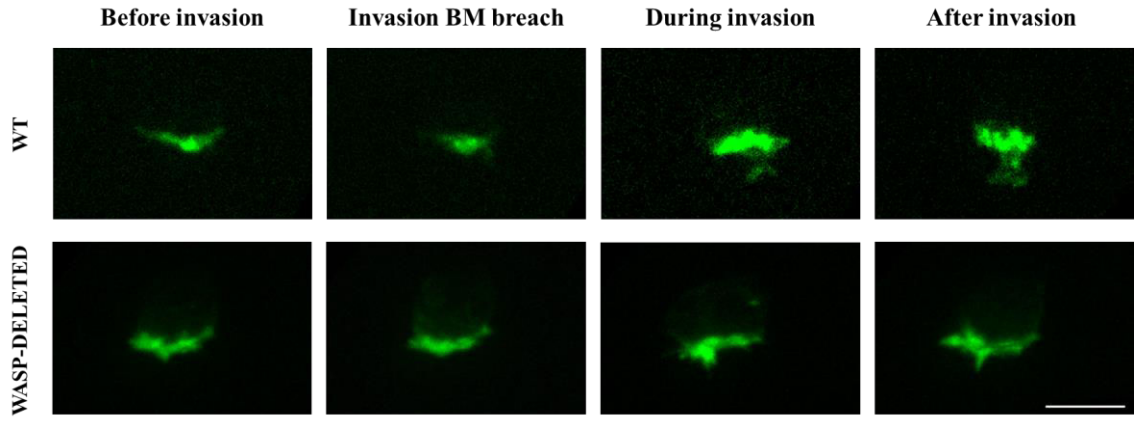

Figure 4.3 Protrusion growth. Representative maximum intensity projections from spinning disk movies of the AC (Lifeact::GFP) over about 1 hour for WT (top panels) and WASP-deleted (bottom panels). WT images are from before invasion, just at the moment of BM breach, during and after invasion, and WASP-deleted images are taken over about an hour from the 4-cell stage when the AC should have invaded. Alleles *wsp-1(gm324)* and *qyIs242*; see **Chapter 3**. Scale bar 5 µm.

To quantify differences the area of the maximum intensity projection of the actin protrusion at each time point was measured and plotted over time. WT worms showed an expansion of the protrusion over time during invasion attaining an average maximum area of 10 μm^2 while the WASP-deleted worms showed a smaller protrusion that did not grow over time but remained at a constant area of 5 μm^2 **(Figure 4.4).**

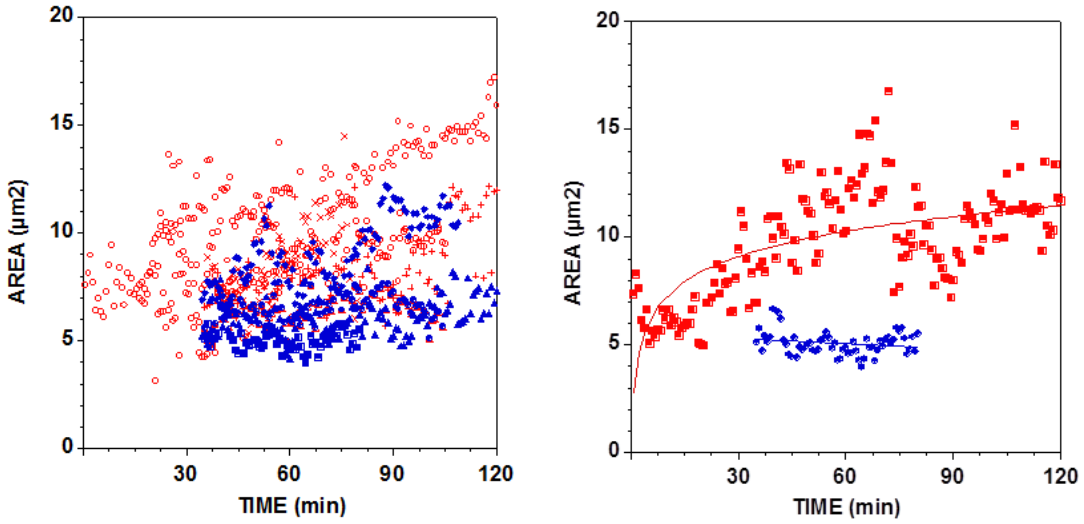

Figure 4.4 Analysis of the size of the AC protrusion over the time course of invasion. Left: plot of the area of the actin-filled protrusion in WT worms (red, N=6) and WASP-deleted worms (blue, N=6). All WT traces were aligned so that invasion started at about 30 minutes, and WASP-deleted traces were placed at 30 minutes as well. The cloud of blue points is lower than the cloud of red points. Right: plot of the time course of a single representative cell taken from the previous plot. The red and blue lines are guides to the eyes.

Next the dynamics of the protrusion were evaluated by comparing consecutive frames of time-lapse movies, and calculating the amount of unshared area between consecutive frames **(Figure 4.5)**. WT protrusions were more dynamic and displayed shape changes between consecutive frames during invasion of around 3 μm^2 while WASP-deleted protrusions fluctuated less, with an average shape change between frames of only about 1 μm^2 **(Figure 4.5).** Overall from this analysis I concluded that the WASP-deleted worms displayed an actin protrusion in the AC during invasion that was not only smaller but less dynamic than in WT worms, pointing to a role for WASP in the formation and dynamics of filamentous actin in the invasive protrusion.

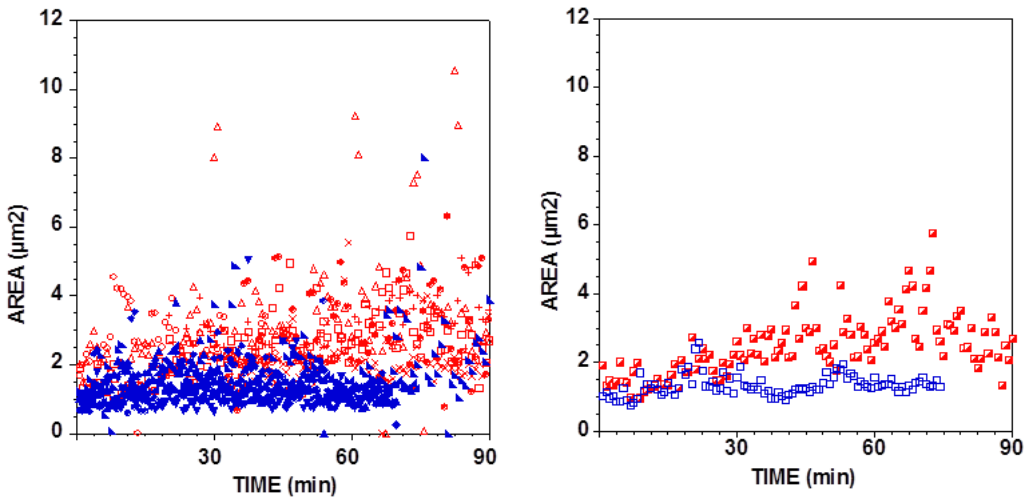

Figure 4.5 AC protrusion dynamics during invasion. Left: the area of unshared regions between consecutive time points was plotted for WT worms (red N=6) and WASP-deleted worms (blue N=6). The cloud of red points is clustered around 3 μm^2, while the blue points cluster around 1 μm^2. The traces are shorter than in **Figure 4.4** because only post-BM breach points were considered for WT. Right: plot of shape changes of a single representative invasive event taken from the previous plot.

4.2.3 AC INVASION IN THE ABSENCE OF WAVE

In the case of WASP deletion, the protrusion was not entirely absent. Indeed WASP-deleted worms were still able to invade, but with a 40 minute delay as compared to the normal developmental program, suggesting that another component assured invasion in the absence of WSP-1/WASP. A possible candidate was the other Arp2/3 complex activator, WVE-1/WAVE.

To evaluate the contribution of WVE-1/WAVE to AC invasion, I measured the size of the F-actin protrusion of the AC of worms treated with *wve-1* RNAi. The protrusion was slightly, but significantly, smaller than WT, about 8 μm^2 as opposed to 10 μm^2 at the 4-cell stage of invasion **(Figure 4.6).**

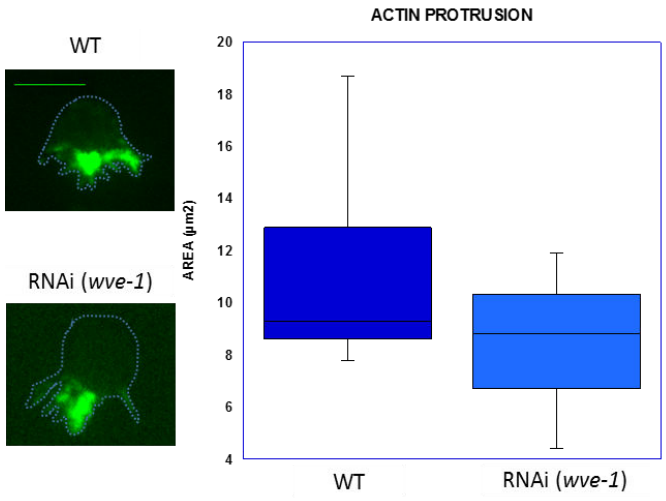

Figure 4.6 Area of the actin-rich protrusion from maximum intensity projections. WT animals and worms treated with RNAi against *wve-1*. N ≥ 6. The difference is small but significant ($p < 0.098$). The dotted line shows the perimeter of the AC. Alleles *wsp-1(gm324)* and *qyIs127*; see **Chapter 3**. Scale bar 5 µm.

In order to probe further the role of WVE-1/WAVE in AC invasion, invasion was scored in different mutant and RNAi backgrounds at the 4-cell stage by DIC microscopy as described above. First a WAVE-deleted worm was evaluated, strain OX308, genotype *wve-1(ne350)*, which contains an early stop codon giving non-functional protein (Patel et al., 2008). The WVE-1/WAVE deletion is embryonic lethal so this worm strain was maintained as a heterozygote. Homozygotic WAVE-deleted larval worms were isolated for the analysis and further treated with RNAi targeting *wve-1* to eliminate maternally contributed WVE-1/WAVE as much as possible. As compared to an RNAi control, WAVE-deleted worms treated with *wve-1* RNAi showed no significant reduction in invasion efficiency and almost 100% of the animals showed full invasion at the 4-cell stage **(Figure 4.7).**

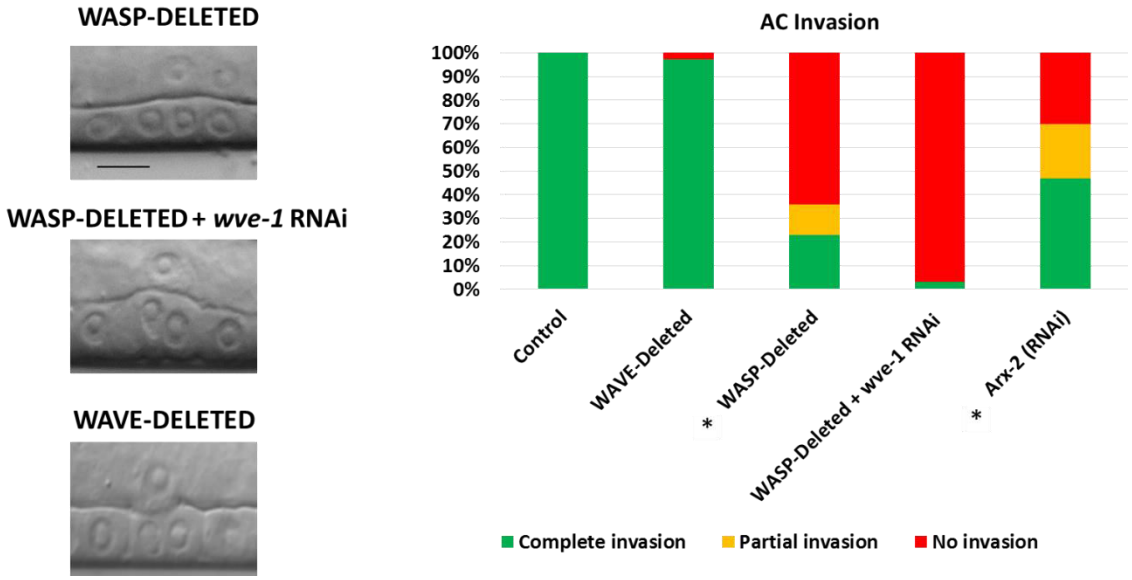

Figure 4.7 AC invasion upon WVE-1/WAVE and WSP-1/WASP disruption. Left: representative DIC images of the major phenotype observed in the indicated conditions. Right: score of AC invasion in different mutant and RNAi backgrounds. WASP-deleted and WAVE-deleted, alleles *wsp-1(gm324)* and *wve-1(ne350)*; see **Chapter 3**. N>40. Scale bar 5µm. *Same data as shown in **Table 4.1**, represented here for comparison.

These worms then produced mostly dead eggs indicating that indeed the worms were carrying low levels of WVE-1/WAVE. As mentioned previously, WASP-deleted worms displayed only 20% invasion at the 4-cell stage. This was reduced to 3% invasion when the WASP-deleted worms were treated with RNAi targeting *wve-1* **(Figure 4.7).** These results strongly suggested that AC invasion was dependent on Arp2/3 complex-driven actin polymerization downstream of both WSP-1/WASP and WVE-1/WAVE activation. The WASP/WAVE double perturbation was stronger than RNAi against the Arp2/3 complex itself **(Figure 4.7)**, probably due to low RNAi efficiency against the Arp2/3 complex as mentioned above.

4.2.4 Dominant negative inhibition of Arp2/3 complex activity

To get around this limitation, we employed a dominant negative approach to inhibit the Arp2/3 complex that had been shown to be effective in mammalian cells (Machesky and Insall, 1998) **(Figure 4.8)**. This consisted in expressing under control of an AC-specific promoter the VCA domain of WASP, the part of WASP that binds and activates the Arp2/3 complex. The cytosolic expression of VCA sequesters the Arp2/3 complex in the cytosol away from its normal membrane localization and thus acts as a dominant negative without disturbing other known pathways for actin polymerization that are Arp2/3 complex-independent (Koestler et al., 2013).

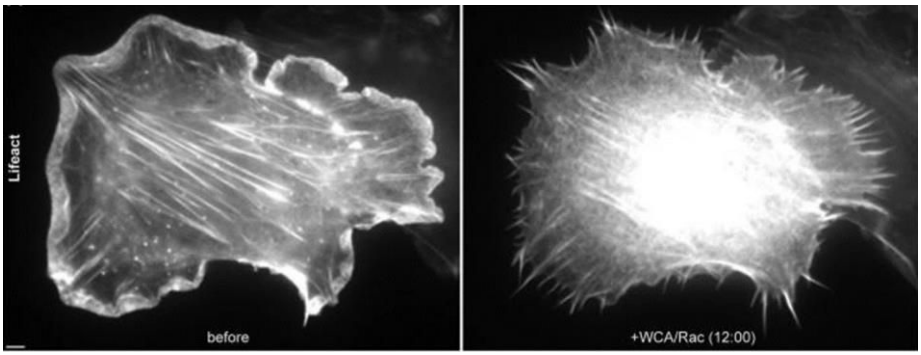

Figure 4.8: Effect of VCA treatment in mammalian cells. Left: untreated cell. Right: the same cell microinjected with purified VCA. Lamellipodial actin networks are diminished by the treatment, but non-Arp2/3 complex-dependent structures like stress fibers and filopodia increase. NIH3T3 cells; actin structures are labeled with fluorescent Lifeact. Scale bar 3 µm. Adapted from (Koestler et al., 2013)

Expression of VCA in the AC completely blocked invasion at the 4-cell stage (0% invasion, N=30), and F-actin was distributed throughout the cell instead of being concentrated predominantly in the protrusion as observed for WT (**Figure 4.9**).

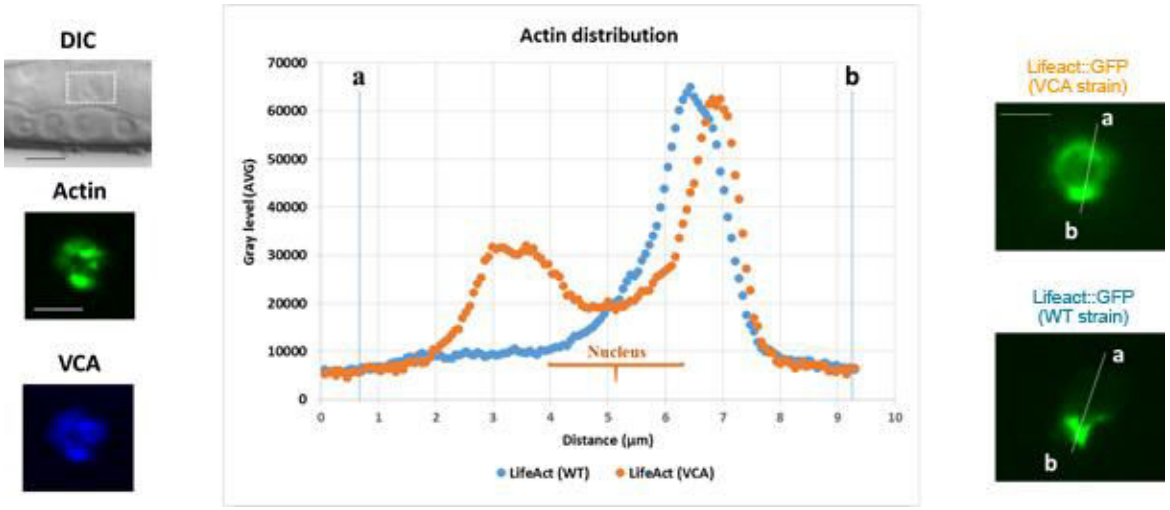

Figure 4.9 Effect of VCA expression on AC invasion, 4-cell stage. Left: representative images of a VCA-expressing AC. The boxed region in the DIC is shown in the green and blue channels, single plane spinning disk images. F-actin is visualized with Lifeact::GFP and VCA is labeled with tagBFP. Middle and right: actin distribution line scan for WT (blue curve) and VCA strain (orange curve) for the images shown on the right. Alleles *curIs20* and *curEx21*; see **Chapter 3**. Spinning disk microscopy addition projection image. Scale bars 5µm.

Indeed even at later stages of vulval morphogenesis, the BM remained intact in 90% of the VCA-expressing worms (**Figure 4.10**), the vulva did not form properly, and worms "bagged", that is eggs hatched inside the mothers instead of being laid. We concluded from these results that AC invasion is very strongly dependent on Arp2/3 complex-based actin nucleation, and except for rare events, AC invasion does not occur when the Arp2/3 complex at the invasive leading edge is completely turned off.

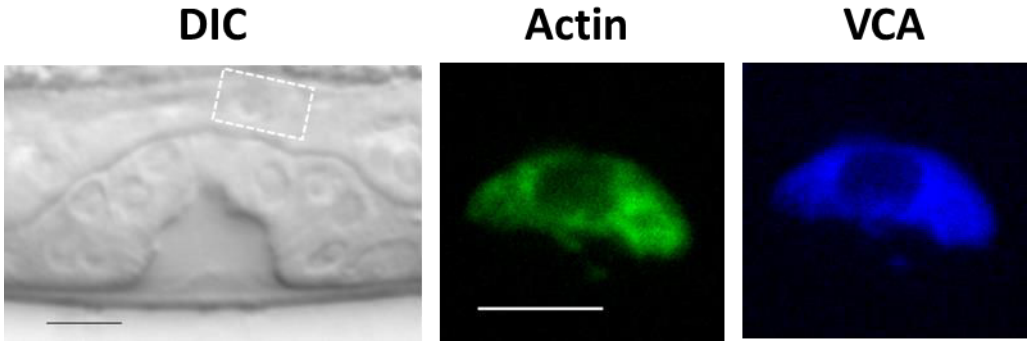

Figure 4.10 Effect of VCA expression on AC invasion, late stage. Left: the unbroken line of the BM in DIC indicates a full block of invasion. Middle and right: the boxed region in the DIC is shown in the green channel (LifeACT::GFP) and blue channel (VCA::tagBFP). Spinning disk microscopy. Maximum intensity projection. Alleles *curIs20* and *curEx21*; see **Chapter 3**. Scale bars 5µm.

4.2.5 Interplay of WASP and WAVE for AC invasion

As mentioned above, invasion driven by Arp2/3 complex-based polymerization still happened in WASP-deleted worms seemingly due to the presence of WVE-1/WAVE. In order to provide evidence for this, I examined where endogenous WSP-1/WASP and WVE-1/WAVE were localized during AC invasion, using a worm strain carrying GFP-labeled WSP-1/WASP and RFP-labeled WVE-1/WAVE, produced via genome modification by CRISPR (courtesy of the Guangshuo Ou laboratory, alleles *cas723* and *cas762*, respectively (Zhu et al., 2016)). In this background, we introduced Lifeact::tagBFP to visualize where WVE-1/WAVE and WSP-1/WASP were in relation to the actin cytoskeleton during AC invasion.

We observed that WSP-1/WASP was present in the AC before (2-cell stage) and after (4-cell stage) invasion, and also present at cell junctions in the vulval and uterine tissue, while WVE-1/WAVE, although faint in the vulva and uterine tissue, was more expressed at the leading edge of the invading AC **(Figure 4.11)**. To measure the co-localization of WSP-1/WASP, WVE-1/WAVE and actin in the AC protrusion, linescans were drawn along the leading edge of the protrusion and the fluorescence of actin, WVE-1/WAVE and WSP-1/WASP were measured. This analysis was performed before and after invasion, and showed that WVE-1/WAVE was co-localized with WSP-1/WASP in the actin-rich protrusion at both stages **(Figure 4.11).** This analysis showed that WVE-1/WAVE was present in the right place and at the right time to contribute to the formation of the invasive protrusion, and explained how the protrusion could still form in the absence of WSP-1/WASP.

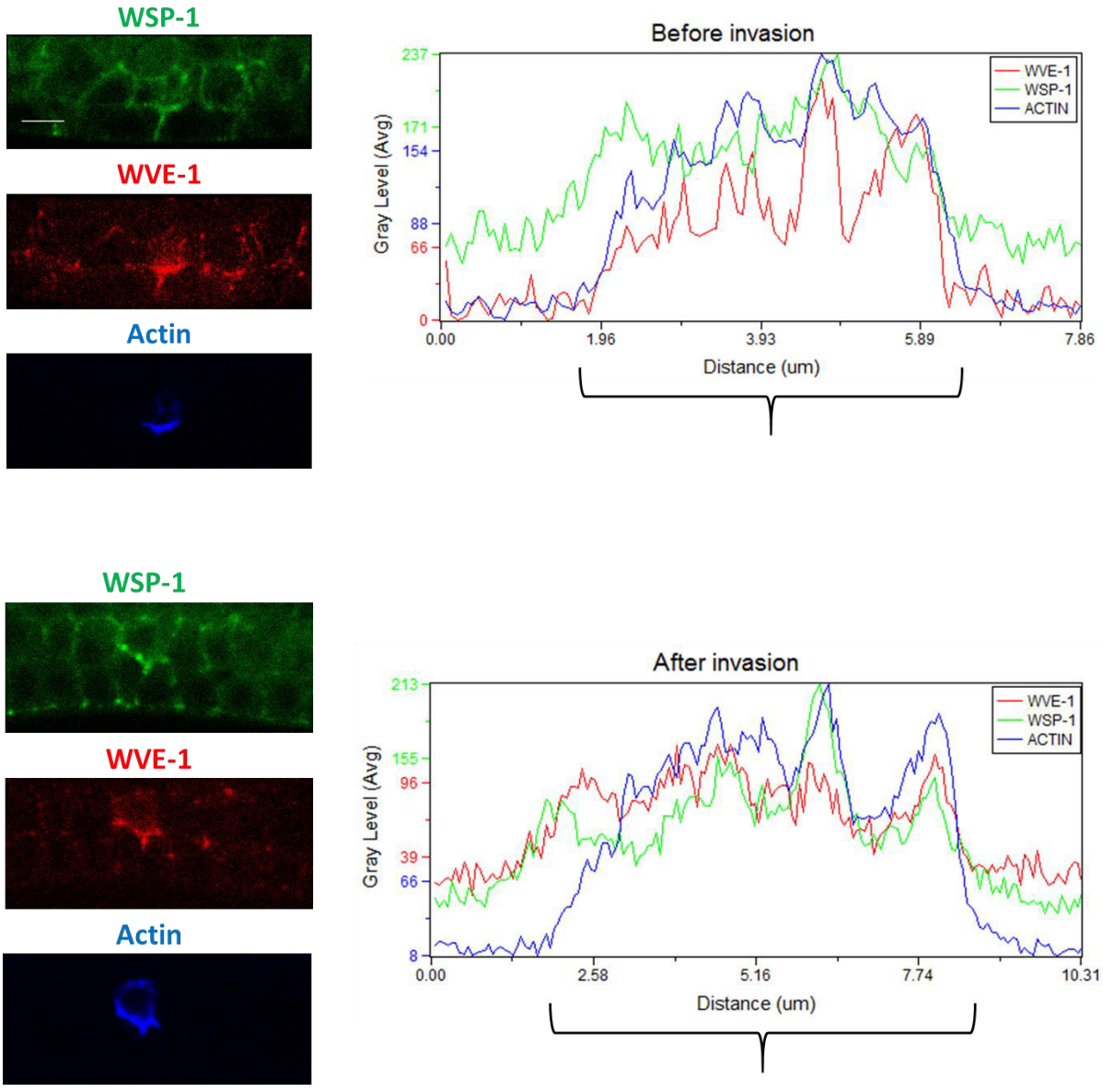

Figure 4.11 Localization of WASP and WAVE in relation to actin in the invading AC. Left: images of the AC before (top panels) and after (bottom panels) invasion. Actin in the AC labeled by LifeAct::tagBFP and WVE-1::RFP and WSP-1::GFP are shown. Right: linescans were drawn along the protruding edge of the AC. The borders of the AC are marked with a bracket on the linescans. Alleles *cas762*, *cas723*, *curEx22*; see **Chapter 3**. Scale bar 5µm.

4.2.6 Relative roles of WASP and WAVE in AC invasion

WVE-1/WAVE played a minor role in AC invasion as compared to WSP-1/WAVE despite their similar function of activating the Arp2/3 complex for branched actin polymerization nucleation. The upstream activators of WVE-1/WAVE have been shown to be present at the invasive front (Ziel et al., 2009), in keeping with my observed localization analysis above, so it was not clear why there was such an unequal contribution to invasion of the two Arp2/3 complex activators. One possibility was a reduced efficiency of WVE-1/WVE to activate the Arp2/3 complex in comparison to WSP-1/WAVE to form a branched protrusion able to push

aside the BM. Mammalian WAVEs are known to be less active than mammalian WASP molecules due to differences in acidity of the C-terminal, Arp2/3 complex-binding domain (Zalevsky et al., 2001b). To see if this was likewise the case with *C. elegans* WASP and WAVE, a pyrene-actin assay was performed using the purified VCA domains from *C. elegans* WSP-1/WASP and WVE-1/WAVE in presence of the Arp2/3 complex. A pyrene assay is a spectroscopic method to evaluate the speed of formation of actin filaments over time, and more efficient Arp2/3 complex activation gives steeper polymerization curves (Doolittle et al., 2013).

Representative polymerization curves for WSP-1/WASP and WVE-1/WAVE are shown in **Figure 4.12**. Both drastically increased the amount of filamentous actin formed over the no addition control, but WSP-1/WASP was 40% faster reaching the plateau than WVE-1/WAVE at identical concentration. Applying some assumptions, the number of filament barbed ends can be roughly calculated using the slopes at half-maximum of such polymerization curves (Higgs et al., 1999). The number of barbed ends formed by each activator in the presence of Arp2/3 complex as a function of concentration showed that WSP-1/WASP created 40% more barbed ends **(Figure 4.12)**. This difference could explain why WVE-1/WAVE plays a less important role in AC invasion as compared to WSP-1/WASP.

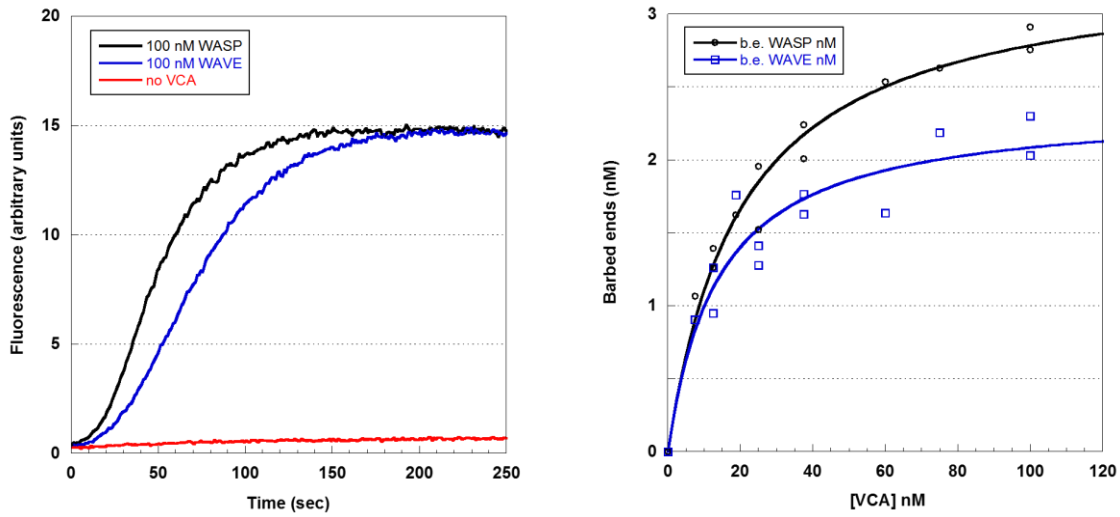

Figure 4.12 Pyrene assay comparison of WSP-1/WASP and WVE-1/WAVE activity.
Left: pyrene actin curves 4 µM actin, 12 µM profilin, 50 nM Arp2/3 complex. Red is no VCA addition, blue is 100 nM VCA(WVE-1) addition, and black is 100 nM VCA(WSP-1) addition. WSP-1 gets to the plateau faster than WVE-1. Right: amount of barbed ends (nM) formed by VCA activation of Arp2/3 complex at different VCA concentrations. The data was fit to a saturation curve (Michaelis-Menten) to get the plateau. Plateau for WSP-1 is 3.4 ± 0.1 nM and for WVE-1 2.4 ± 0.2 nM.

4.2.7 LOCALIZATION OF INVASIVE COMPONENTS UPON WASP DELETION

Given the known role of WASP in endocytosis and in protease delivery in invadopodia (Campellone and Welch, 2010; Yu et al., 2012), it was possible that the effect of WASP deletion on invasion was related to a defect in trafficking of invasive components to the leading edge.

In order to test this idea I knocked down *wsp-1* by RNAi and measured the localization of fluorescently labeled UNC-40/DCC, the metalloprotease ZMP-1 and a marker for PI(4,5)P2, components known to be involved in AC invasion and enriched at the invasive membrane (see **Chapter 2**). Enrichment was quantified by dividing the mean intensity of the invasive membrane by the mean intensity of the apical and lateral membranes (the non-invasive membranes) using a single plane where the lateral, apical and invasive membranes were most visible. As shown in **Figure 4.13**, in WT worms, all 3 components were enriched by a factor of 2-3 in the invasive membrane as compared to the non-invasive membrane, and there was no significant difference ($p < 0.9$) in polarization in WT worms as compared to those blocked by *wsp-1* RNAi.

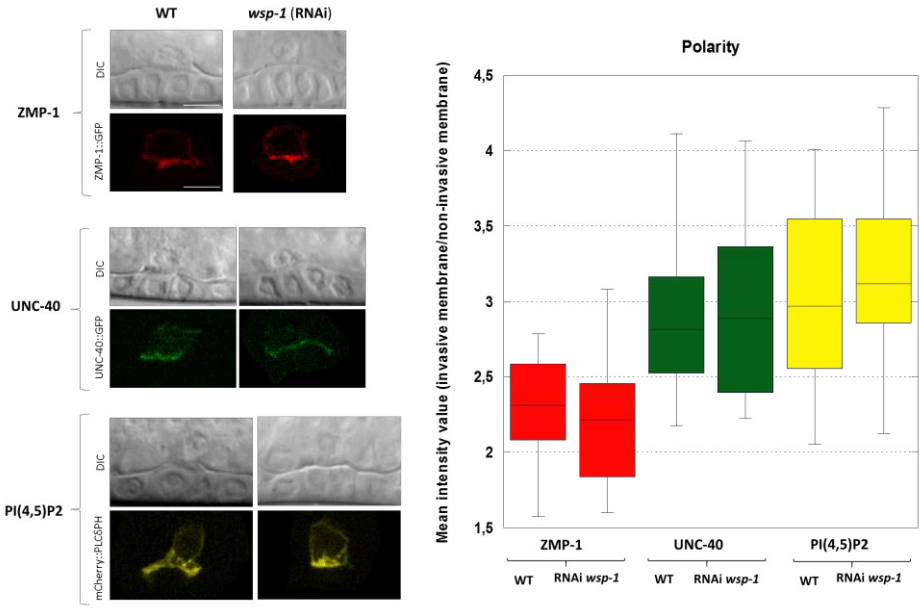

Figure 4.13 *wsp-1* RNAi effect on the polarity of key invasive components ZMP-1, UNC-40 and PI(4,5)P2. Left: representative images of a single plane by DIC and fluorescence in WT and *wsp-1*RNAi treated animals. Right: quantification of enrichment/polarity as described in the text. N>12. Alleles *qyEx260*, *qyIs67* and *qyIs108*; see **Chapter 3**. Scale bar 5µm.

This data confirmed that WASP deletion was not affecting localization, and presumably trafficking, of essential components to the invasive edge. This supported the idea that the branched actin network made by WASP was not playing a passive scaffolding role, but was actively driving the invasive process by applying forces on the BM.

4.3 ROLES OF UPSTREAM REGULATORS OF WASP AND WAVE IN AC INVASION

Despite its reduced activity, WVE-1/WAVE appeared to "stand in" for WSP-1/WASP to ensure AC invasion, albeit with a smaller, less dynamic protrusion and a corresponding delay in BM invasion. If WSP-1/WASP and WVE-1/WAVE were working together in this way, this should be reflected in the upstream regulatory pathways involving GTPases. In *C. elegans*, WASP is known to be regulated by both CDC-42/Cdc-42 and MIG-2/Rac, while WVE-1/WAVE is activated by the CED-10/Rac (Walck-Shannon et al., 2015). We therefore set out to probe the role of these upstream regulators, in order to lend evidence to the idea that there were two independent pathways for activating the Arp2/3 complex for AC invasion.

Interfering with the GTPase regulators individually gave little or no invasion defect: RNAi against *cdc-42* gave a slight defect (14% no invasion) (Lohmer et al., 2016), *mig-2* mutant worms had 100% normal invasion (Ziel et al., 2009) and *ced-10* mutant worms with *ced-10* RNAi to eliminate maternal contribution (it was a balanced strain) had 97% full invasion at the 4-cell stage. RNAi against *cdc-42* and *mig-2* in the WASP-deleted strain gave no additional effect above the 20% invasion already observed for WASP-deleted alone, confirming that CDC-42 and MIG-2 were in the same pathway as WSP-1/WASP **(Figure 4.14A and B)**. However when *ced-10* was knocked down in the WASP-deleted strain, full invasion decreased to 7%, very similar to what was obtained with RNAi against WVE-1/WAVE in the WASP-deleted background **(Figure 4.14A** and see **Figure 4.7)**.

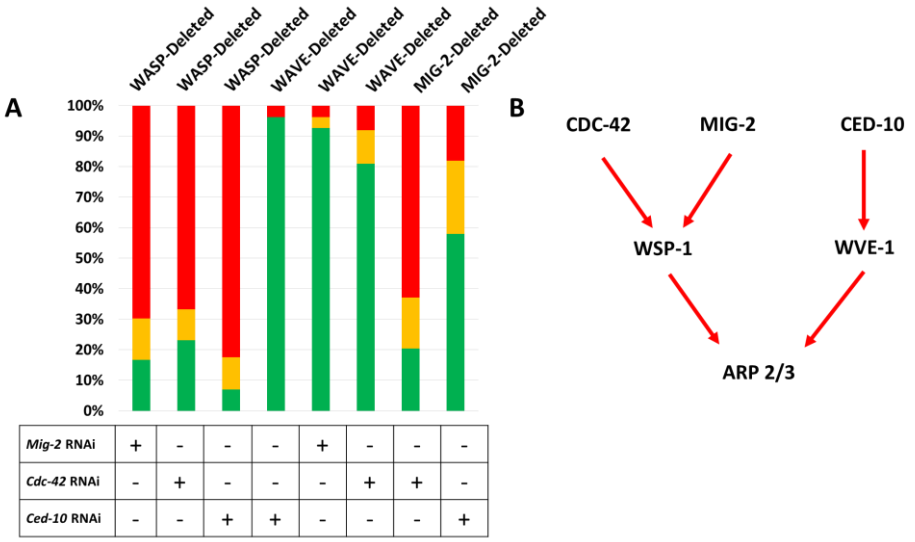

Figure 4.14 A) Evaluation of the role of RhoGTPases in relation to WSP-1/WASP and WVE-1/WAVE in AC invasion. Score of AC invasion after RNAi knock-down of *mig-2*, *cdc-42* and *ced-10* in WASP-deleted and WAVE-deleted worms, and of *cdc-42* and *ced-10* knock-down in MIG-2-deleted worms. Green is full invasion, yellow is partial and red is no invasion. N>40 for each condition. Alleles *wsp-1(gm324), wve-1(ne350)* and *mig-2(mu28)*; see **Chapter 3**. **B)** Regulatory pathways involving the RhoGTPases.

Conversely when *ced-10* was knocked down in the WAVE-deleted background, there was no reduction of invasion efficiency as compared to WVE-1/WAVE mutant alone (full invasion 96%). When the WSP-1/WASP regulators *mig-2* and *cdc-42* were knocked down separately in the WVE-1/WAVE null background, there was little effect on invasion (full invasion 92% and 83%, respectively), indicating that either one sufficed for WSP-1/WASP activation for invasion. Indeed when *cdc-42* was knocked down in a *mig-2*-deleted worm, this gave only 20% full invasion similar to that observed with the WASP-deleted worms **(Figure 4.14A)**. Compromising *mig-2* and *ced-10* pathways together gave a less severe invasion defect (58% full invasion). All together these results confirmed data obtained in **Section 4.2**: WSP-1/WASP, downstream of CDC-42/Cdc-42, was the principal pathway by which the Arp2/3 complex was activated in the AC. However MIG-2/Rac could assure almost WT levels of invasion in the absence of CDC-42/Cdc-42. On the other hand WVE-1/WAVE, downstream of CED-10/Rac, served as a backup, but could assure some invasion in the absence of the CDC-42/Cdc-42-MIG-2/Rac-WSP-1/WASP activation **(Figure 4.14B)**.

4.4 Role of formins in AC invasion

From the results of the dominant negative Arp2/3 complex activator study, it seemed unlikely that formins played a role in AC invasion. Indeed in studies on cells, when the Arp2/3 complex is inhibited by the VCA dominant negative approach or other methods, lamellipodia

collapse, but actin structures that are dependent on other nucleators such as formins become more pronounced (Koestler et al., 2013; Suraneni et al., 2012; Wu et al., 2012). The fact that the VCA-expressing AC did not display actin spikes or other structures was an indication that other nucleators, including formins, were not active in the AC, see **Figure 4.9** and **4.10**.

In order to confirm that formins were not playing a role, I evaluate the invasion for all 6 known *C. elegans* formin mutants separately, and also evaluated a triple formin mutant that included EXC-6, a formin strongly and specifically expressed in the AC (Matus et al., 2015). All of these animals showed WT invasion at the 4-cell stage **(Table 4.2)**. Perhaps EXC-6 is strongly expressed in the AC because it is needed in later stages of vulval morphogenesis, during lumen formation for example (Estes and Hanna-Rose, 2009). EXC-6 is known to be important for lumen formation during secretory canal development (Shaye and Greenwald, 2015). These RNAi results, together with the unspikey appearance of ACs treated with the VCA dominant negative, suggested that formins did not nucleate actin for AC invasion.

	AC Invasion		
FORMINS	**Complete Invasion**	**partial Invasion**	**No Invasion**
Control	100%	0%	0%
frl-1(ok460)	100%	0%	0%
fhod-1(tm2363)	100%	0%	0%
cyk-1(ok2300)	100%	0%	0%
daam-1(tm2133)	100%	0%	0%
inft-2(ok1296)	99%	1%	0%
exc-6(rh103)	99%	1%	0%
exc-6(rh103)+cyk-1(RNAi)	95%	5%	0%
cyk-1(or596ts),inft-2(ok1296),exc-6(gk386)	93%	3%	4%

Table 4.2 Evaluation of AC invasion in formin mutants. Formins were reduced by a combination of mutants (as specified) or RNAi (when indicated). CYK-1 is the equivalent of mammalian Dia, while EXC-6 and INFT-2 are similar to mammalian Inverted Formins INF proteins. FHOD and DAAM carry the same names as their mammalian counterparts. Score of AC invasion at the 4-cell stage by DIC microscopy. N>40 for each condition. Alleles as indicated in the table; see also **Chapter 3**.

4.5 ROLE OF ACTIN FILAMENT CROSSLINKERS IN AC INVASION

As mentioned previously, actin crosslinkers play important roles in the mechanics of actin structures in general, and the actin bundler fascin is key for invadopodia formation in particular (Schoumacher et al., 2010). In order to know if the actin crosslinkers were playing a role in AC cell invasion, I performed RNAi and evaluated mutants of the 3 main actin crosslinkers in the *C. elegans* genome: ATN-1/α-actinin, PLST-1/plastin (fimbrin) and FLN-

1/filamin. Mutations knocking out the activity of individual cross-linkers did not affect AC invasion **(Table 4.3)**. To bypass possible redundancy amongst crosslinkers, I constructed a strain that was mutant in ATN-1/α-actinin and PLST-1/plastin (fimbrin) and I further knocked down *fln-1* by RNAi in this background. These worms also displayed near WT levels of invasion **(Table 4.3)**. From this I concluded that crosslinkers were not essential for AC invasion. It has been shown that entanglement due to a high degree of branching can provide cohesion in an actin network despite the absence of crosslinkers (Achard et al., 2010; Dayel et al., 2009). Experiments using super-resolution microscopy **(Chapter 5)** indicated that the actin network in the AC protrusion was very dense, suggesting that additional crosslinking was unnecessary.

	AC Invasion		
CROSSLINLERKS	**Complete Invasion**	**partial Invasion**	**No Invasion**
atn-1(ok84)	100%	0%	0%
plst-1(tm4255)	100%	0%	0%
fln-1 (tm545)	91%	7%	2%
atn-1(ok84) ; plst-1(tm4255)+fln-1 (RNAi)	96%	4%	0%

Table 4.3 Evaluation of AC invasion in the absence of crosslinkers. Crosslinkers were reduced by a combination of mutants (as specified) or RNAi (when indicated). ATN-1 is α-actinin, PLST-1 is plastin/fimbrin and FLN-1 is filamin. Score of AC invasion at the 4-cell stage by DIC microscopy. N>40 for each condition. Alleles as indicated in the table; see also **Chapter 3**.

4.6 CONCLUSION: WASP AND WAVE ACTIVATE THE ARP2/3 COMPLEX FOR BM INVASION

I show that AC invasion is almost exclusively driven by the Arp2/3 complex, which is activated at the invasive membrane by both WSP-1/WASP and WVE-1/WAVE working together. WSP-1/WASP is the main contributor since it is a more efficient activator of the Arp2/3 complex than WVE-1/WAVE **(Figure 4.15)**.

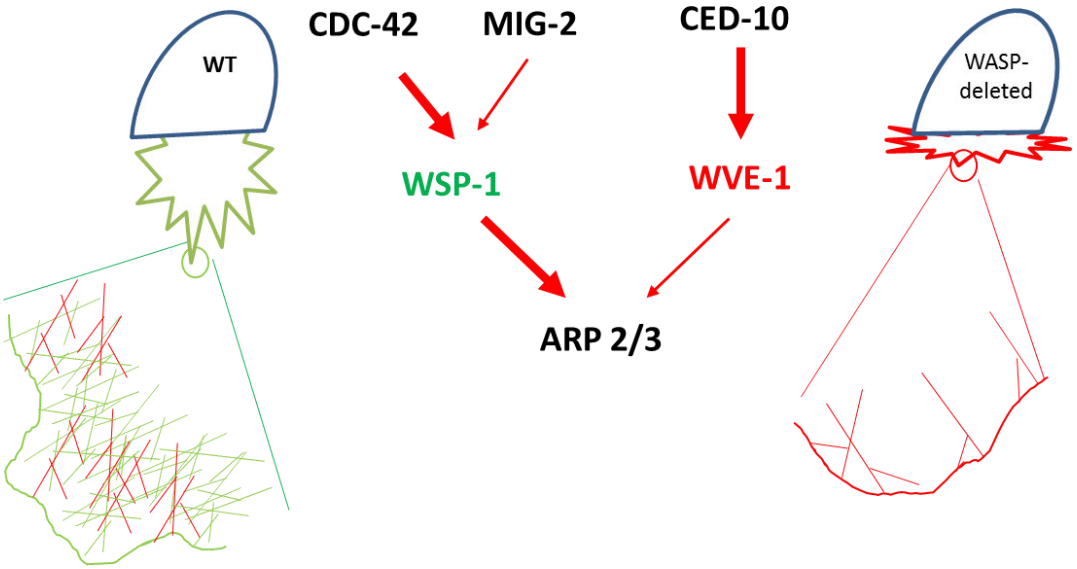

Figure 4.15 Summary of the main results of this study. The main regulatory pathways of the Arp2/3 complex are shown, and their relative abilities to generate branched filaments in order to expand the protrusion during invasion are presented as green filaments issuing from WSP-1/WASP activation of the Arp2/3 complex and red filaments from WVE-1/WAVE.

Similar observations, showing the contribution of both WSP-1/WASP and WVE-1/WAVE were reported for cell movements in the *C. elegans* embryo during a process known as dorsal intercalation (Walck-Shannon et al., 2015) and during axon migration (Shakir et al., 2008). On the other hand an analysis of WSP-1/WASP and WVE-1/WAVE during Q neuroblast migration, a process where a single cell migrates through the body cavity in *C. elegans,* showed that WVE-1/WAVE is the main Arp2/3 complex activator for motility although WSP-1/WASP can relocalize upon WVE-1/WAVE depletion to compensate (Zhu et al., 2016). In other lamellipodial-type protrusions, like that of the ventral epidermal cells during ventral enclosure, WSP-1/WASP plays no role in actin assembly dynamics, which are entirely dependent on WVE-1/WAVE (Havrylenko et al., 2015; Patel et al., 2008). Likewise WAVE elimination in mammalian cells abolishes lamellipodia formation and WASP is not localized at the leading edge (Leithner et al., 2016), and it is generally accepted that Rac signaling to WAVE is what forms lamellipodia while Cdc42 signaling to WASP has other functions (Campellone and Welch, 2010; Rotty et al., 2013).

In AC invasion, this is not the case, and the lamellipodial-like protrusion of the AC is mostly WSP-1/WASP driven with some contribution from WVE-1/WAVE. This is similar to cancer cell invadopodia, as presented in **Chapter 2**, where there is strong evidence for WASP activity in invadopodia while the role of WAVE in invadopodia is less clear. My results point

clearly to a role for WAVE as a back-up player to WASP in invasive protrusion formation, and adds to a growing list of recent studies showing that the two molecules play more similar roles than previously thought (Fritz-Laylin et al., 2017; Zhu et al., 2016). I also show that the strong dependence of AC invasion on actin polymerization via WASP is not due to its trafficking or scaffolding role: 3 main players in AC invasion, including a protease, are correctly localized in the absence of WASP. Despite the presence of the key components, WASP-deleted ACs do not invade with normal timing, presumably because insufficient actin is produced to breach and push aside the BM.

The results of this chapter and some elements from the next chapter will be included in a publication that is currently in preparation: Cáceres R., Bojanala N., Kelley L.C., Dreier J., Manzi J., Di Federico F., Chi Q., Risler T., Testa I., Sherwood D.R. and Plastino J "WASP and WAVE activate the Arp2/3 complex for actin-based force production during basement membrane invasion".

CHAPTER 5: SUPER-RESOLUTION MICROSCOPY STUDY OF THE AC PROTRUSION

5.1 MOTIVATION FOR SUPER-RESOLUTION MICROSCOPY OF THE INVASIVE AC PROTRUSION

Actin filaments have a diameter of 7-10 nm depending on where along the double helix the measurement is taken (Aebi et al., 1986). Filaments can pack close together in structures such as crosslinked bundles with individual filaments only 8-24 nm apart (Goldstein et al., 1979; Jansen et al., 2011; Volkmann et al., 2001) or cell cortices that have a mesh size of only 50–200 nm (Morone et al., 2006). In addition to being tightly packed, actin structures in the cell can sometimes be quite small such as filopodia that can be under 100 nm in diameter (Lewis and Bridgman, 1992; Svitkina et al., 2003). The small size and tight packing of actin structures limits the structural information that can be obtained by conventional light microscopy techniques. Indeed the limit of fluorescence microscopy, the diffraction limitation, was described by Ernst Abbé in 1873: $d = \frac{\lambda}{2NA}$, where the resolution of the image d is equal to the wavelength of incident light λ divided by 2 times the numerical aperture NA. With numerical apertures of around 1 and illumination with green light for example, this means that the resolution of the image is approximately 250 nm, so structures that are closer together than 250 nm will be seen as a single object. Because of these issues, almost all information concerning actin architecture in protrusions has been obtained via electron microscopy, a technique that is incompatible with live-cell imaging.

The visualization of actin structures in invadopodia is a particularly difficult problem even for electron microscopy due to the 3D nature of invasive protrusions. The only structural information available for an invasive protrusion comes from electron microscopy of thin sections of cells invading into BM mimic-coated pores (images shown **Chapter 1**, **Section 1.3.1**) (Schoumacher et al., 2010). The goal of this part of my PhD was to apply super-resolution microscopy to AC invasion, in view of obtaining for the first time structural information on the actin cytoskeleton during BM invasion in vivo. The choice of the technique, RESOLFT, was a result of discussions with Ilaria Testa (KTH, Sweden) who gave a seminar at Institut Curie in 2016. This technique also offered the exciting possibility of doing super-resolution dynamics (time-lapse), since the samples are not fixed. I will first

introduce super-resolution in general before describing RESOLFT and its predecessor STED, and the results I obtained with the former.

5.2 SUPER-RESOLUTION MICROSCOPY

5.2.1 OVERVIEW OF SUPER-RESOLUTION TECHNIQUES RELATED TO RESOLFT

In order to increase the resolution of the light microscope, and be able visualize two adjacent filopodia for example, a decrease in the wavelength or an increase in the numerical aperture is needed, something that in practice is difficult to do with conventional confocal, bright field, and spinning disk microscopy. These techniques are limited by the wavelengths of available probes and the NA of the objectives. However in 1994 Hell and Wichmann broke the diffraction limited using an approach based on spatial minimization of the focal spot created by the laser, increasing the resolution of confocal fluorescence microscopy (Hell and Wichmann, 1994). This technique is called Stimulated Emission Depletion Fluorescence Microscopy (STED) and it can achieve a resolution of around 70 nm (Willig et al., 2006a). I will come back in more detail to this technique in **Section 5.2.2**. REversible Saturable Optical Linear Fluorescence (RESOLFT) relies on the same idea as STED, but additionally using reversible photoswitching between a fluorescent "on" state and a dark "off" state to decrease the focal spot (Hell et al., 2003; Testa et al., 2012). I will describe RESOLFT more fully in **Section 5.2.3**.

At about the same time as STED, other super-resolution techniques were being developed, including Photo-Activated Localization Microscopy (PALM) (Betzig, 1995; Betzig et al., 2006). PALM uses a different approach to break the diffraction limit, based on repeated cycles of photoactivation and photobleaching: fluorophores such as photoactivatable GFP are stochastically activated, an image is taken and then the fluorophores are bleached, allowing for the pinpointing of individual fluorescent molecules. Once all the single fluorophore positions are obtained, a reconstruction produces a final super-resolution image. A similar strategy can be used with photoswitchable fluorophores, such as Eos and Dendra, in order to turn “on” and “off” different sub-sets of fluorophores in the same region. This approach is known as stochastic optical reconstruction microscopy (STORM) (Rust et al., 2006). PALM, STORM and STED super-resolution techniques use long acquisition times (5-30 minutes) (Shroff et al., 2013) and high intensity light of $MW.cm^{-2}$ (Li et al., 2015), and are thus suited to studies of fixed samples but not to following the dynamics of a cellular process. This is not

the case with RESOLFT, which was one of the reasons we chose this technique to image F-actin in the AC.

5.2.2 Stimulated Emission Depletion Fluorescence Microscopy (STED)

I will describe STED before moving on to RESOLFT, since pedagogically and historically, RESOLFT was inspired by STED. STED consists in the overlapping of 2 synchronized lasers that illuminate the same position. One is responsible for activating the fluorophore (excitation laser) while the second one turns off the excitation (depletion laser). The depletion laser has a doughnut-shaped pattern and thus sharpens the excitation laser and decreases the focal spot. This doughnut-shaped depletion is accomplished using a phase mask in the path of the depletion laser (**Figure 5.1**). The depletion laser works by de-exciting fluorophores from the excited state to the ground state without photon emission.

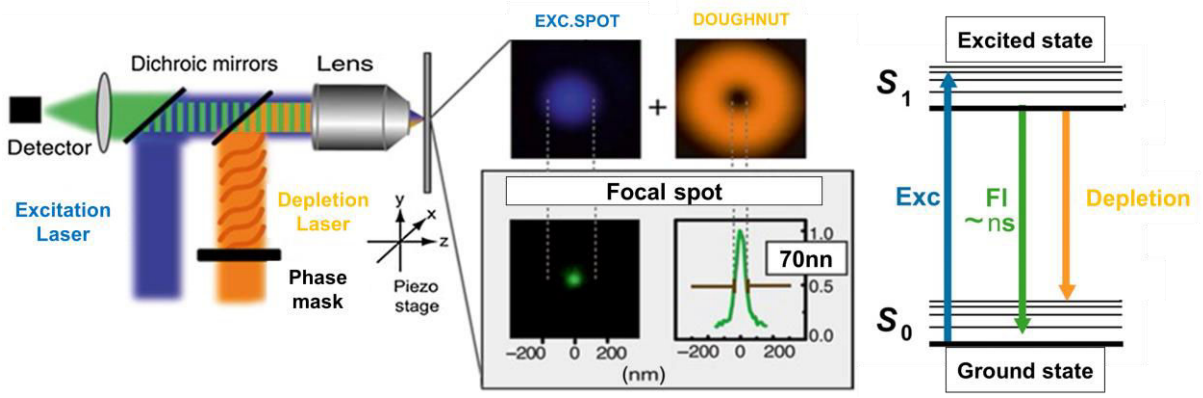

Figure 5.1 Principle of STED microscopy. Left: the excitation beam (blue) and the depletion doughnut-shaped laser (orange) with a phase mask. The overlap of the lasers decreases the focal spot achieving a resolution around 70 nm. Adapted from (Willig et al., 2006b). Right: energy diagram of fluorescence (FI, green arrow) which occurs at the focal spot and depletion (de-excitation of fluorophores) by the depletion laser of the doughnut. Adapted from (Donnert et al., 2006).

The probability that the fluorophore will remain in a high energy state decreases in an exponential manner with increasing intensity of the depletion laser **(Figure 5.2)**. In practice, STED is performed at a laser intensity where almost all the exited fluorophores are turned off, I_s. This intensity is called a "saturated intensity", but if a higher intensity is used (I in **Figure 5.2**), this will not only increase the probability of turning off the exited fluorophores, but also increase the resolution in an inversely proportional manner **(Figure 5.2)**. When I equals I_s, the equation is reduced to the Abbé diffraction limit, but if I is larger than I_s, the focal spot becomes very narrow achieving super-resolution. To achieve this gain in resolution, the depletion laser must be high enough in energy to send all the exciting fluorophores to the

ground state before they release fluorescence which happens in less than 2 ns. For this reason high depletion laser energies, on the order of MW.cm^{-2}, are required.

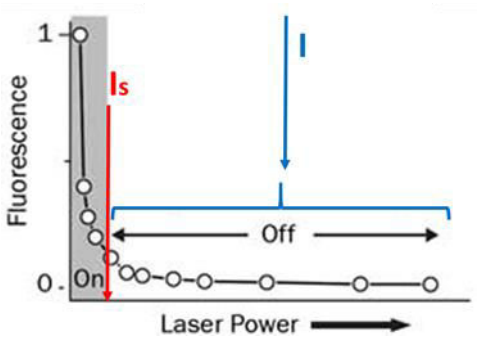

$$d = \frac{\lambda}{2NA\sqrt{1 + \frac{I}{I_s}}}$$

Figure 5.2 Laser power and resolution for STED microscopy. Left: representation of fluorophore intensity vs depletion laser intensity. I_s saturated intensity, I depletion laser intensity used during STED microscopy. Right: the modified Abbé equation showing how altering depletion laser intensity (I) and the saturated intensity (I_s) can increase resolution. Adapted from (Christian et al., 2009).

5.2.3 REVERSIBLE SATURABLE OPTICAL LINEAR FLUORESCENCE (RESOLFT)

The concept of RESOLFT was developed in order to reduce the intensity levels required in STED (Hell et al., 2003). This technique uses on/off switching as in STED but with reversible photoswitchable fluorophores (rsFPs) such as the molecule Dronpa. On/off states reflect cis-trans molecular isomerization within the fluorophore of the fluorescent protein label (Grotjohann et al., 2011). These states have long lifetimes (µs-ms), reducing the light intensity needed to perform depletion to W.cm^{-2} to kW.cm^{-2}, around 10^5 lower than STED (Stefan et al., 2015). As for STED, the gain in spatial resolution is due to use of a doughnut-shaped light pattern to transiently silence the florescence of rsFPs, and allow only the fluorophores from the center of the doughnut to contribute to the fluorescence signal **(Figure 5.3)**. In order to achieve nano-resolution, the rsFPs need to survive several "on" and "off" cycles. Nevertheless due to the low energies used, studies on living neurons show that after 2 hours of continuous scanning there is no obvious photodamage (Testa et al., 2012).

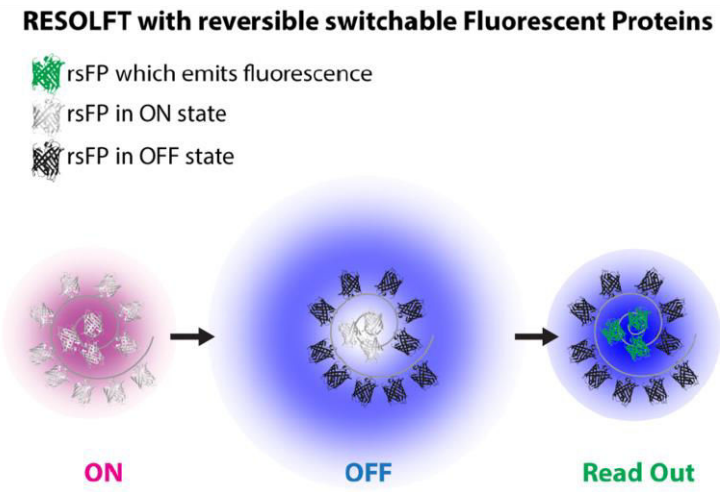

Figure 5.3 Principle of RESOLFT microscopy. Schematic representation of the light patterns used during RESOLFT microscopy. Adapted from (Stefan et al., 2015).

5.3 SUPER-RESOLUTION VISUALIZATION OF F-ACTIN STRUCTURES DURING AC INVASION

Results described in **Chapter 4** strongly suggest that AC protrusion is mainly driven by a branched actin network that indents the BM before invasion and pushes it aside during invasion. However the actin architecture in the invasive protrusion is not resolvable with conventional microscopy techniques, as seen from the images presented in **Chapter 4**. In order to overcome this obstacle, and after having tried other techniques such as structured illumination and light sheet microscopy without success, I decided to do RESOLFT imaging in collaboration with Ilaria Testa, one of the authors of the first RESOLFT publication. I constructed a worm strain expressing an rsFP, DronpaM159T, fused to Lifeact specifically in the AC as an integrated transgenic line. The M159T variant is a faster switcher than the original Dronpa (Kaucikas et al., 2015). I took these worms to Sweden, and spent about 3 weeks in the Testa laboratory to perform RESOLFT imaging.

Experiments were performed on live anesthetized worms in view to doing super-resolution of the invasive protrusion over time. However with the point scanning acquisition mode of the RESOLFT microscope, acquiring a stack that covered the entire AC took around 3 minutes, a window of time much too long considering that the whole invasion process only lasted about 30 minutes. In order to remedy this problem, the scanning time was reduced to around 1.5 minutes by reducing the number of z-planes, and only acquiring those planes where the AC actin protrusion was most visible. Image acquisition of 1.5 minutes was still very long, especially considering that even with an interval of 45 seconds on the spinning disk,

consecutive frames appeared discontinuous, indicating that structures formed and collapsed faster than the stacks could be acquired. However with the 3D nature of the AC and the slow scan speed imposed by the point-scanning set-up and RESOLFT technology, 1.5 minute image acquisition was the best that could be achieved. Reducing the number of z-planes also helped reduce photodamage, but even with this restricted z-stack mode, we were only able to image AC invasion for around 15 minutes before fluorophore bleaching, not enough time to acquire the entire AC invasion process. So in the end, acquiring RESOLFT images of AC invasion over time turned out not to be practicable, due mostly to insufficient time resolution.

As concerns resolution, RESOLFT showed dense patches of actin at the invasive front of the AC, unresolvable into individual structures, indicating that the actin network was very dense in these regions **(Figure 5.4)**. Some fine structure could be observed on the edges of the invasive protrusion, and appeared to be branched-type structures as opposed to needle-like filopodia **(Figure 5.4)**

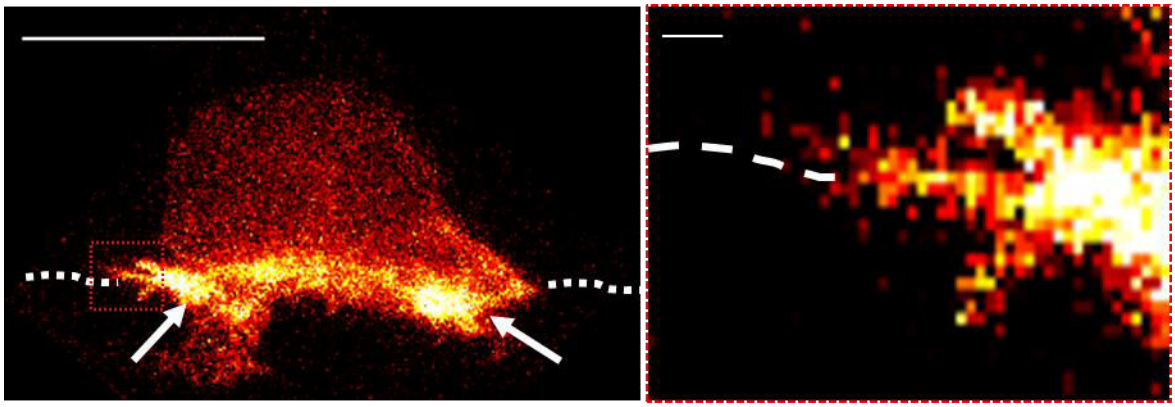

Figure 5.4 RESOLFT image of an AC during invasion. Left: arrows indicate the dense actin regions, the white dotted line represents the BM, red box indicates the presence of a branched structure in close proximity to the BM. Scale bar 5µm. Right: zoom of the red box shown on the left. Scale 0.2 µm. Allele *curIs23*; see **Chapter 3**.

The dense unresolvable core was also visible in post-invasion stages, where the BM hole started to expand beyond the AC edges and the protrusion was bigger **(Figure 5.5)**. In addition to short branch-type structures at the edges of the BM hole as observed pre-invasion (above), a few elongated structures were also visualized on the shaft of the AC protrusion, emanating from the dense core **(Figure 5.5)**. These structures resembled filopodia protruding from a lamellipodia network. In this regard it should be remembered that some formins such as EXC-6 are highly expressed in the AC, and although they don't appear to play a role in invasion (**Chapter 4, Section 4.4**), they could participate in the formation of post-invasive structures such as these filopodia-like protrusions.

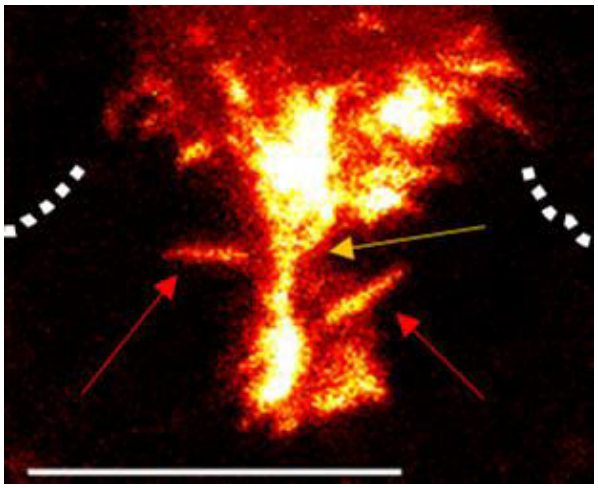

Figure 5.5 RESOLFT image of an AC protrusion at a later stage when tissue invagination begins. Red arrows point to elongated structures coming from an actin dense region indicated by a yellow arrow. BM is represented by the white dotted line. Allele *curIs23*; see **Chapter 3**. Scale bar 5µm.

5.4 CONCLUSION: AC PROTRUSION IS A HIGHLY DENSE ACTIN NETWORK

On a technological level, the study of the AC protrusion is a proof-of-concept as to the potential of RESOLFT microscopy for following cellular events on live samples. In addition it shows that complex thick tissues can be successfully imaged with RESOLFT. Since RESOLFT is a relatively new technique, this is useful information for the Testa laboratory.

As to understanding more about the architecture of the invasive protrusion, the RESOLFT study was not as informative as I had hoped. Partly due to the long acquisition time and the dynamic movements of the sample, the amount of additional detail observable by RESOLFT as compared to spinning disk was not dramatic. In the AC, RESOLFT microscopy distinguishes actin structures around 100 nm thick on the edges of the protrusion. However the actin core of the protrusion can't be resolved by RESOLFT. This is a piece of information in itself, indicating that the protrusion is very densely packed with actin filaments. This supports my results in **Chapter 4,** showing that strong filament branching via both WASP and WAVE activation of the Arp2/3 complex is occurring during normal invasion.

CHAPTER 6: ROLE OF ACTO-MYOSIN CONTRACTION DURING AC INVASION IN THE ABSENCE OF PROTEASES

6.1 CONTEXT OF THE STUDY: AC INVASION AND MMPS

Up until recently the role of proteases in AC invasion was not clear. As discussed in **Chapter 2**, an MMP, ZMP-1, was known to be expressed in the AC under control of the transcription factors responsible for AC identity. However knocking out *zmp-1* on its own had no effect on AC invasion (Sherwood et al., 2005). Furthermore RNAi knock-down of 90% of the *C. elegans* genes that possessed a predicted protease or protease inhibitor domain gave no perturbations of AC invasion (Ihara et al., 2011). This lack of effect may be due to protease redundancy, so a study was undertaken by our collaborators to remove all MMPs in the *C. elegans* genome. As opposed to the mammalian genome that has 20+ MMPs, *C. elegans* only possesses 6, one of which is not expressed in the AC at the relevant stage (Hagedorn and Sherwood, 2011) and (L. Kelley and D. Sherwood, unpublished). Based on this, L. Kelley and coworkers from the Sherwood lab created a worm strain that was mutated in all 5 relevant MMPs, hereafter referred to as "MMP-" conditions. Somewhat surprisingly AC invasion in these worms was only slightly affected, with 84% of the ACs invading by the 4-cell stage. Given what was known about protease-independent invasion of cancer cells **(Chapter 1, Section 1.3.2)**, I undertook the study of the role of myosin in AC invasion in MMP- worms, with the hypothesis that, in analogy to cancer cells, enhanced contractility might compensate for reduced proteolysis of ECM barriers.

6.2 ACTO-MYOSIN MACHINERY DURING AC INVASION IN ABSENCE OF MMPS

In order to test for compensation, I compared the effects of RNAi in WT versus in MMP-, looking for knock-downs that affected MMP- invasion while having no effect in WT worms. I knocked down by RNAi the genes for myosin heavy chain *nmy-2*, *mlc-4*, a regulatory light chain for non-muscle myosin, *mel-11*, a myosin phosphatase and negative regulator of myosin activity, and two other main regulators of myosin contraction, the Rho kinase *let-502* and the myosin light chain kinase *mrck-1* (see also **Chapter 2**, **Section 2.3**). All of these components are implicated in myosin-based processes like embryonic elongation in *C. elegans* (Gally et al., 2009). Scoring was performed at the 4-cell stage as either invaded or not.

As shown in **Table 6.1**, none of the treatments had an impact on WT worms, indicating that myosin contractility was not important for AC invasion. The effectiveness of the RNAi treatment was confirmed by the presence of vulval malformations and a reduction in egg-laying for *mlc-4* and *mell-11* probes. From this it appeared that myosin activity was necessary for later stages of vulval development in keeping with other studies (Farooqui et al., 2012), but not for AC invasion in itself. The same RNAi treatments were applied to MMP- worms, and as compared to control RNAi treatment containing empty vector, there were no differences in the % of ACs invaded at the 4-cell stage **(Table 6.1)**. This very clearly indicated that myosin contractility was not important either in WT or in MMP- worms for effective AC invasion.

RNAi Treatment	WT	MMP-
Control	98%	84%
nmy-2	96%	90%
mrck-1	92%	93%
let-502	97%	90%
mlc-4	98%	87%
mel-11	100%	89%

Table 6.1 Evaluation of myosin participation in invasion. Percentage of full invasion at the 4-cell stage after RNAi knock down. Control is empty vector. N>40 for each condition. WT were carrying the alleles *qyIs108* and *qyIs23* for BM and AC membrane label, respectively. MMP- worms were additionally carrying alleles for the 5 MMPs: *cg115, tm3482, tm3078, tm3073 and tm3209*; see **Chapter 3**.

In keeping with this, a GFP fusion of MRCK-1 expressed under the endogenous promotor as a transgene was not expressed in the AC **(Figure 6.1)**, nor was its substrate MLC-4, although MEL-11, LET-502 and NMY-2 were all present in the AC at the 4-cell stage (L. Kelley unpublished results). The fact that some of the essential myosin machinery was missing from the AC at the critical time was further evidence that myosin activity was not important for invasion. Of note MRCK-1::GFP was observed in the VPCs **(Figure 6.1)**, indicating that the transgene was active. This localization is probably related to the importance of myosin contraction for normal vulva development during lumen formation that starts in the stage just after AC invasion (Farooqui et al., 2012).

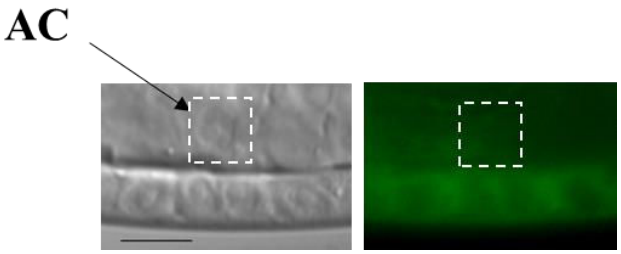

Figure 6.1 MRCK-1 expression at the 4-cell stage. MRCK::GFP is not expressed in the AC but is present in the VPCs. Allele *mcEx551*; see **Chapter 3**. Scale bar 5 µm.

6.3 ACTO-MYOSIN CORTEX DURING AC INVASION

In parallel with this RNAi study, I approached the question from another angle, examining WT and MMP- ACs during invasion to see if the AC exhibited a cortex. Since myosin contributes to invasion and motility by contracting the cell cortex at the back of the cell **(Chapter 1, Section 1.2.3 and 1.2.5)**, it was expected that a cortex would be visible in the AC if myosin contractility was playing a role. In order to visualize the actin cytoskeleton in MMP- worms, I induced the expression of Lifeact::BFP in the AC and did the same in WT as a control. Imaging the AC at the 4-cell stage revealed the presence of both cortical and protrusive actin in WT worms **(Figure 6.2).** Surprisingly in MMP- worms, F-actin was concentrated in the AC protrusion and barely detectable in the cortex **(Figure 6.2),** as if actin polymerization was enhanced in the protrusion to compensate for the absence of MMPs. This difference was quantified by calculating the actin ratio: the mean intensity of the protrusion (maximum intensity projection) was divided by the mean intensity of the cortex (single cortical plane) using the AC membrane (mCherry::PH) as a marker to detect the plane where the cortex was most in focus. As shown in **Figure 6.2**, the ratio protrusion/cortex in MMP- was double that of WT, meaning that F-actin was much more polarized toward the invasive edge of the cell in MMP- worms as compared to WT. In fact, as evident in **Figure 6.2,** cortical actin was so sparse that it appeared to be absent in many cases. This data added to the RNAi data in confirming that myosin contraction of the cortex was not helping the cell squeeze through the BM.

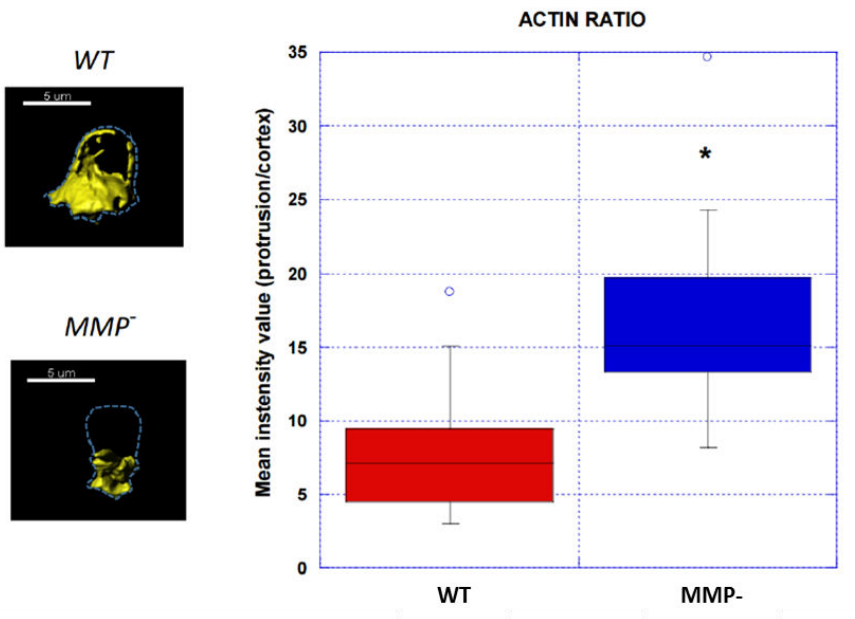

Figure 6.2 Cortex analysis in WT and MMP- worms. Left: actin isosurface renderings made from z-stacks of WT and MMP- worms expressing Lifeact::BFP in the AC. Dashed blue line represents the AC membrane, labeled by AC-specific expression of mCherry::PH. Right: N>13. Alleles for WT were *qyls108*, *qyIs23* and *curEx24*; MMP- additionally carried *cg115, tm3482, tm3078, tm3073 and tm3209*; see **Chapter 3**. Scale bar 5 μm.

6.4 BLEB VISUALIZATION DURING AC INVASION

The worms strains that I constructed for the previous section allowed me to visualize F-actin, AC membrane and BM in both WT and MMP- backgrounds. In MMP- only, I sometimes observed membrane bulges coming off the front of the protrusion **(Figure 6.3)**. These could be called blebs since they contained no F-actin, however I was never able to obtain any dynamics, so it was not clear how these bulges formed. Some appeared to have no connection to the AC body, implying that they were severed membrane fragments. Although these structures were observed at low frequency (5% of worms examined), they were consistently seen in MMP- as opposed to WT. MMP- ACs appeared to be more constricted by the BM during invasion, giving rise to "onion"-type shapes **(Figure 6.2** and **Figure 6.3)**. Perhaps membrane bulges originated from rupture events as the protrusion attempted to squeeze through small openings in the BM. Given the lack of certain myosin components in the AC, although I couldn't rule out that they were just at undetectable levels, it seemed unlikely that these were real blebs created by contraction and cortex detachment as described in **Chapter 1, Section 1.2.3**.

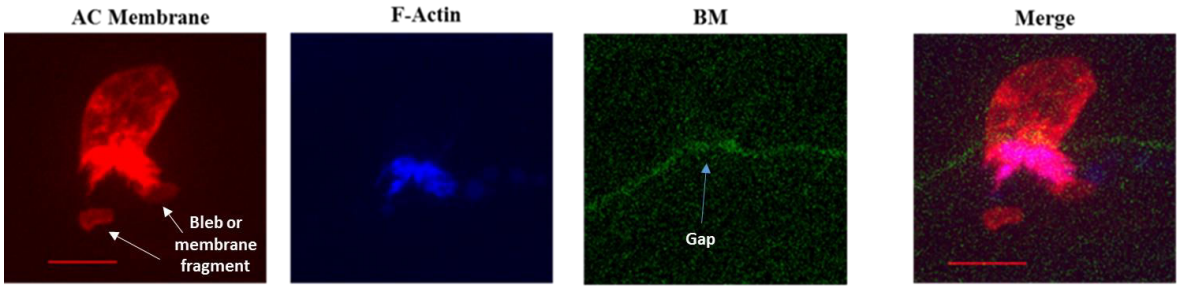

Figure 6.3 Membranous structures observed during AC invasion in MMP- worms. Membrane bulges that lack filamentous actin were observed that could be blebs or membrane fragments (indicated by arrows). Maximum intensity projections of AC membrane and F-actin in the AC. For BM, a single plane shows the small gap (arrow) that constricts the AC. Scale bars 5µm.

6.5 CONCLUSION: MYOSIN IS NOT ESSENTIAL FOR AC INVASION

The conclusion of this chapter is that myosin contractility is not important for AC invasion even in the absence of proteases. So unlike cancer cells in in vitro 3D environments (Wolf et al., 2003), the AC does not switch to a bleb-based mode of invasion powered by myosin contractility when MMPs are inhibited. In this context it should be mentioned that the Wolf et al. study was somewhat controversial due to the uncrosslinked nature of the reconstituted ECM used. Other laboratories found that cancer cells were unable to migrate without MMPs in ECM mimics that were physiologically crosslinked (Sabeh et al., 2004). Indeed in our AC study, native BM was used, so this might explain why invasion in the absence of MMPs was not powered by myosin contractility. Another reason is that the physical context of the AC is very different from a solitary invading cancer cell. The AC is part of a tissue, adhering to adjacent cells at its back and sides as well as to the BM that it is invading. Indeed AC invasion is not a real transmigration event in that the back of the cell does not move forward and cross over the BM. AC invasion is a lamellipodia-type protrusion event, and myosin is not known to play a role in the formation of this kind of protrusion.

Our collaborators have continued their studies of the MMP- strain, looking for components that are responsible for invasion in this background. They find that mitochondrial proteins are necessary, implying that energy consumption is increased in the MMP- case as compared to WT. The hypothesis is that the cell needs more ATP, probably to power actin polymerization, in order to break through a BM in the absence of proteases. These results and the results in this chapter will make up a publication that is currently in preparation: Kelley L.C, Hastie E.L., Cáceres R., Matus D.Q., Chi Q., Plastino J. and Sherwood D.R. “Localized ATP

production and F-actin polymerization drive basement membrane invasion in the absence of MMPs".

Overall this study of MMP-independent invasion emphasizes the plasticity of the invading cell to adapt its machinery in order to accomplish its invasive program. This is a crucial point that needs to be better understood in order to develop new treatments targeting cell invasion in disease.

GENERAL CONCLUSION

In this thesis I analyzed the acto-myosin cytoskeleton during a cell invasion event that occurs during *C. elegans* development, with the long-term perspective of better understanding the similar process of cancer cell invasion. Although relatively well-characterized as far as signaling and genetics were concerned, AC invasion had not been much thought of in terms of physical mechanisms. The ease of genetics and imaging in the worm made quantitative measurements possible while respecting the native microenvironment.

In **Chapter 4** taking advantage of *C. elegans* genetic and imaging tools, as well as using the actin biochemistry strengths of the host lab (the dominant negative approach, the in vitro analysis…), I provided evidence for actin polymerization-based forces in the invading cell, produced by teamwork between WASP and WAVE. In **Chapter 5** I used RESOLFT to visualize in more detail the actin cytoskeleton. This study confirmed that the actin network in the AC during invasion was unresolvably dense, but some dendritic-like structures were visible. During this study in Ilaria Testa's lab, I was lucky to work with an expert in optics, Jess Dreier. I experienced first-hand the power of super-resolution techniques, but also the constraints of working with opticians. In **Chapter** 6 I participated in the characterization of a new invasion strategy in the absence of proteases, independent of myosin contraction, but relying on increased ATP production in the invading cell. Here again I was lucky to collaborate with Laura Kelley and David Sherwood, experts in the field of AC development. The results of this study are not contradictory to previous studies with human cancer cells, but it shows the importance of studying cellular processes in their native environment.

Overall the main contribution of this PhD was to provide evidence that mechanical forces generated by the cytoskeleton are important during cell invasion, an idea that is not universally accepted in the invasion field. AC invasion and other cell movements in the worm could be powerful models for studying the cell biology and biophysics of cell motility, but they need to be better exploited at the mechanical and structural level.

REFERENCES

Achard, V., J.-L. Martiel, A. Michelot, C. Guérin, A.-C. Reymann, L. Blanchoin, and R. Boujemaa-Paterski. 2010. A "Primer"-Based Mechanism Underlies Branched Actin Filament Network Formation and Motility. *Curr. Biol.* 20:423-428.

Adams, J.C. 2004. Roles of fascin in cell adhesion and motility. *Current Opinion in Cell Biology*. 16:590-596.

Aebi, U., R. Millonig, H. Salvo, and A. Engel. 1986. The Three-Dimensional Structure of the Actin Filament Revisiteda. *Annals of the New York Academy of Sciences*. 483:100-119.

Aguilar-Cuenca, R., A. Juanes-García, and M. Vicente-Manzanares. 2014. Myosin II in mechanotransduction: master and commander of cell migration, morphogenesis, and cancer. *Cellular and Molecular Life Sciences*. 71:479-492.

Akin, O., and R.D. Mullins. 2008. Capping Protein Increases the Rate of Actin-based Motility by Promoting Filament Nucleation by the Arp2/3 Complex. *Cell*. 133:841-851.

Alberts, A.S. 2001. Identification of a Carboxyl-terminal Diaphanous-related Formin Homology Protein Autoregulatory Domain. *Journal of Biological Chemistry*. 276:2824-2830.

Alvarado, J., M. Sheinman, A. Sharma, F.C. MacKintosh, and G.H. Koenderink. 2013. Molecular motors robustly drive active gels to a critically connected state. *Nature Physics*. 9:591-597.

Aoyagi, K., I. Shima, M. Wang, Y. Hu, F.U. Garcia, and M.E. Stearns. 1998. Specific transcription factors prognostic for prostate cancer progression. *Clinical Cancer Research*. 4:2153-2160.

Baldassarre, M., Z. Razinia, N. N. Brahme, R. Buccione, and D.A. Calderwood. 2012. Filamin A controls matrix metalloproteinase activity and regulates cell invasion in human fibrosarcoma cells. *Journal of Cell Science*. 125:3858-3869.

Bartles, J.R. 2000. Parallel Actin Bundles and Their Multiple Actin-bundling Proteins. *Current Opinion in Cell Biology*. 12:72-78.

Barzik, M., T.I. Kotova, H.N. Higgs, L. Hazelwood, D. Hanein, F.B. Gertler, and D.A. Schafer. 2005. Ena/VASP Proteins Enhance Actin Polymerization in the Presence of Barbed End Capping Proteins. *Journal of Biological Chemistry*. 280:28653-28662.

Benesch, S., S. Lommel, A. Steffen, T.E.B. Stradal, N. Scaplehorn, M. Way, J. Wehland, and K. Rottner. 2002. Phosphatidylinositol 4,5-Biphosphate (PIP2)-induced Vesicle Movement Depends on N-WASP and Involves Nck, WIP, and Grb2. *Journal of Biological Chemistry*. 277:37771-37776.

Bergert, M., S.D. Chandradoss, R.A. Desai, and E. Paluch. 2012. Cell mechanics control rapid transitions between blebs and lamellipodia during migration. *Proceedings of the National Academy of Sciences of the United States of America*. 109:14434-14439.

Blanchoin, L., R. Boujemaa-Paterski, C. Sykes, and J. Plastino. 2014. Actin Dynamics, Architecture, and Mechanics in Cell Motility. *Physiological Reviews*. 94:235-263.

Bovellan, M., Y. Romeo, M. Biro, A. Boden, P. Chugh, A. Yonis, M. Vaghela, M. Fritzsche, D. Moulding, R. Thorogate, A. Jégou, Adrian J. Thrasher, G. Romet-Lemonne, Philippe P. Roux, Ewa K. Paluch, and G. Charras. 2014. Cellular Control of Cortical Actin Nucleation. *Current Biology*. 24:1628-1635.

Bowden, E.T., E. Onikoyi, R. Slack, A. Myoui, T. Yoneda, K.M. Yamada, and S.C. Mueller. 2006. Co-localization of cortactin and phosphotyrosine identifies active invadopodia in human breast cancer cells. *Experimental Cell Research*. 312:1240-1253.

Breitsprecher, D., A.K. Kiesewetter, J. Linkner, C. Urbanke, G.P. Resch, J.V. Small, and J. Faix. 2008. Clustering of VASP actively drives processive, WH2 domain-mediated actin filament elongation. *EMBO Journal*. 27:2943-2954.

Breitsprecher, D., A.K. Kiesewetter, J. Linkner, M. Vinzenz, T. Stradal, J.V. Small, U. Curth, R.B. Dickinson, and J. Faix. 2011. Molecular mechanism of Ena/VASP-mediated actin-filament elongation. *EMBO Journal*. 30:456-467.

Bretscher, A., and K. Weber. 1980. Fimbrin, a new microfilament-associated protein present in microvilli and other cell surface structures. *The Journal of Cell Biology*. 86:335-340.

Caceres, R., and J. Plastino. 2017. Cytoskeleton dynamics: actin in cell invasion *Encyclopedia of Life Sciences*. DOI: 10.1002/9780470015902.a0001254.pub2.

Campellone, K.G., and M.D. Welch. 2010. A nucleator arms race: cellular control of actin assembly. *Nature Reviews Molecular Cell Biology.* 11:237-251.

Carmona, G., U. Perera, C. Gillett, A. Naba, A.L. Law, V.P. Sharma, J. Wang, J. Wyckoff, M. Balsamo, F. Mosis, M. De Piano, J. Monypenny, N. Woodman, R.E. McConnell, G. Mouneimne, M. Van Hemelrijck, Y. Cao, J. Condeelis, R.O. Hynes, F.B. Gertler, and M. Krause. 2016. Lamellipodin promotes invasive 3D cancer cell migration via regulated interactions with Ena/VASP and SCAR/WAVE. *Oncogene*. 35:5155-5169.

Caruso, J.A., and P.M. Stemmer. 2011. Proteomic profiling of lipid rafts in a human breast cancer model of tumorigenic progression. *Clinical and Experimental Metastasis*. 28:529-540.

Charras, G., and E. Paluch. 2008. Blebs lead the way: how to migrate without lamellipodia. *Nature Reviews Molecular Cell Biology.* 9:730-736.

Charras, G.T., M. Coughlin, T.J. Mitchison, and L. Mahadevan. 2008. Life and Times of a Cellular Bleb. *Biophysical Journal*. 94:1836-1853.

Charras, G.T., C.-K. Hu, M. Coughlin, and T.J. Mitchison. 2006. Reassembly of contractile actin cortex in cell blebs. *The Journal of Cell Biology*. 175:477-490.

Chen, Xing J., Anna J. Squarr, R. Stephan, B. Chen, Theresa E. Higgins, David J. Barry, Morag C. Martin, Michael K. Rosen, S. Bogdan, and M. Way. 2014. Ena/VASP Proteins Cooperate with the WAVE Complex to Regulate the Actin Cytoskeleton. *Developmental Cell*. 30:569-584.

Chesarone, M.A., A.G. DuPage, and B.L. Goode. 2010. Unleashing formins to remodel the actin and microtubule cytoskeletons. *Nature Reviews Molecular Cell Biology*. 11:62-74.

Christian, R., H. Ben, M. Claas von, M. Rebecca, H. Alf, W. Richard, L. Marcel, S. Andreas, W.H. Stefan, and E. Christian. 2009. Exploring single-molecule dynamics with fluorescence nanoscopy. *New Journal of Physics*. 11:103054.

Co, C., D.T. Wong, S. Gierke, V. Chang, and J. Taunton. 2007. Mechanism of Actin Network Attachment to Moving Membranes: Barbed End Capture by N-WASP WH2 Domains. *Cell*. 128:901-913.

Courson, D.S., and R.S. Rock. 2010. Actin Cross-link Assembly and Disassembly Mechanics for α-Actinin and Fascin. *The Journal of Biological Chemistry*. 285:26350-26357.

Dayel, M.J., O. Akin, M. Landeryou, V. Risca, A. Mogilner, and R.D. Mullins. 2009. In silico reconstitution of actin-based symmetry breaking and motility. *PLOS Biol.* 7:1000201.

de Arruda, M.V., S. Watson, C.S. Lin, J. Leavitt, and P. Matsudaira. 1990. Fimbrin is a homologue of the cytoplasmic phosphoprotein plastin and has domains homologous with calmodulin and actin gelation proteins. *The Journal of Cell Biology*. 111:1069-1079.

DeMaso, C.R., I. Kovacevic, A. Uzun, and E.J. Cram. 2011. Structural and Functional Evaluation of C. elegans Filamins FLN-1 and FLN-2. *PLOS One*. 6:e22428.

Di Vizio, D., J. Kim, M.H. Hager, M. Morello, W. Yang, C.J. Lafargue, L.D. True, M.A. Rubin, R.M. Adam, R. Beroukhim, F. Demichelis, and M.R. Freeman. 2009. Oncosome Formation in Prostate Cancer: Association with a Region of Frequent Chromosomal Deletion in Metastatic Disease. *Cancer Research*. 69:5601-5609.

Ding, W.Y., H.T. Ong, Y. Hara, J. Wongsantichon, Y. Toyama, R.C. Robinson, F. Nédélec, and R. Zaidel-Bar. 2017. Plastin increases cortical connectivity to facilitate robust polarization and timely cytokinesis. *The Journal of Cell Biology*. 216:1371-1386.

Donnert, G., J. Keller, R. Medda, M.A. Andrei, S.O. Rizzoli, R. Lührmann, R. Jahn, C. Eggeling, and S.W. Hell. 2006. Macromolecular-scale resolution in biological fluorescence microscopy. *Proc. Natl. Acad. Sci. USA*. 103:11440-11445.

Doolittle, L.K., M.K. Rosen, and S.B. Padrick. 2013. Measurement and Analysis of in vitro Actin Polymerization. *Methods in molecular biology*. 1046:273-293.

Eden, S., R. Rohatgi, A.V. Podtelejnikov, M. Mann, and M.W. Kirschner. 2002. Mechanism of regulation of WAVE1-induced actin nucleation by Rac1 and Nck. *Nature*. 418:790-793.

Eilken, H.M., and R.H. Adams. 2010. Dynamics of endothelial cell behavior in sprouting angiogenesis. *Current Opinion in Cell Biology*. 22:617-625.

Engler, A.J., S. Sen, H.L. Sweeney, and D.E. Discher. 2006. Matrix Elasticity Directs Stem Cell Lineage Specification. *Cell*. 126:677-689.

Estes, K.A., and W. Hanna-Rose. 2009. The anchor cell initiates dorsal lumen formation during C. elegans vulval tubulogenesis. *Developmental Biology*. 328:297-304.

Farooqui, S., Mark W. Pellegrino, I. Rimann, Matthias K. Morf, L. Müller, E. Fröhli, and A. Hajnal. 2012. Coordinated Lumen Contraction and Expansion during Vulval Tube Morphogenesis in Caenorhabditis elegans. *Developmental Cell*. 23:494-506.

Flanagan, L.A., J. Chou, H. Falet, R. Neujahr, J.H. Hartwig, and T.P. Stossel. 2001. Filamin A, the Arp2/3 complex, and the morphology and function of cortical actin filaments in human melanoma cells. *The Journal of Cell Biology*. 155:511-518.

Fletcher, D.A., and R.D. Mullins. 2010. Cell mechanics and the cytoskeleton. *Nature*. 463:485-492.

Fraley, S.I., Y. Feng, R. Krishnamurthy, D.-H. Kim, A. Celedon, G.D. Longmore, and D. Wirtz. 2010. A distinctive role for focal adhesion proteins in threedimensional cell motility. *Nature Cell Biology*. 12:598-604.

Francis, G.R., and R.H. Waterston. 1985. Muscle organization in Caenorhabditis elegans: localization of proteins implicated in thin filament attachment and I-band organization. *The Journal of Cell Biology*. 101:1532-1549.

Friedl, P., and K. Wolf. 2003. Tumour-cell invasion and migration: diversity and escape mechanisms. *Nature Reviews Cancer*. 3:362-374.

Fritz-Laylin, L.K., S.J. Lord, and R.D. Mullins. 2017. WASP and SCAR are evolutionarily conserved in actin-filled pseudopod-based motility. *The Journal of Cell Biology*. 216:1673-1688.

Fukumoto, M., S. Kurisu, T. Yamada, and T. Takenawa. 2015. α-Actinin-4 Enhances Colorectal Cancer Cell Invasion by Suppressing Focal Adhesion Maturation. *PLOS One*. 10:e0120616.

Gally, C., F. Wissler, H. Zahreddine, S. Quintin, F. Landmann, and M. Labouesse. 2009. Myosin II regulation during C. elegans embryonic elongation: LET-502/ROCK, MRCK-1 and PAK-1, three kinases with different roles. *Development*. 136:3109-3119.

Geraldo, S., A. Simon, N. Elkhatib, D. Louvard, L. Fetler, and D.M. Vignjevic. 2012. Do cancer cells have distinct adhesions in 3D collagen matrices and in vivo? *European Journal of Cell Biology*. 91:930-937.

Giri, A., S. Bajpai, N. Trenton, H. Jayatilaka, G.D. Longmore, and D. Wirtz. 2013. The Arp2/3 complex mediates multigeneration dendritic protrusions for efficient 3-dimensional cancer cell migration. *The FASEB Journal*. 27:4089-4099.

Gitai, Z., T.W. Yu, E.A. Lundquist, M. Tessier-Lavigne, and C.I. Bargmann. 2003. The Netrin Receptor UNC-40/DCC Stimulates Axon Attraction and Outgrowth through Enabled and, in Parallel, Rac and UNC-115/AbLIM. *Neuron*. 37:53-65.

Goldstein, M.A., J.P. Schroeter, and R.L. Sass. 1979. The Z lattice in canine cardiac muscle. *The Journal of Cell Biology*. 83:187-204.

Gorlin, J.B., R. Yamin, S. Egan, M. Stewart, T.P. Stossel, D.J. Kwiatkowski, and J.H. Hartwig. 1990. Human endothelial actin-binding protein (ABP-280, nonmuscle filamin): a molecular leaf spring. *The Journal of Cell Biology*. 111:1089-1105.

Grotjohann, T., I. Testa, M. Leutenegger, H. Bock, N.T. Urban, F. Lavoie-Cardinal, K.I. Willig, C. Eggeling, S. Jakobs, and S.W. Hell. 2011. Diffraction-unlimited all-optical imaging and writing with a photochromic GFP. *Nature*. 478:204-208.

Hagedorn, E.J., L.C. Kelley, K.M. Naegeli, Z. Wang, Q. Chi, and D.R. Sherwood. 2014. ADF/cofilin promotes invadopodial membrane recycling during cell invasion in vivo. *The Journal of Cell Biology*. 204:1209-1218.

Hagedorn, E.J., and D.R. Sherwood. 2011. Cell invasion through basement membrane: the anchor cell breaches the barrier. *Current Opinion in Cell Biology*. 23:589-596.

Hagedorn, E.J., H. Yashiro, J.W. Ziel, S. Ihara, Z. Wang, and D.R. Sherwood. 2009. Integrin Acts Upstream of Netrin Signaling to Regulate Formation of the Anchor Cell's Invasive Membrane in C. elegans. *Developmental Cell*. 17:187-198.

Hagedorn, E.J., J.W. Ziel, M.A. Morrissey, L.M. Linden, Z. Wang, Q. Chi, S.A. Johnson, and D.R. Sherwood. 2013. The netrin receptor DCC focuses invadopodia-driven basement membrane transmigration in vivo. *The Journal of Cell Biology*. 201:903-913.

Hanein, D., and A.R. Horwitz. 2012. The structure of cell–matrix adhesions: the new frontier. *Current Opinion in Cell Biology*. 24:134-140.

Hansen, S.D., and R.D. Mullins. 2015. Lamellipodin promotes actin assembly by clustering Ena/VASP proteins and tethering them to actin filaments. *eLife*. 4:e06585.

Hartwig, J.H., K.A. Chambers, and T.P. Stossel. 1989. Association of gelsolin with actin filaments and cell membranes of macrophages and platelets. *The Journal of Cell Biology*. 108:467-479.

Hartwig, J.H., and T.P. Stossel. 1981. Structure of macrophage actin-binding protein molecules in solution and interacting with actin filaments. *Journal of Molecular Biology*. 145:563-581.

Havrylenko, S., P. Noguera, M. Abou-Ghali, J. Manzi, F. Faqir, A. Lamora, C. Guérin, L. Blanchoin, and J. Plastino. 2015. WAVE binds Ena/VASP for enhanced Arp2/3 complex-based actin assembly. *Molecular Biology of the Cell*. 26:55-65.

Hell, S.W., S. Jakobs, and L. Kastrup. 2003. Imaging and writing at the nanoscale with focused visible light through saturable optical transitions. *Applied Physics A*. 77:859-860.

Hell, S.W., and J. Wichmann. 1994. Breaking the diffraction resolution limit by stimulated emission: stimulated-emission-depletion fluorescence microscopy. *Optics Letters*. 19:780-782.

Higgs, H.N., L. Blanchoin, and T.D. Pollard. 1999. Influence of the C terminus of Wiskott-Aldrich syndrome protein (WASp) and the Arp2/3 complex on actin polymerization. *Biochemistry*. 38:15212-15222.

Higgs, H.N., and T.D. Pollard. 2000. Activation by Cdc42 and Pip(2) of Wiskott-Aldrich Syndrome Protein (Wasp) Stimulates Actin Nucleation by Arp2/3 Complex. *The Journal of Cell Biology*. 150:1311-1320.

Hohenester, E., and P.D. Yurchenco. 2013. Laminins in basement membrane assembly. *Cell Adhesion and Migration*. 7:56-63.

Huang, F.-K., S. Han, B. Xing, J. Huang, B. Liu, F. Bordeleau, C.A. Reinhart-King, J.J. Zhang, and X.-Y. Huang. 2015. Targeted inhibition of fascin function blocks tumour invasion and metastatic colonization. *Nature Communications*. 6.

Hwang, B.J., A.D. Meruelo, and P.W. Sternberg. 2007. *C. elegans* EVI1 proto-oncogene, EGL-43, is necessary for Notch-mediated cell fate specification and regulates cell invasion. *Development*. 134:669-679.

Ihara, S., E.J. Hagedorn, M.A. Morrissey, Q. Chi, F. Motegi, J.M. Kramer, and D.R. Sherwood. 2011. Basement membrane sliding and targeted adhesion remodels tissue boundaries during uterine vulval attachment in Caenorhabditis elegans. *Nature Cell Biology*. 13:641-651.

Ismail, A.M., S.B. Padrick, B. Chen, J. Umetani, and M.K. Rosen. 2009. The WAVE Regulatory Complex is Inhibited. *Nature structural & molecular biology*. 16:561-563.

Jansen, S., A. Collins, C. Yang, G. Rebowski, T. Svitkina, and R. Dominguez. 2011. Mechanism of Actin Filament Bundling by Fascin. *Journal of Biological Chemistry*. 286:30087-30096.

Kaucikas, M., M. Tros, and J.J. van Thor. 2015. Photoisomerization and Proton Transfer in the Forward and Reverse Photoswitching of the Fast-Switching M159T Mutant of the Dronpa Fluorescent Protein. *The Journal of Physical Chemistry B*. 119:2350-2362.

Kelley, L.C., L.L. Lohmer, E.J. Hagedorn, and D.R. Sherwood. 2014. Traversing the basement membrane in vivo: A diversity of strategies. *The Journal of Cell Biology*. 204:291-302.

Kiema, T., Y. Lad, P. Jiang, C.L. Oxley, M. Baldassarre, K.L. Wegener, I.D. Campbell, J. Ylänne, and D.A. Calderwood. 2006. The Molecular Basis of Filamin Binding to Integrins and Competition with Talin. *Molecular Cell*. 21:337-347.

Koestler, S.A., A. Steffen, M. Nemethova, M. Winterhoff, N. Luo, J.M. Holleboom, J. Krupp, S. Jacob, M. Vinzenz, F. Schur, K. Schlüter, P.W. Gunning, C. Winkler, C. Schmeiser, J. Faix, T.E.B. Stradal, J.V. Small, and K. Rottner. 2013. Arp2/3 complex is essential for actin network treadmilling as well as for targeting of capping protein and cofilin. *Molecular Biology of the Cell*. 24:2861-2875.

Kovacs, E.M., R.S. Makar, and F.B. Gertler. 2006. Tuba stimulates intracellular N-WASP-dependent actin assembly. *Journal of Cell Science*. 119:2715-2726.

Kovar, D.R., E.S. Harris, R. Mahaffy, H.N. Higgs, and T.D. Pollard. 2006. Control of the Assembly of ATP- and ADP-Actin by Formins and Profilin. *Cell*. 124:423-435.

Kurisu, S., and T. Takenawa. 2009. The WASP and WAVE family proteins. *Genome Biology*. 10:226.

Kurisu, S., and T. Takenawa. 2010. WASP and WAVE family proteins: Friends or foes in cancer invasion? *Cancer Science*. 101:2093-2104.

Lämmermann, T., and M. Sixt. 2009. Mechanical modes of 'amoeboid' cell migration. *Current Opinion in Cell Biology*. 21:636-644.

Laurent, V., T.P. Loisel, B. Harbeck, A. Wehman, L. Gröbe, B.M. Jockusch, J. Wehland, F.B. Gertler, and M.-F. Carlier. 1999. Role of proteins of the Ena-VASP family in actin-based motility of Listeria monocytogenes. *The Journal of Cell Biology*. 144:1245-1258.

Law, A.-L., A. Vehlow, M. Kotini, L. Dodgson, D. Soong, E. Theveneau, C. Bodo, E. Taylor, C. Navarro, U. Perera, M. Michael, G.A. Dunn, D. Bennett, R. Mayor, and M. Krause. 2013. Lamellipodin and the Scar/WAVE complex cooperate to promote cell migration in vivo. *The Journal of Cell Biology*. 203:673-689.

Lee, K., J.L. Gallop, K. Rambani, and M.W. Kirschner. 2010. Self-assembly of filopodia-like structures on supported lipid bilayers. *Science*. 329:1341-1345.

Leithner, A., A. Eichner, J. Müller, A. Reversat, M. Brown, J.P. Schwarz, J. Merrin, D.J.J. de Gorter, F. Schur, J. Bayerl, I. de Vries, S. Wieser, R. Hauschild, F.P.L. Lai, M. Moser, D. Kerjaschki, K. Rottner, J.V. Small, T.E.B. Stradal, and M. Sixt. 2016. Diversified actin protrusions promote environmental exploration but are dispensable for locomotion of leukocytes. *Nature Cell Biology*. 18:1253-1259.

Levayer, R., and T. Lecuit. 2012. Biomechanical regulation of contractility: spatial control and dynamics. *Trends in Cell Biology*. 22:61-81.

Lewis, A.K., and P.C. Bridgman. 1992. Nerve growth cone lamellipodia contain two populations of actin filaments that differ in organization and polarity. *The Journal of Cell Biology*. 119:1219-1243.

Li, D., L. Shao, B.-C. Chen, X. Zhang, M. Zhang, B. Moses, D.E. Milkie, J.R. Beach, J.A. Hammer, M. Pasham, T. Kirchhausen, M.A. Baird, M.W. Davidson, P. Xu, and E. Betzig. 2015. Extended-resolution structured illumination imaging of endocytic and cytoskeletal dynamics. *Science* 349:aab3500-aab3500.

Liang, L., J. Guan, Y. Zeng, J. Wang, X. Li, X. Zhang, and Y. Ding. 2011. Down-regulation of formin-like 2 predicts poor prognosis in hepatocellular carcinoma. *Human Pathology*. 42:1603-1612.

Linder, S., C. Wiesner, and M. Himmel. 2011. Degrading Devices: Invadosomes in Proteolytic Cell Invasion. *Annual Review of Cell and Developmental Biology*. 27:185-211.

Liu, Y.-J., M. Le Berre, F. Lautenschlaeger, P. Maiuri, A. Callan-Jones, M. Heuzé, T. Takaki, R. Voituriez, and M. Piel. 2015. Confinement and Low Adhesion Induce Fast Amoeboid Migration of Slow Mesenchymal Cells. *Cell*. 160:659-672.

Lizárraga, F., R. Poincloux, M. Romao, G. Montagnac, G. Le Dez, I. Bonne, G. Rigaill, G. Raposo, and P. Chavrier. 2009. Diaphanous-Related Formins Are Required for Invadopodia Formation and Invasion of Breast Tumor Cells. *Cancer Research*. 69:2792-2800.

Lohmer, L.L., M.R. Clay, K.M. Naegeli, Q. Chi, J.W. Ziel, E.J. Hagedorn, J.E. Park, R. Jayadev, and D.R. Sherwood. 2016. A Sensitized Screen for Genes Promoting Invadopodia Function In Vivo: CDC-42 and Rab GDI-1 Direct Distinct Aspects of Invadopodia Formation. *PLOS Genetics*. 12:e1005786.

Lundquist, E.A., P.W. Reddien, E. Hartwieg, H.R. Horvitz, and C.I. Bargmann. 2001. Three *C. elegans* Rac proteins and several alternative Rac regulators control axon guidance, cell migration and apoptotic cell phagocytosis. *Development*. 128:4475-4488.

Luther, P.K. 2000. Three-Dimensional Structure of a Vertebrate Muscle Z-band: Implications for Titin and α-Actinin Binding. *Journal of Structural Biology*. 129:1-16.

Machesky, L.M., and R.H. Insall. 1998. Scar1 and the related Wiskott-Aldrich syndrome protein, WASP, regulate the actin cytoskeleton through the Arp2/3 complex. *Curr. Biol.* 8:1347-1356.

Machesky, L.M., R.D. Mullins, H.N. Higgs, D.A. Kaiser, L. Blanchoin, R.C. May, M.E. Hall, and T.D. Pollard. 1999. Scar, a WASp-related protein, activates nucleation of actin filaments by the Arp2/3 complex. *Proceedings of the National Academy of Sciences of the United States of America*. 96:3739-3744.

Marchand, J.-B., D.A. Kaiser, T.D. Pollard, and H.N. Higgs. 2001. Interaction of WASP/Scar proteins with actin and vertebrate Arp2/3 complex. *Nature Cell Biology*. 3:76-82.

Matsuoka, T., and M. Yashiro. 2014. Rho/ROCK signaling in motility and metastasis of gastric cancer. *World Journal of Gastroenterology* 20:13756-13766.

Matus, D.Q., E. Chang, S.C. Makohon-Moore, M.A. Hagedorn, Q. Chi, and D.R. Sherwood. 2014. Cell Division and Targeted Cell Cycle Arrest Opens and Stabilizes Basement Membrane Gaps. *Nature Communications*. 5:4184-4184.

Matus, D.Q., X.-Y. Li, S. Durbin, D. Agarwal, Q. Chi, S.J. Weiss, and D.R. Sherwood. 2010. In Vivo Identification of Regulators of Cell Invasion Across Basement Membranes. *Science Signaling*. 3:1-9.

Matus, David Q., Lauren L. Lohmer, Laura C. Kelley, Adam J. Schindler, Abraham Q. Kohrman, M. Barkoulas, W. Zhang, Q. Chi, and David R. Sherwood. 2015. Invasive Cell Fate Requires G1 Cell-Cycle Arrest and Histone Deacetylase-Mediated Changes in Gene Expression. *Developmental Cell*. 35:162-174.

McClatchey, S.T.H., Z. Wang, L.M. Linden, E.L. Hastie, L. Wang, W. Shen, A. Chen, Q. Chi, and D.R. Sherwood. 2016. Boundary cells restrict dystroglycan trafficking to control basement membrane sliding during tissue remodeling. *eLife*. 5:e17218.

McGough, A.M., C.J. Staiger, J.-K. Min, and K.D. Simonetti. 2003. The gelsolin family of actin regulatory proteins: modular structures, versatile functions. *FEBS Lett.* 552:75-81.

Miki, H., S. Suetsugu, and T. Takenawa. 1998. WAVE, a novel WASP-family protein involved in actin reorganization induced by Rac. *EMBO Journal*. 17:6932-6941.

Miki, H., and T. Takenawa. 2003. Regulation of actin dynamics by WASP family proteins. *Journal of Biochemistry*. 134:309-313.

Morone, N., T. Fujiwara, K. Murase, R.S. Kasai, H. Ike, S. Yuasa, J. Usukura, and A. Kusumi. 2006. Three-dimensional reconstruction of the membrane skeleton at the plasma membrane interface by electron tomography. *The Journal of Cell Biology*. 174:851-862.

Morrissey, M.A., D.P. Keeley, E.J. Hagedorn, S.T.H. McClatchey, Q. Chi, D.H. Hall, and D.R. Sherwood. 2014. B-LINK: a hemicentin, plakin, and integrin-dependent adhesion system that links tissues by connecting adjacent basement membranes. *Developmental Cell*. 31:319-331.

Moulder, G.L., G.H. Cremona, J. Duerr, J.N. Stirman, S.D. Fields, W. Martin, H. Qadota, G.M. Benian, H. Lu, and R.J. Barstead. 2010. α-actinin is Required for Proper Assembly of Z-disk / Focal Adhesion-Like Structures and for Efficient Locomotion in Caenorhabditis elegans. *Journal of Molecular Biology*. 403:516-528.

Mullins, R.D., J.A. Heuser, and T.D. Pollard. 1998. The interaction of Arp2/3 complex with actin: Nucleation, high affinity pointed end capping, and formation of branching networks of filaments. *Proceedings of the National Academy of Sciences of the United States of America*. 95:6181-6186.

Murphy, D.A., and S.A. Courtneidge. 2011. The 'ins' and 'outs' of podosomes and invadopodia: characteristics, formation and function. *Nature Reviews Molecular Cell Biology*. 12:413-426.

Nezhad, A.S., and A. Geitmann. 2013. The cellular mechanics of an invasive lifestyle. *Journal of Experimental Botany* 64:4709-4728.

Nürnberg, A., T. Kitzing, and R. Grosse. 2011. Nucleating actin for invasion. *Nature Reviews Cancer*. 11:177-187.

Nusblat, L.M., A. Dovas, and D. Cox. 2011. The non-redundant role of N-WASP in podosome-mediated matrix degradation in macrophages. *European Journal of Cell Biology*. 90:205-212.

Ohta, Y., N. Suzuki, S. Nakamura, J.H. Hartwig, and T.P. Stossel. 1999. The small GTPase RalA targets filamin to induce filopodia. *Proceedings of the National Academy of Sciences of the United States of America*. 96:2122-2128.

Oikawa, T., H. Yamaguchi, T. Itoh, M. Kato, T. Ijuin, D. Yamazaki, S. Suetsugu, and T. Takenawa. 2004. PtdIns(3,4,5)P3 binding is necessary for WAVE2-induced formation of lamellipodia. *Nature Cell Biology*. 6:420-426.

Oser, M., H. Yamaguchi, C.C. Mader, J.J. Bravo-Cordero, M. Arias, X. Chen, V. DesMarais, J. van Rheenen, A.J. Koleske, and J. Condeelis. 2009. Cortactin regulates cofilin and N-WASp activities to control the stages of invadopodium assembly and maturation. *The Journal of Cell Biology*. 186:571-587.

Otey, C.A., and O. Carpen. 2004. α-actinin revisited: A fresh look at an old player. *Cell Motility and the Cytoskeleton*. 58:104-111.

Paluch, E., M. Piel, J. Prost, M. Bornens, and C. Sykes. 2005. Cortical Actomyosin Breakage Triggers Shape Oscillations in Cells and Cell Fragments. *Biophysical Journal*. 89:724-733.

Paszek, M.J., N. Zahir, K.R. Johnson, J.N. Lakins, G.I. Rozenberg, A. Gefen, C.A. Reinhart-King, S.S. Margulies, M. Dembo, D. Boettiger, D.A. Hammer, and V.M. Weaver. 2005. Tensional homeostasis and the malignant phenotype. *Cancer Cell*. 8:241-254.

Patel, F.B., Y.Y. Bernadskaya, E. Chen, A. Jobanputra, Z. Pooladi, K.L. Freeman, C. Gally, W.A. Mohler, and M.C. Soto. 2008. The WAVE/SCAR complex promotes polarized cell movements and actin enrichment in epithelia during C. elegans embryogenesis. *Developmental Biology*. 324:297-309.

Paul, N.R., J.L. Allen, A. Chapman, M. Morlan-Mairal, E. Zindy, G. Jacquemet, L. Fernandez del Ama, N. Ferizovic, D.M. Green, J.D. Howe, E. Ehler, A. Hurlstone, and P.T. Caswell. 2015. α5β1 integrin recycling promotes Arp2/3-independent cancer cell invasion via the formin FHOD3. *The Journal of Cell Biology*. 210:1013-1031.

Petrie, R.J., N. Gavara, R.S. Chadwick, and K.M. Yamada. 2012. Nonpolarized signaling reveals two disctinct modes of 3D cell migration. *The Journal of Cell Biology*. 197:439-455.

Petrie, R.J., and K.M. Yamada. 2012. At the leading edge of three-dimensional cell migration. *Journal of Cell Science*. 125:5917-5926.

Piekny, A.J., A. Wissmann, and P.E. Mains. 2000. Embryonic Morphogenesis in *Caenorhabditis elegans* Integrates the Activity of LET-502 Rho-Binding Kinase, MEL-11 Myosin Phosphatase, DAF-2 Insulin Receptor and FEM-2 PP2c Phosphatase. *Genetics*. 156:1671-1689.

Pinner, S., and E. Sahai. 2008. Imaging amoeboid cancer cell motility in vivo. *Journal of Microscopy*. 231:441-445.

Pollard, T.D. 1986. Rate constants for the reactions of ATP- and ADP-actin with the ends of actin filaments. *The Journal of Cell Biology*. 103:2747-2754.

Pollard, T.D., and G.G. Borisy. 2003. Cellular Motility Driven by Assembly and Disassembly of Actin Filaments. *Cell*. 112:453-465.

Pring, M., A. Weber, and M.R. Bubb. 1992. Profilin-actin complexes directly elongate actin filaments at the barbed end. *Biochemistry*. 31:1827-1836.

Randall, T.S., and E. Ehler. 2014. A formin-g role during development and disease. *European Journal of Cell Biology*. 93:205-211.

Reiner, D.J., and E.A. Lundquist. 2016. Small GTPases. *Wormbook*:1-99.

Revach, O.-Y., and B. Geiger. 2014. The interplay between the proteolytic, invasive, and adhesive domains of invadopodia and their roles in cancer invasion. *Cell Adhesion and Migration*. 8:215-225.

Revenu, C., R. Athman, S. Robine, and D. Louvard. 2004. The co-workers of actin filaments: from cell structures to signals. *Nature Reviews Molecular Cell Biology*. 5:635-646.

Rimann, I., and A. Hajnal. 2007. Regulation of anchor cell invasion and uterine cell fates by the egl-43 Evi-1 proto-oncogene in Caenorhabditis elegans. *Developmental Biology*. 308:187-195.

Rohatgi, R., L. Ma, H. Miki, M. Lopez, H. Kirchausen, T. Takenawa, and M. Kirschner. 1999. The interaction between N-Wasp and the Arp2/3 complex links Cdc42-dependent signals to actin assembly. *Cell*. 97:221-231.

Romero, S., C. Le Clainche, D. Didry, C. Egile, D. Pantaloni, and M.-F. Carlier. 2004. Formin is a processive motor that requires profilin to accelerate actin assembly and associated ATP hydrolysis. *Cell*. 119:419-429.

Rottner, K., B. Behrendt, J.V. Small, and J. Wehland. 1999. VASP dynamics during lamellipodia protrusion. *Nature Cell Biology*. 1:321-322.

Rotty, J.D., C. Wu, and J.E. Bear. 2013. New insights into the regulation and cellular functions of the Arp2/3 complex. *Nature Reviews Molecular Cell Biology*. 14:7-12.

Rowe, R.G., and S.J. Weiss. 2009. Navigating ECM Barriers at the Invasive Front: The Cancer Cell–Stroma Interface. *Annual Review of Cell and Developmental Biology.* 25:567-595.

Rust, M.J., M. Bates, and X. Zhuang. 2006. Stochastic optical reconstruction microscopy (STORM) provides sub-diffraction-limit image resolution. *Nature Methods*. 3:793-795.

Sabeh, F., I. Ota, K. Holmbeck, H. Birkedal-Hansen, P. Soloway, M. Balbin, C. Lopez-Otin, S. Shapiro, M. Inada, S. Krane, E. Allen, D. Chung, and S.J. Weiss. 2004. Tumor cell traffic through the extracellular matrix is controlled by the membrane-anchored collagenase MT1-MMP. *The Journal of Cell Biology*. 167:769-781.

Sabeh, F., R. Shimizu-Hirota, and S.J. Weiss. 2009. Protease-dependent versus -independent cancer cell invasion programs: three-dimensional amoeboid movement revisited. *The Journal of Cell Biology*. 185:11-19.

Saez, E., S.E. Rutberg, E. Mueller, H. Oppenheim, J. Smoluk, S.H. Yuspa, and B.M. Spiegelman. 1995. c-fos is required for malignant progression of skin tumors. *Cell*. 82:721-732.

Sawa, M., S. Suetsugu, A. Sugimoto, H. Miki, M. Yamamoto, and T. Takenawa. 2003. Essential role of the *C.elegans* Arp2/3 complex in cell migration during ventral enclosure. *Journal of Cell Science*. 116:1505-1518.

Schliwa, M., and J. van Blerkom. 1981. Structural interaction of cytoskeletal components. *The Journal of Cell Biology*. 90:222-235.

Schmid, T., and A. Hajnal. 2015. Signal transduction during *C. elegans* vulval development: a NeverEnding story. *Current Opinion in Genetics and Development*. 32:1-9.

Schoumacher, M., R.D. Goldman, D. Louvard, and D.M. Vignjevic. 2010. Actin, microtubules, and vimentin intermediate filaments cooperate for elongation of invadopodia. *The Journal of Cell Biology*. 189:541-556.

Sept, D., and J.A. McCammon. 2001. Thermodynamics and Kinetics of Actin Filament Nucleation. *Biophysical Journal*. 81:667-674.

Shakir, M.A., K. Jiang, E.C. Struckhoff, R.S. Demarco, F.B. Patel, M.C. Soto, and E.A. Lundquist. 2008. The Arp2/3 activators WAVE and WASP have distinct genetic interactions with Rac GTPases in *Caenorhabditis elegans* axon guidance. *Genetics*. 179:1957-1971.

Shao, H., S. Li, S.C. Watkins, and A. Wells. 2014. α-Actinin-4 Is Required for Amoeboid-type Invasiveness of Melanoma Cells. *Journal of Biological Chemistry*. 289:32717-32728.

Shaye, Daniel D., and I. Greenwald. 2015. The Disease-Associated Formin INF2/EXC-6 Organizes Lumen and Cell Outgrowth during Tubulogenesis by Regulating F-Actin and Microtubule Cytoskeletons. *Developmental Cell*. 32:743-755.

Shelton, C.A., J.C. Carter, G.C. Ellis, and B. Bowerman. 1999. The Nonmuscle Myosin Regulatory Light Chain Gene *mlc-4* Is Required for Cytokinesis, Anterior-Posterior Polarity, and Body Morphology during *Caenorhabditis elegans* Embryogenesis. *The Journal of Cell Biology*. 146:439-451.

Shemesh, T., T. Otomo, M.K. Rosen, A.D. Bershadsky, and M.M. Kozlov. 2005. A novel mechanism of actin filament processive capping by formin: solution of the rotation paradox. *The Journal of Cell Biology*. 170:889-893.

Sherwood, D.R., J.A. Butler, J.M. Kramer, and P.W. Sternberg. 2005. FOS-1 Promotes Basement-Membrane Removal during Anchor-Cell Invasion in *C. elegans*. *Cell*. 121:951-962.

Sherwood, D.R., and P.W. Sternberg. 2003. Anchor Cell Invasion into the Vulval Epithelium in C. elegans. *Developmental Cell*. 5:21-31.

Shroff, H., H. White, and E. Betzig. 2013. Photoactivated Localization Microscopy (PALM) of Adhesion Complexes. *Current Protocols in Cell Biology*. 58:4.21.21-24.21.28.

Skop, A.R., H. Liu, J. Yates, B.J. Meyer, and R. Heald. 2004. Dissection of the Mammalian Midbody Proteome Reveals Conserved Cytokinesis Mechanisms. *Science*. 305:61-66.

Small, J.V., T. Stradal, E. Vignal, and K. Rottner. 2002. The lamellipodium: where motility begins. *Trends in Cell Biology*. 12:112-120.

Smith, B.A., S.B. Padrick, L.K. Doolittle, K. Daugherty-Clarke, I.R. Corrêa, M.-Q. Xu, B.L. Goode, M.K. Rosen, and J. Gelles. 2013. Three-color single molecule imaging shows WASP detachment from Arp2/3 complex triggers actin filament branch formation. *eLife*. 2:e01008.

Stefan, W.H., J.S. Steffen, B. Mark, Z. Xiaowei, H. Rainer, J.B. Martin, B. Joerg, S. Gleb, H. Harald, T. Philip, H. Alf, J. Stefan, T. Ilaria, C. Laurent, L. Brahim, E. Helge, J.D. Simon, E. Christian, K. David, I.W. Katrin, V. Giuseppe, C. Marco, D. Alberto, and C. Thorben. 2015. The 2015 super-resolution microscopy roadmap. *Journal of Physics D: Applied Physics*. 48:443001.

Stevenson, R.P., D. Veltman, and L.M. Machesky. 2012. Actin-bundling proteins in cancer progression at a glance. *Journal of Cell Science*. 125:1073-1079.

Stossel, T.P., J. Condeelis, L. Cooley, J.H. Hartwig, A. Noegel, M. Schleicher, and S.S. Shapiro. 2001. Filamins as integrators of cell mechanics and signalling. *Nature Reviews Molecular Cell Biology*. 2:138-145.

Suei, S., J. Plastino, and L. Kreplak. 2012. Fascin and VASP synergistically increase the Young's modulus of actin comet tails. *J. Struct. Biol.* 177:40-45.

Suraneni, P., B. Rubinstein, J.R. Unruh, M. Durnin, D. Hanein, and R. Li. 2012. The Arp2/3 complex is required for lamellipodia extension and directional fibroblast cell migration. *The Journal of Cell Biology*. 197:239-251.

Svitkina, T.M., and G.G. Borisy. 1999. Arp2/3 Complex and Actin Depolymerizing Factor/Cofilin in Dendritic Organization and Treadmilling of Actin Filament Array in Lamellipodia. *The Journal of Cell Biology*. 145:1009-1026.

Svitkina, T.M., E.A. Bulanova, O.Y. Chaga, D.M. Vignjevic, S.-i. Kojima, J.M. Vasiliev, and G.G. Borisy. 2003. Mechanism of filopodia initiation by reorganization of a dendritic network. *The Journal of Cell Biology*. 160:409-421.

Takahashi, K., and K. Suzuki. 2011. WAVE2, N-WASP, and mena facilitate cell invasion via phosphatidylinositol 3-kinase-dependent local accumulation of actin filaments. *Journal of Cellular Biochemistry*. 112:3421-3429.

Takenawa, T. 2010. Phosphoinositide-binding interface proteins involved in shaping cell membranes. *Proceedings of the Japan Academy. Series B, Physical and Biological Sciences*. 86:509-523.

Testa, I., Nicolai T. Urban, S. Jakobs, C. Eggeling, Katrin I. Willig, and Stefan W. Hell. 2012. Nanoscopy of Living Brain Slices with Low Light Levels. *Neuron*. 75:992-1000.

Thiam, H.-R., P. Vargas, N. Carpi, C.L. Crespo, M. Raab, E. Terriac, M.C. King, J. Jacobelli, A.S. Alberts, T. Stradal, A.-M. Lennon-Dumenil, and M. Piel. 2016. Perinuclear Arp2/3-driven actin polymerization enables nuclear deformation to facilitate cell migration through complex environments. *Nature Communications*. 7:10997.

Thiery, J.P. 2002. Epithelial-mesenchymal transitions in tumour progression. *Nature Reviews Cancer*. 2:442-454.

Tinevez, J.-Y., U. Schulze, G. Salbreux, J. Roensch, J.-F. Joanny, and E. Paluch. 2009. Role of cortical tension in bleb growth. *Proceedings of the National Academy of Sciences of the United States of America*. 106:18581-18586.

Tseng, Y., T.P. Kole, J.S.H. Lee, E. Fedorov, S.C. Almo, B.W. Schafer, and D. Wirtz. 2005. How actin crosslinking and bundling proteins cooperate to generate an enhanced cell mechanical response. *Biochemical and Biophysical Research Communications*. 334:183-192.

Vargas, P., P. Maiuri, M. Bretou, P.J. Saez, P. Pierobon, M. Maurin, M. Chabaud, D. Lankar, D. Obino, E. Terriac, M. Raab, H.-R. Thiam, T. Brocker, S.M. Kitchen-Goosen, A.S. Alberts, P. Sunareni, S. Xia, R. Li, R. Voituriez, M. Piel, and A.-M. Lennon-Dumenil. 2016. Innate control of actin nucleation determines two distinct migration behaviours in dendritic cells. *Nature Cell Biology*. 18:43-53.

Vestweber, D. 2015. How leukocytes cross the vascular endothelium. *Nature Reviews Immunology*. 15:692-704.

Vicente-Manzanares, M., and A.R. Horwitz. 2011. Adhesion dynamics at a glance. *Journal of Cell Science*. 124:3923-3927.

Vignjevic, D., S.-i. Kojima, Y. Aratyn, O. Danciu, T. Svitkina, and G.G. Borisy. 2006. Role of fascin in filopodial protrusion. *The Journal of Cell Biology*. 174:863-875.

Vignjevic, D., M. Schoumacher, N. Gavert, K.-P. Janssen, G. Jih, M. Laé, D. Louvard, A. Ben-Ze'ev, and S. Robine. 2007. Fascin, a Novel Target of β-Catenin-TCF Signaling, Is Expressed at the Invasive Front of Human Colon Cancer. *Cancer Research*. 67:6844-6853.

Voisin, M.-B., D. Pröbstl, and S. Nourshargh. 2010. Venular Basement Membranes Ubiquitously Express Matrix Protein Low-Expression Regions: Characterization in Multiple Tissues and Remodeling during Inflammation. *The American Journal of Pathology*. 176:482-495.

Volkmann, N., D. DeRosier, P. Matsudaira, and D. Hanein. 2001. An Atomic Model of Actin Filaments Cross-Linked by Fimbrin and Its Implications for Bundle Assembly and Function. *The Journal of Cell Biology*. 153:947-956.

Walck-Shannon, E., B. Lucas, I. Chin-Sang, D. Reiner, K. Kumfer, H. Cochran, W. Bothfeld, and J. Hardin. 2016. CDC-42 orients cell migration during epithelial intercalation in the *Caenorhabditis elegans* epidermis. *PLOS Genetics*. 12:e1006415.

Walck-Shannon, E., D. Reiner, and J. Hardin. 2015. Polarized Rac-dependent protrusions drive epithelial intercalation in the embryonic epidermis of *C. elegans*. *Development*. 142:3549-3560.

Wang, L., W. Shen, S. Lei, D. Matus, D. Sherwood, and Z. Wang. 2014a. MIG-10 (Lamellipodin) stabilizes invading cell adhesion to basement membrane and is a negative transcriptional target of EGL-43 in C. elegans. *Biochemical and Biophysical Research Communications*. 452:328-333.

Wang, Z., Q. Chi, and D.R. Sherwood. 2014b. MIG-10 (lamellipodin) has netrin-independent functions and is a FOS-1A transcriptional target during anchor cell invasion in *C. elegans*. *Development*. 141:1342-1353.

Wang, Z., L.M. Linden, K.M. Naegeli, J.W. Ziel, Q. Chi, E.J. Hagedorn, N.S. Savage, and D.R. Sherwood. 2014c. UNC-6 (netrin) stabilizes oscillatory clustering of the UNC-40 (DCC) receptor to orient polarity. *The Journal of Cell Biology*. 206:619-633.

Watanabe, N., T. Kato, A. Fujita, T. Ishizaki, and S. Narumiya. 1999. Cooperation between mDia1 and ROCK in Rho-induced actin reorganization. *Nature Cell Biology*. 1:136-143.

Willig, K.I., R.R. Kellner, R. Medda, B. Hein, S. Jakobs, and S.W. Hell. 2006a. Nanoscale resolution in GFP-based microscopy. *Nature Methods*. 3:721-723.

Willig, K.I., S.O. Rizzoli, V. Westphal, R. Jahn, and S.W. Hell. 2006b. STED microscopy reveals that synaptotagmin remains clustered after synaptic vesicle exocytosis. *Nature*. 440:935-939.

Wissmann, A., J. Ingles, and P.E. Mains. 1999. TheCaenorhabditis elegans mel-11Myosin Phosphatase Regulatory Subunit Affects Tissue Contraction in the Somatic Gonad and the Embryonic Epidermis and Genetically Interacts with the Rac Signaling Pathway. *Developmental Biology*. 209:111-127.

Withee, J., B. Galligan, N. Hawkins, and G. Garriga. 2004. *Caenorhabditis elegans* WASP and Ena/VASP protiens play compensatory roles in morphogenesis and neuronal cell migration. *Genetics*. 167:1165-1176.

Wolf, K., I. Mazo, H. Leung, K. Engelke, U.H. von Andrian, E.I. Deryugina, A.Y. Strongin, E.-B. Bröcker, and P. Friedl. 2003. Compensation mechanism in tumor cell migration: mesenchymal–amoeboid transition after blocking of pericellular proteolysis. *The Journal of Cell Biology*. 160:267-277.

Wolf, K., M. te Lindert, M. Krause, S. Alexander, J. te Riet, A.L. Willis, R.M. Hoffman, C.G. Figdor, S.J. Weiss, and P. Friedl. 2013. Physical limits of cell migration: Control by ECM space and nuclear deformation and tuning by proteolysis and traction force. *The Journal of Cell Biology*. 201:1069-1084.

Wood, J.A., S.J. Liliensiek, P. Russell, P.F. Nealey, and C.J. Murphy. 2010. Biophysical Cueing and Vascular Endothelial Cell Behavior. *Materials*. 3:1620.

Wu, C., S.B. Asokan, M.E. Berginski, E.M. Haynes, N.E. Sharpless, J.D. Griffith, S.M. Gomez, and J.E. Bear. 2012. Arp2/3 is critical for lamellipodia and response to extracellular matrix cues but is dispensable for chemotaxis. *Cell*. 148:973-987.

Xu, Y., T.A. Bismar, J. Su, B. Xu, G. Kristiansen, Z. Varga, L. Teng, D.E. Ingber, A. Mammoto, R. Kumar, and M.A. Alaoui-Jamali. 2010. Filamin A regulates focal adhesion disassembly and suppresses breast cancer cell migration and invasion. *The Journal of Experimental Medicine*. 207:2421-2437.

Yamaguchi, H., M. Lorenz, S. Kempiak, C. Sarmiento, S. Coniglio, M. Symons, J. Segall, R. Eddy, H. Miki, T. Takenawa, and J. Condeelis. 2005. Molecular mechanisms of invadopodium formation: the role of the N-WASP–Arp2/3 complex pathway and cofilin. *The Journal of Cell Biology*. 168:441-452.

Yang, C., and T. Svitkina. 2011. Filopodia initiation. *Cell Adhesion and Migration*. 5:402-408.

Yu, X., T. Zech, L. McDonald, E.G. Gonzalez, A. Li, I. Macpherson, J.P. Schwarz, H. Spence, K. Futó, P. Timpson, C. Nixon, Y. Ma, I.M. Anton, B. Visegrády, R.H. Insall, K. Oien, K. Blyth, J.C. Norman, and L.M. Machesky. 2012. N-WASP coordinates the delivery and F-actin–mediated capture of MT1-MMP at invasive pseudopods. *The Journal of Cell Biology*. 199:527-544.

Zalevsky, J., I. Grigorova, and R.D. Mullins. 2001a. Activation of the Arp2/3 Complex by the *Listeria* ActA Protein. *Journal of Biological Chemistry*. 276:3468-3475.

Zalevsky, J., L. Lempert, H. Kranitz, and R.D. Mullins. 2001b. Different WASP family proteins stimulate different Arp2/3 complex-dependent actin-nucleating activities. *Current Biology*. 11:1903-1913.

Zhu, X.-L., L. Liang, and Y.-Q. Ding. 2008. Overexpression of FMNL2 is closely related to metastasis of colorectal cancer. *International Journal of Colorectal Disease*. 23:1041.

Zhu, Z., Y. Chai, Y. Jiang, W. Li, H. Hu, W. Li, J.-W. Wu, Z.-X. Wang, S. Huang, and G. Ou. 2016. Functional Coordination of WAVE and WASP in C. elegans Neuroblast Migration. *Developmental Cell*. 39:224-238.

Ziel, J.W., E.J. Hagedorn, A. Audhya, and D.R. Sherwood. 2009. UNC-6 (Netrin) Orients the Invasive Membrane of the Anchor Cell in *C. elegans*. *Nature Cell Biology*. 11:183-189.

ANNEXE 1: PUBLISHED REVIEW ARTICLE 2017

Cytoskeleton Dynamics: Actin in Cell Invasion

Rodrigo Cáceres, *Institut Curie, PSL Research University, CNRS, Université Paris Descartes, Paris, France*

Julie Plastino, *Institut Curie, PSL Research University, CNRS, Université Pierre et Marie Curie,, Paris, France*

Advanced article

Article Contents

Online posting date: 17th April 2017

Basement membrane (BM) is a dense sheet of specialised extracellular matrix that separates epithelial layers of cells from the underlying tissue. The penetration of cells through BM barriers, called 'invasion', is an important process during normal tissue development and in cancer metastasis. To enable invasion, the cell adopts different shapes and creates different protrusive structures powered mainly by actin cytoskeleton dynamics. However, the exact cytoskeletal strategy that the cell uses to cross the physical BM barrier depends on the physiological context and the physical environment, as observed by examining actin structures in invading cancer and immune cells, and in cells that invade during developmental processes such as angiogenesis and anchor cell invasion in *Caenorhabditis elegans*.

Introduction

Basement membrane (BM) is a two-dimensional layer of specialised extracellular matrix (ECM) composed principally of laminin, type IV collagen polymers and glycoproteins that separate epithelia from the underlying tissue (Hohenester and Yurchenco, 2013). Owing to the small pore size of BM, non-permissive to cell passage, cells must enable specific cellular programs to invade across BMs. Cell invasion occurs during tissue development and also in pathologies such as cancer progression and is controlled by genetics and signalling, as well as by the physical properties and mechanical activity of invasive cells (Wirtz *et al.*, 2011).

eLS subject area: Cell Biology

How to cite:
Cáceres, Rodrigo and Plastino, Julie (April 2017) Cytoskeleton Dynamics: Actin in Cell Invasion. In: eLS. John Wiley & Sons, Ltd: Chichester.
DOI: 10.1002/9780470015902.a0001254.pub2

The mechanical properties of cells are determined in large part by the actin cytoskeleton, a network of biopolymers that continuously assemble and disassemble inside the cell in a directional manner due to the polarity of actin filaments that have dynamic (barbed) ends and less dynamic (pointed) ends (Blanchoin *et al.*, 2014). Filaments also slide past each other by the action of the molecular motor myosin, which can recognise the polarity of the actin filament and move directionally. One of the main structures of the moving cell is the actin-rich protrusion, the lamellipodium, formed by polarised polymerisation of the actin network beneath the plasma membrane, which creates enough force to deform the membrane and pull the cell forward via adhesions to the substrate (Pollard and Borisy, 2003). Filopodia, finger-like actin protrusions, are also observed at the leading edge of cells (Faix and Rottner, 2006). At the back of the moving cell is the cell cortex, an actomyosin network that lies just underneath the plasma membrane. Myosin contraction of actin filaments serves to squeeze forward the back of the cell during cell motility and also drives other aspects of cell motility and cell shape changes (Salbreux *et al.*, 2012). Cycles of contraction and detachment from the substrate at the back of the cell, coupled with protrusion and the formation of new cell–matrix adhesions at the front, allow the cell to move forward.

Depending on the environment, different strategies are employed by the cell in order to cross BM barriers. In most invasion events, the breach in the BM is mediated by a lamellipodia-type protrusion, generally known as an invadopodium. Actin assembly dynamics in invadopodia are essential for invasion (Nürnberg *et al.*, 2011). Making holes in BMs is also known to depend on matrix metalloproteases (MMPs) that are displayed on the surface of invadopodia and digest the matrix fibres (Rowe and Weiss, 2009). However, protease-independent mechanisms of invasion have also been reported, involving the cell squeezing through matrix gaps due to actomyosin contractility (Wolf *et al.*, 2003).The objective of this article is to summarise the roles of cytoskeleton dynamics and actin-binding proteins in different modes of cell invasion. Studies on cancer cell invasion, immune cell invasion of endothelia and developmental models such as angiogenesis and anchor cell (AC) invasion in *Caenorhabditis elegans* will be used to illustrate the different strategies used by cells to breach BMs.

The Actin Cytoskeleton

To better understand the actin structures that participate in cell invasion, we will briefly introduce the main concepts of actin architecture and the role of actin-binding proteins in different structures. For more details, see also Blanchoin *et al.* (2014) and **Actin and Actin Filaments**.

Branched networks

Cellular lamellipodia are composed principally of branched actin networks produced by the activity of the Arp2/3 complex (Pollard and Borisy, 2003). This complex catalyses the polymerisation of a new actin filament on the side of a preexisting filament and is thus called 'a nucleator', creating a Y-branched actin structure. The Arp2/3 complex on its own has a very low nucleating capacity and must be activated by a nucleation-promoting factor from the WASP (Wiskott–Aldrich Syndrome protein)/WAVE family of proteins. The activity of WASP/WAVE proteins, which are constitutively inactive due to inhibitory interactions, is in turn controlled by Rho family GTPases (Rho, Cdc42 and Rac) and by the lipids phosphatidylinositol-(4,5)-bisphosphate (PIP2) and phosphatidylinositol-(3,4,5)-bisphosphate (PIP3) [for review, see Campellone and Welch, (2010)]. For WASP activation, in response to extra- or intracellular signals, the autoinhibited conformation of WASP is recruited to the plasma membrane through binding to membrane-bound Cdc42-GTP which, in cooperation with PIP2, switches WASP into an active conformation. On the other hand, WAVE, which exists in an inhibited complex with other components, is activated by binding PIP3 and via an indirect interaction with Rac-GTP. Both mechanisms expose the binding site for the Arp2/3 complex on the WASP/WAVE molecule and thus trigger Arp2/3 complex-based actin assembly. Another important component of actin networks nucleated by the Arp2/3 complex is the protein cortactin. Cortactin synergises with WASP to enhance Arp2/3 complex activation by triggering the release of WASP from nascent branch points, permitting new filaments to elongate from the branching point [(Blanchoin *et al.*, 2014) and references therein].

Two other important components for branched actin network dynamics are capping proteins and ADF/cofilin. Capping protein binds growing filament ends, stopping their growth, and is believed to promote branched network growth by helping to maintain the pool of monomeric actin for branch formation and elongation. Similarly, ADF/cofilin, in association with other cellular factors such as Aip1 in the cell, severs filaments, thus contributing to actin dynamics by creating more filament ends that can disassemble to provide monomers for subsequent rounds of polymerisation [(Blanchoin *et al.*, 2014) and references therein].

Unbranched filament arrangements

The Arp2/3 complex is not the only actin polymerisation nucleator in the cell. There exists another class of nucleators that form unbranched filaments, including a family of proteins called formins. Formins exist in an inactive, autoinhibited conformation that can be switched to an active conformation by interaction with Rho-GTP or Cdc42-GTP. In the active conformation, the formin homology domains FH1 and FH2 work together to nucleate and elongate unbranched filaments, with FH2 attaching to the growing filament end and FH1 recruiting profilin–actin to fuel barbed end elongation (Goode and Eck, 2007). The dynamics of growing filaments is also controlled by Ena/VASP proteins, which enhance barbed end elongation, compete with capping protein and crosslink filaments together (Bear and Gertler, 2009). Unbranched filaments formed by formins and Ena/VASP proteins can organise into parallel bundles, with barbed ends pointing in the same direction, and such structures are preferentially stabilised and rigidified by actin crosslinking proteins such as fascin. *In vivo* such structures are observed in filopodia. Unbranched filaments can also adopt an antiparallel orientation in bundles stabilised by α-actinin, while crosslinkers such as plastin/fimbrin bundle both parallel and antiparallel filaments. Plastin/fimbrin and α-actinin, as well as filamin, a T-crosslinker, confer mechanical stability to unorganised networks formed by both formins and the Arp2/3 complex (Blanchoin *et al.*, 2014)

Actomyosin cortex

Another actin structure in the cell, important for cell shape changes, is the cell cortex. The cortex is a layer of actin attached to the inner leaflet of the plasma membrane by the ERM proteins (ezrin, radixin and moesin), which have the ability to interact with both the plasma membrane and actin filaments (McClatchey and Fehon, 2009). The actin layer also contains minifilaments of myosin that can contract the actin network due to their bipolar nature. The actin network in the cell cortex is generated by both Arp2/3 complex- and formin-based nucleation, making a mix of branched and unbranched filaments (Bovellan *et al.*, 2014). The balance between branched and unbranched filaments, their interaction with myosin mini filaments and the actin crosslinkers α-actinin and filamin act together to tune the properties of the cortical actomyosin network.

The actomyosin cortex dynamically polymerises, depolymerises and contracts, deforming the plasma membrane. However, if the attachment between the cortex and the membrane ruptures or if a rupture occurs in the cortex itself, a phenomenon known as blebbing occurs (Charras and Paluch, 2008). A bleb is a bubble of naked membrane that is forced out by myosin contraction of the cortex of the cell, downstream of Rho/ROCK signalling. This membrane bulge will be either retracted or stabilised by subsequent actin polymerisation to make a protrusion. In the latter case, cellular blebs can drive migration, in what is commonly called amoeboid migration based on its resemblance to the bleb-based motility of amoeba.

Actin Cytoskeleton in Cancer Cell Invasion

One of the first steps of cancer metastasis from epithelial tissues, the origin of many cancers, is the invasion of tumour cells across the BM that underlies the epithelia. They subsequently invade the

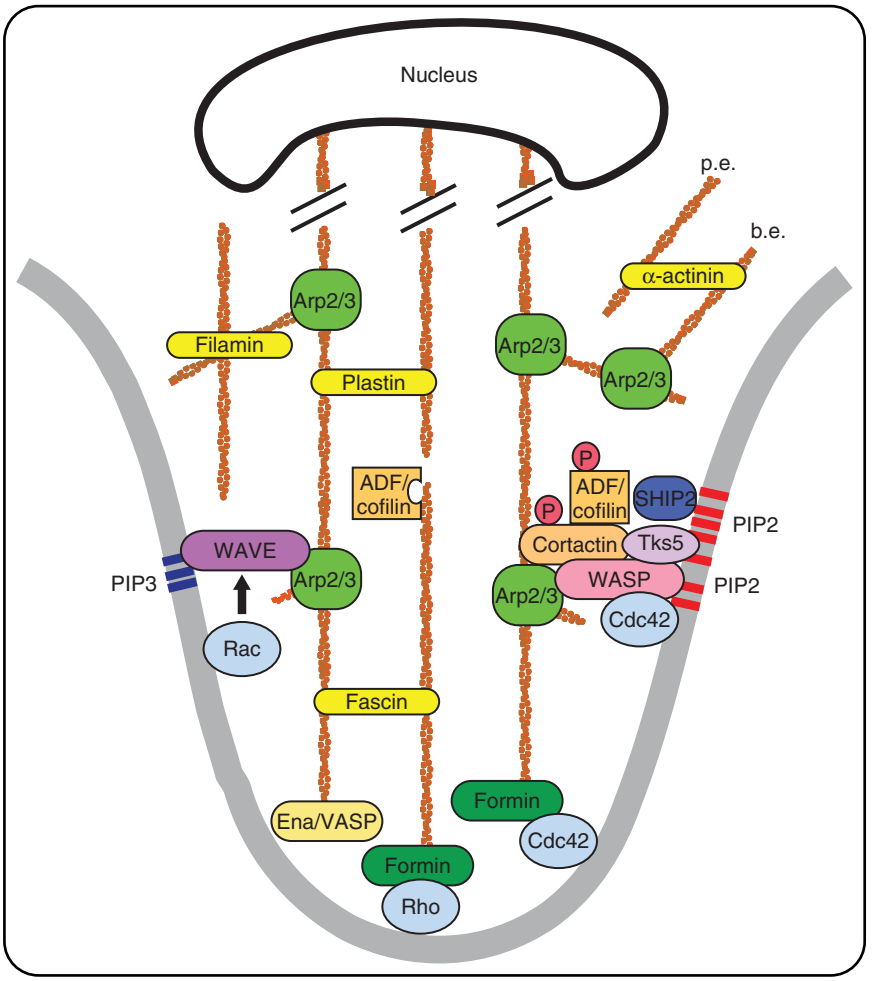

Figure 1 **Actin biochemistry in invadopodia**. Scheme of a hypothetical invadopodium, summarising all actin-binding proteins reported to be present in invasive structures in different contexts. The lipid bilayer of the cell membrane is represented by a thick grey line. Actin filaments are represented in orange, with barbed ends labelled 'b.e.' and pointed ends labelled 'p.e.'.

stroma and migrate towards the blood stream, from which they are disseminated to new sites to develop metastasis. Two main modes of cancer cell invasion have been described: mesenchymal and amoeboid.

Mesenchymal-type invasion

The epithelial–mesenchymal transition is a process by which epithelial cells lose their polarity and their cell–cell adhesion attributes that make them part of a cohesive tissue (Thiery, 2002). Once the cell is no longer part of the epithelial tissue, it can acquire characteristics that allow it to move and invade, including increased adhesion to the substrate and the production of actin-rich protrusions capable of remodelling the ECM, invadopodia (**Figure 1**).

There is very little structural information concerning the actin network of invadopodia, but one electron microscopy study indicates that invadopodia are composed of a mixture of a dendritic, branched network and unbranched, bundled filaments (Schoumacher *et al.*, 2010). In keeping with this, both formins and the Arp2/3 complex are necessary for invadopodia formation (Nürnberg *et al.*, 2011). The dynamics of Arp2/3 complex-based networks in invadopodia have been shown to be controlled by an interplay between the actin-binding proteins ADF/cofilin and cortactin, modified by phosphorylation (Sibony-Benyamini and Gil-Henn, 2012). However, it is not entirely clear what the upstream activator of the Arp2/3 complex is for invadopodia formation. As mentioned before, both WASP and WAVE can activate the Arp2/3 complex; however, only N-WASP has been clearly visualised in invadopodia, with WAVE localisation very dim or absent (Yamaguchi *et al.*, 2005). Other studies show that the inhibition of different forms of WAVE can upregulate or downregulate cancer cell invasion, depending on the context (Kurisu and Takenawa, 2010).Other actin-binding proteins associated with invadopodia and enhanced invasion efficiency are the Ena/VASP proteins and various filament bundling proteins, including α-actinin, fascin, filamin and plastin/fimbrin (Stevenson *et al.*, 2012) .

How all of these proteins come together temporally to construct an invadopodium is not clear. One study presents at least a partial picture involving some of the previously mentioned components (Sharma *et al.*, 2013). Invadopodia precursors are initiated by the association of cofilin, cortactin, actin and N-WASP, which is stabilised by the adaptor protein Tks5 that also binds PIP2 at the future invadopodial membrane. The maturation phase involves intense actin polymerisation, augmented by the recruitment of SHIP2, a 5′-inositol phosphatase, that locally produces more PIP2, thus retaining the Tks5 complex at the invading membrane and maintaining strong polymerisation (**Figure 1**). Other studies indicate that there is a subsequent elongation phase involving filopodia-type machinery, including fascin (Schoumacher *et al.*, 2010). A recent study shows that the distal ends of invadopodia extend into the cytosol and abut the nucleus, indenting it (Revach *et al.*, 2015). This implies that mature invadopodia are mechanically supported for invasion by bracing against the nucleus, 'pushing off' from the relatively rigid nuclear surface to help drive the protrusion through the ECM.

Amoeboid-type invasion

Cancer cells have also been reported to undergo bleb-based invasion, independent of invadopodia. For example, cancer cells migrating in three-dimensional matrices via invadopodia switch to amoeboid motion upon inhibition of MMPs (Wolf *et al.*, 2003). From this study, it was concluded that when BM holes cannot be made by digestion and actin pushing, cells use actomyosin contractility to squeeze through existing BM gaps. Switches in motility mode can also be observed in two-dimensional situations, where inhibiting lamellipodia by reducing the Arp2/3 complex or reducing cell–substrate adhesion triggers bleb-based motility, while increasing lamellipodial dynamics by activating Rac suppresses bleb formation (Bergert *et al.*, 2012). For some cancer cell types in three-dimensional environments, a rounded migration mode is observed with bleb-like protrusions at the back of the cell (Poincloux *et al.*, 2011). This motility mode is independent of the Arp2/3 complex but dependent on actomyosin contractility components that are believed to squeeze the cell through the ECM. Similar behaviour is observed when cancer cells are confined in channels passivated to decrease the level of cell adhesion to the substrate (Liu *et al.*, 2015). Under these conditions, slow-moving mesynchymal-type cells show fast bleb-based locomotion. Overall, it is clear that invading cancer cells can exhibit both mesenchymal and amoeboid modes of invasion and can switch between the two depending on the three-dimensional environment and the balance among actin protrusivity, actomyosin contractility and adhesion (Lämmermann and Sixt, 2009).

Actin Cytoskeleton in Invasion in Nonpathological Contexts

Actin in anchor cell invasion in *C. elegans*

Most of what is known about the role of actin cytoskeleton in cell invasion comes from the study of cultured cancer cells invading artificial BM mimics due to the difficulty of studying cancer cell invasion in living animals. BM mimics do not reflect the stiff microenvironment of the tumour (Paszek *et al.*, 2005), and the invadopodia observed in such conditions may therefore not be representative of what happens *in vivo*. In this context, it is useful to study cell invasion in near native conditions, using developmental models where nonpathologic invasion occurs at specified times during organ development. An example of such a process is AC invasion in the development of the vulva of *C. elegans*. This process starts at an early larval stage of *C. elegans*, where the uterine and vulva cells are separated by a double BM, one laid down by the vulval epithelial cells and the other by the gonadal tissue. The double BM is held together by a tight adhesion known as BM-LINKage (B-LINK), consisting of a hemicentin linker between the adjacent BMs that is regulated by signalling from the AC (Morrissey *et al.*, 2014). During the third larval stage, the AC pierces the BM by extending a protrusion, making a hole that will later become the vulva (**Figure 2a**).

The AC protrusion resembles cancer cell invadopodia visually and also in some important biochemical respects (**Figure 2b**). The AC protrusion is full of actin filaments, and a mutant for ADF/cofilin (UNC-60), which accumulates large amounts of nondynamic filamentous actin in its AC, shows a drastically reduced invasion efficiency (Hagedorn *et al.*, 2014). From this study, it appears that dynamic actin filaments must be present at the invading membrane to actuate invasion, as is the case in invasive cancer cells. Indeed, much of the signalling that happens in the AC could potentially feed into actin dynamics, including the netrin-DCC pathway. Netrin (UNC-6) is produced by the ventral nerve cord, diffuses to the AC and binds to the DCC receptor (UNC-40) on the AC membrane (Hagedorn *et al.*, 2013; Wang *et al.*, 2014; Ziel *et al.*, 2009). This receptor polarises PIP2 to the AC invading membrane (Ziel *et al.*, 2009), which could in turn participate in the activation of actin polymerisation as discussed earlier. Indeed, the same study shows that a double mutant of two *C. elegans* RacGTPases, MIG-2 and CED-10, displays a significant reduction in invasion, suggesting the participation of downstream effectors such as WAVE and the Arp2/3 complex (Ziel *et al.*, 2009). Loss of another GTPase, Cdc-42, as well as its downstream effector WASP (WSP-1), also results in delayed BM breaching (Lohmer *et al.*, 2016). Two other actin-binding proteins important for actin dynamics in lamellipodia, Ena/VASP (UNC-34) and lamellipodin (MIG-10), are also known to contribute to AC invasion (Wang *et al.*, 2014).

Future work will address what exact combination of actin polymerisation nucleators and actin filament bundlers is necessary for AC invasion as well as the potential role of myosin in this process. It is interesting to note that certain components known to be key for invasion of cancer cells, such as fascin and cortactin, are lacking in the *C. elegans* genome, implying that other molecules fulfil these roles in AC invasion.

Actin in sprouting angiogenesis

The term 'angiogenesis' commonly refers to the process of vessel growth, including vessel sprouting from pre-existing ones. In stable vessels, endothelial cells typically form a monolayer of

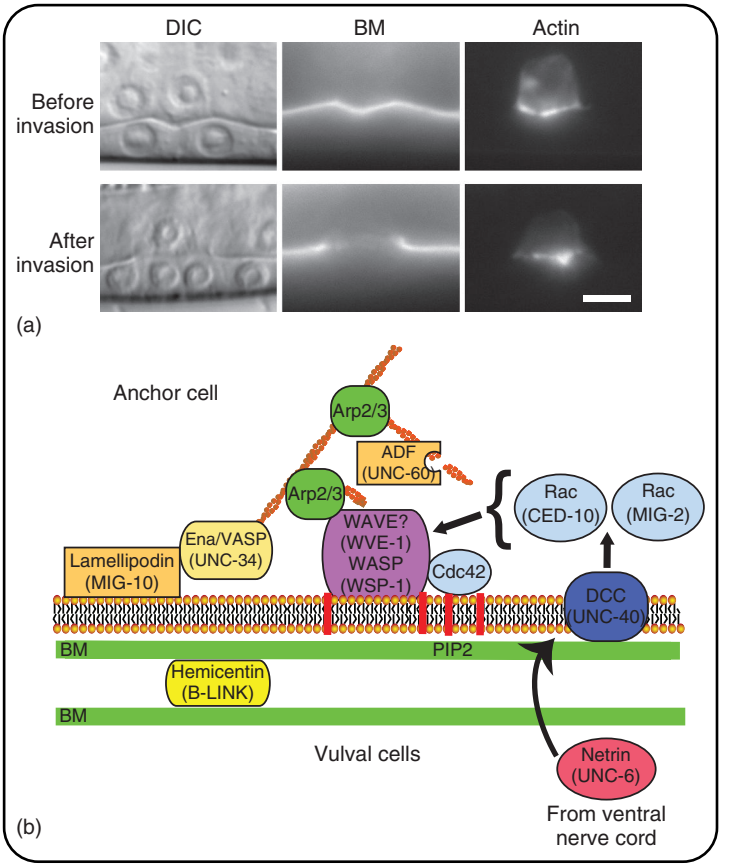

Figure 2 **Anchor cell invasion in *C. elegans*.** (a) DIC and epifluorescence images of AC invasion in an early stage (before BM penetration) and in a late stage (BM effaced), showing the accumulation of filamentous actin at the AC/BM interface just before BM breaching and the actin-rich protrusion that forms during invasion. Actin in the AC is labelled with Life act-GFP and BM with mCherry-laminin. Bar 5 µm. Rodrigo Cáceres, unpublished, 2016. (b) Scheme of what is known about actin dynamics in the AC. Actin filaments are represented in orange.

polarised cells that make up the blood vessel wall. However, in the presence of proangiogenesis signals such as vascular endothelial growth factor (VEGF), the endothelial cells initiate motile and invasive behaviour. During this process, leading cells, called 'tip cells', elongate, principally by employing filopodia, whereas the following cells, 'stalk cells', are less protrusive and play a role in establishing a lumen and proliferating to support sprout elongation (Eilken and Adams, 2010).

An *in vivo* imaging study in zebrafish shows that the filopodia of the tip cells are promoted by Cdc42, which binds a formin, FMNL3, to nucleate actin polymerisation (Wakayama *et al.*, 2015). A similar role forCdc42 in tip cells is reported using human dermal microvascular endothelial cells (Fantin *et al.*, 2015). However, lamellipodia are also observed on protruding tip cells, and in keeping with this, proteins such as WAVE and Ena/VASP are required for vascular formation and remodelling (Furman *et al.*, 2007; Yamazaki *et al.*, 2003).

In addition to filopodia and lamellipodia, structures called podosomes have recently been implicated in sprouting angiogenesis [for review, see Seano and Primo (2015)]. Similar to invadopodia, podosomes are actin-rich structures that can degrade the ECM; however, one main difference is their life time. Podosomes are relatively short lived (2–20 min), whereas invadopodia can persist for several hours (Murphy and Courtneidge, 2011). Another main difference is their structure. Podosomes consist of a ring of cell–substrate adhesion molecules called integrins with an actin core that can further organise into clusters called rosettes (Juin *et al.*, 2013).

The actin core of the podosome is known to contain the actin nucleating machinery Cdc42, WASP and the Arp2/3 complex, as well as associated proteins such as cortactin, α-actinin, fimbrin and the filament capping/severing protein gelsolin (Linder and Aepfelbacher, 2003). In another physiological context, podosome assembly in osteoclasts is observed to proceed through steps involving first assembly and then core consolidation by α-actinin (Luxenburg *et al.*, 2012). Actomyosin contraction does not appear to play a role during podosome actin core enlargement; however, it plays a role in clustering of adjacent podosomes (Meddens *et al.*, 2016).

Overall from what is known concerning actin dynamics in invasion during angiogenesis, invasion of endothelial cells shares many features with cancer cell invasion and AC invasion.

Actin in leukocyte transmigration

In the preceding sections, invasion has been described in specific pathological or developmental contexts, but in fact, BM invasion is a common occurrence in the blood and lymphatic systems. Immune cells, the leukocytes, must continually pass back and forth across the BMs of the vasculature in order to mount the immune response, in a process known as transmigration. The vasculature barrier that leukocytes cross is made up of a uniform layer of endothelial cells and a discontinuous layer of pericytes that sandwich a BM which presents uneven expression of collagen IV and laminins because of the discontinuous nature of the pericytes (Voisin *et al.*, 2010). This must be kept in mind as BM in other invasion events is generally uniform. Indeed, a recent study shows that leukocytes preferentially cross the BM in patchy regions and that gaps can further be enlarged by pericyte shape change (Proebstl *et al.*, 2012).

Although much is known about the rearrangement and dynamics of actin in underlying endothelial cells during leukocyte transmigration (Vestweber, 2015), relatively little is known about how actin is reorganised in an invading leukocyte to penetrate not only the endothelial cell layer but also the supporting BM. In fact, most studies on the actin cytoskeleton in immune cell migration have been performed in confining devices that mimic the geometry of invasion in the absence of BM. Using such devices, it appears that formin-based nucleation of actin polymerisation at the back of the cell is the driving force for migration through small openings, while Arp2/3 complex-dependent polymerisation is necessary for other immune cell functions (Vargas *et al.*, 2016). Another report indicates that Arp2/3 complex-based networks around the nucleus are necessary for the nuclear deformation that accompanies cell passage through constrictions (Thiam *et al.*, 2016).

Conclusion

Overall, the molecular signature of the actin cytoskeleton is similar in different types of invasive protrusions, and many of the same actin polymerisation nucleators, adaptors and structuring proteins are found in different contexts. On the other hand, modes of invasion can be very clearly distinguished based on the biochemistry of the actin cytoskeleton, with myosin driving bleb-based invasion and the Arp2/3 complex playing the predominant role in invadopodia-type invasion. Despite distinct modes, the system is inherently plastic, and many invasive cell types are capable of switching modes in order to adapt to the microenvironment and realise their migratory program. This point needs to be taken into account when developing therapies targeting invasive cell motility.

Acknowledgements

R.C. was funded by a PhD fellowship from ITMO Cancer. J.P. acknowledges financial support from the Fondation pour la Recherche Médicale (Grant Number DEQ20120323737) and the Fondation ARC (Grant Number PJA 20151203487). Additionally R.C. and J.P. have received support under the program ≪Investissements d'Avenir≫ launched by the French Government and implemented by ANR with the references ANR-10-LABX-0038 and ANR-10-IDEX-0001-02 PSL.

References

Bear JE and Gertler FB (2009) Ena/VASP: towards resolving a pointed controversy at the barbed end. *Journal of Cell Science* **122**: 1947–1953.

Bergert M, Chandradoss SD, Desai RA and Paluch E (2012) Cell mechanics control rapid transitions between blebs and lamellipodia during migration. *Proceedings of the National Academy of Sciences of the United States of America* **109**: 14434–14439.

Blanchoin L, Boujemaa-Paterski R, Sykes C and Plastino J (2014) Actin dynamics, architecture, and mechanics in cell motility. *Physiological Reviews* **94**: 235–263.

Bovellan M, Romeo Y, Biro M, *et al.* (2014) Cellular control of cortical actin nucleation. *Current Biology* **24**: 1628–1635.

Campellone KG and Welch MD (2010) A nucleator arms race: cellular control of actin assembly. *Nature Reviews Molecular Cell Biology* **11**: 237–251.

Charras G and Paluch E (2008) Blebs lead the way: how to migrate without lamellipodia. *Nature Reviews Molecular Cell Biology* **9**: 730–736.

Eilken HM and Adams RH (2010) Dynamics of endothelial cell behavior in sprouting angiogenesis. *Current Opinion in Cell Biology* **22**: 617–625.

Faix J and Rottner K (2006) The making of filopodia. *Current Opinion in Cell Biology* **18**: 18–25.

Fantin A, Lampropoulou A, Gestri G, *et al.* (2015) NRP1 regulates CDC42 activation to promote filopodia formation in endothelial tip cells. *Cell Reports* **11**: 1577–1590.

Furman C, Sieminski AL, Kwiatkowski AV, *et al.* (2007) Ena/VASP is required for endothelial barrier function in vivo. *The Journal of Cell Biology* **179**: 761–775.

Goode BL and Eck MJ (2007) Mechanism and function of formins in the control of actin assembly. *Annual Review of Biochemistry* **76**: 593–627.

Hagedorn EJ, Kelley LC, Naegeli KM, *et al.* (2014) ADF/cofilin promotes invadopodial membrane recycling during cell invasion in vivo. *The Journal of Cell Biology* **204**: 1209–1218.

Hagedorn EJ, Ziel JW, Morrissey MA, *et al.* (2013) The netrin receptor DCC focuses invadopodia-driven basement membrane transmigration in vivo. *The Journal of Cell Biology* **201**: 903–913.

Hohenester E and Yurchenco PD (2013) Laminins in basement membrane assembly. *Cell Adhesion & Migration* **7**: 56–63.

Juin A, Planus E, Guillemot F, *et al.* (2013) Extracellular matrix rigidity controls podosome induction in microvascular endothelial cells. *Biology of the Cell* **105**: 46–57.

Kurisu S and Takenawa T (2010) WASP and WAVE family proteins: friends or foes in cancer invasion? *Cancer Science* **101**: 2093–2104.

Lämmermann T and Sixt M (2009) Mechanical modes of 'amoeboid' cell migration. *Current Opinion in Cell Biology* **21**: 636–644.

Linder S and Aepfelbacher M (2003) Podosomes: adhesion hot-spots of invasive cells. *Trends in Cell Biology* **13**: 376–385.

Liu Y-J, Le Berre M, Lautenschlaeger F, *et al.* (2015) Confinement and low adhesion induce fast amoeboid migration of slow mesenchymal cells. *Cell* **160**: 659–672.

Lohmer LL, Clay MR, Naegeli KM, *et al.* (2016) A sensitized screen for genes promoting invadopodia function in vivo: CDC-42 and Rab GDI-1 direct distinct aspects of invadopodia formation. *PLOS Genetics* **12**: e1005786.

Luxenburg C, Winograd-Katz S, Addadi L and Geiger B (2012) Involvement of actin polymerization in podosome dynamics. *Journal of Cell Science* **125**: 1666–1672.

McClatchey AI and Fehon RG (2009) Merlin and the ERM proteins – regulators of receptor distribution and signaling at the cell cortex. *Trends in Cell Biology* **19**: 198–206.

Meddens MBM, Pandzic E, Slotman JA, *et al.* (2016) Actomyosin-dependent dynamic spatial patterns of cytoskeletal components drive mesoscale podosome organization. *Nature Communications* **7**: 13127.

Morrissey MA, Keeley DP, Hagedorn EJ, *et al.* (2014) B-LINK: a hemicentin, plakin, and integrin-dependent adhesion system that links tissues by connecting adjacent basement membranes. *Developmental Cell* **31**: 319–331.

Murphy DA and Courtneidge SA (2011) The 'ins' and 'outs' of podosomes and invadopodia: characteristics, formation and function. *Nature Reviews Molecular Cell Biology* **12**: 413–426.

Nürnberg A, Kitzing T and Grosse R (2011) Nucleating actin for invasion. *Nature Reviews Cancer* **11**: 177–187.

Paszek MJ, Zahir N, Johnson KR, *et al.* (2005) Tensional homeostasis and the malignant phenotype. *Cancer Cell* **8**: 241–254.

Poincloux R, Collin O, Lizárraga F, *et al.* (2011) Contractility of the cell rear drives invasion of breast tumor cells in 3D matrigel. *Proceedings of the National Academy of Sciences of the United States of America* **108**: 1943–1948.

Pollard TD and Borisy GG (2003) Cellular motility driven by assembly and disassembly of actin filaments. *Cell* **112**: 453–465.

Proebstl D, Voisin M-B, Woodfin A, *et al.* (2012) Pericytes support neutrophil subendothelial cell crawling and breaching of venular walls in vivo. *The Journal of Experimental Medicine* **209**: 1219–1234.

Revach O-Y, Weiner A, Rechav K, *et al.* (2015) Mechanical interplay between invadopodia and the nucleus in cultured cancer cells. *Scientific Reports* **5**: 9466.

Rowe RG and Weiss SJ (2009) Navigating ECM barriers at the invasive front: the cancer cell–stroma interface. *Annual Review of Cell and Developmental Biology* **25**: 567–595.

Salbreux G, Charras G and Paluch E (2012) Actin cortex mechanics and cellular morphogenesis. *Trends in Cell Biology* **22**: 536–545.

Schoumacher M, Goldman RD, Louvard D and Vignjevic DM (2010) Actin, microtubules, and vimentin intermediate filaments cooperate for elongation of invadopodia. *The Journal of Cell Biology* **189**: 541–556.

Seano G and Primo L (2015) Podosomes and invadopodia: tools to breach vascular basement membrane. *Cell Cycle* **14**: 1370–1374.

Sharma VP, Eddy R, Entenberg D, *et al.* (2013) Tks5 and SHIP2 regulate invadopodium maturation, but not initiation, in breast carcinoma cells. *Current Biology* **23**: 2079–2089.

Sibony-Benyamini H and Gil-Henn H (2012) Invadopodia: the leading force. *Eur J Cell Biol* **91**: 896–901.

Stevenson RP, Veltman D and Machesky LM (2012) Actin-bundling proteins in cancer progression at a glance. *Journal of Cell Science* **125**: 1073–1079.

Thiam H-R, Vargas P, Carpi N, *et al.* (2016) Perinuclear Arp2/3-driven actin polymerization enables nuclear deformation to facilitate cell migration through complex environments. *Nature Communications* **7**: 10997.

Thiery JP (2002) Epithelial-mesenchymal transitions in tumour progression. *Nature Reviews Cancer* **2**: 442–454.

Vargas P, Maiuri P, Bretou M, *et al.* (2016) Innate control of actin nucleation determines two distinct migration behaviours in dendritic cells. *Nature Cell Biology* **18**: 43–53.

Vestweber D (2015) How leukocytes cross the vascular endothelium. *Nature Reviews Immunology* **15**: 692–704.

Voisin M-B, Pröbstl D and Nourshargh S (2010) Venular basement membranes ubiquitously express matrix protein low-expression regions: characterization in multiple tissues and remodeling during Inflammation. *The American Journal of Pathology* **176**: 482–495.

Wakayama Y, Fukuhara S, Ando K, Matsuda M and Mochizuki N (2015) Cdc42 mediates Bmp-induced sprouting angiogenesis through Fmnl3-driven assembly of endothelial filopodia in zebrafish. *Developmental Cell* **32**: 109–122.

Wang L, Shen W, Lei S, *et al.* (2014) MIG-10 (Lamellipodin) stabilizes invading cell adhesion to basement membrane and is a negative transcriptional target of EGL-43 in *C. elegans*. *Biochemical and Biophysical Research Communications* **452**: 328–333.

Wirtz D, Konstantopoulos K and Searson PC (2011) The physics of cancer: the role of physical interactions and mechanical forces in metastasis. *Nature Reviews Cancer* **11**: 512–522.

Wolf K, Mazo I, Leung H, *et al.* (2003) Compensation mechanism in tumor cell migration: mesenchymal–amoeboid transition after blocking of pericellular proteolysis. *The Journal of Cell Biology* **160**: 267–277.

Yamaguchi H, Lorenz M, Kempiak S, *et al.* (2005) Molecular mechanisms of invadopodium formation: the role of the N-WASP–Arp2/3 complex pathway and cofilin. *The Journal of Cell Biology* **168**: 441–452.

Yamazaki D, Suetsugu S, Miki H, *et al.* (2003) WAVE2 is required for directed cell migration and cardiovascular development. *Nature* **424**: 452–456.

Ziel JW, Hagedorn EJ, Audhya A and Sherwood DR (2009) UNC-6 (netrin) orients the invasive membrane of the anchor cell in *C. elegans*. *Nature Cell Biology* **11**: 183–189.

Further Reading

Beaty BT and Condeelis J (2014) Digging a little deeper: the stages of invadopodium formation and maturation. *European Journal of Cell Biology* **93**: 438–444.

Friedl P, Sahai E, Weiss S and Yamada KM (2012) New dimensions in cell migration. *Nature Reviews Molecular Cell Biology* **11**: 743–747.

Glentis A, Gurchenkov V and Vignjevic DM (2014) Assembly, heterogeneity and breaching of basement membranes. *Cell Adhesion & Migration* **8**: 236–245.

Hagedorn EJ and Sherwood DR (2011) Cell invasion through basement membrane: the anchor cell breaches the barrier. *Current Opinion in Cell Biology* **23**: 589–596.

Lohmer LL, Kelley LC, Hagedorn EJ and Sherwood DR (2014) Invadopodia and basement membrane invasion in vivo. *Cell Adhesion & Migration* **8**: 246–255.

Parekh A and Weaver AM (2016) Regulation of invadopodia by mechanical signaling. *Experimental Cell Research* **343**: 89–95.

ANNEXE 2: PUBLISHED REVIEW ARTICLE 2015

Biochimica et Biophysica Acta 1853 (2015) 3006–3014

Contents lists available at ScienceDirect

Biochimica et Biophysica Acta

journal homepage: www.elsevier.com/locate/bbamcr

Review

Reconstituting the actin cytoskeleton at or near surfaces *in vitro*☆

Rodrigo Cáceres [a,b,c,d], Majdouline Abou-Ghali [a,b,c], Julie Plastino [a,b,c,*]

[a] Institut Curie, Centre de Recherche, Paris F-75248 France
[b] Centre National de la Recherche Scientifique, Unité Mixte de Recherche 168, Paris F-75248 France
[c] Université Pierre et Marie Curie, Paris F-75248, France
[d] Université Paris Descartes, Paris F-75248, France

ARTICLE INFO

Article history:
Received 9 March 2015
Received in revised form 15 July 2015
Accepted 16 July 2015
Available online 31 July 2015

Keywords:
Actin polymerization
Biomimetic systems
Actin-based motility
Contractility
Actin cortex
Lamellipodium

ABSTRACT

Actin filament dynamics have been studied for decades in pure protein solutions or in cell extracts, but a breakthrough in the field occurred at the turn of the century when it became possible to reconstitute networks of actin filaments, growing in a controlled but physiological manner on surfaces, mimicking the actin assembly that occurs at the plasma membrane during cell protrusion and cell shape changes. The story begins with the bacteria *Listeria monocytogenes*, the study of which led to the reconstitution of cellular actin polymerization on a variety of supports including plastic beads. These studies made possible the development of liposome-type substrates for filament assembly and micropatterning of actin polymerization nucleation. Based on the accumulated expertise of the last 15 years, many exciting approaches are being developed, including the addition of myosin to biomimetic actin networks to study the interplay between actin structure and contractility. The field is now poised to make artificial cells with a physiological and dynamic actin cytoskeleton, and subsequently to put these cells together to make *in vitro* tissues. This article is part of a Special Issue entitled: Mechanobiology.

1. Introduction

Actin is a protein that exists in a globular soluble form and in an assembled filamentous form, echoing a common theme observed in other types of cytoskeleton like microtubules and intermediate filaments. Cell shape changes in general, including cell motility, cell division and cancer cell invasion, are due in part to the controlled assembly of actin into filamentous networks that can push membranes or contract in the presence of the molecular motor myosin thus leading to cell shape changes. The fact that actin filaments are polar, with a dynamic barbed end that grows and shrinks more quickly than the pointed end, is important for the directionality of network growth and for myosin motor activity.

Actin has been studied since the 1940s when it was first isolated from muscle. By the time the last century was drawing to a close, the dynamics of individual actin filaments had been well characterized *in vitro* [1] and much had been discovered about other factors that interacted with both the globular and filamentous forms of actin [2]. The great step forward at the turn of the century was the successful recreation of dynamic actin networks growing at surfaces in a controlled fashion using cellular components, a departure from previous single filament studies where polymerization was generally occurring in the bulk solution. This review will be about the progress over the last 15 years in the field of reconstitution of dynamic actin and acto-myosin networks at surfaces or under confinement, and how technological advances have been used to further our understanding of cellular actin dynamics. Other excellent reviews on reconstitution have been published over the last 5 years concentrating on actin and adhesion, membrane-bound actin and single filament dynamics [3–7]. The focus here is actin and acto-myosin networks at or near surfaces *in vitro*, to mimic cellular confinement and geometry.

2. The beginnings of actin network reconstitution

2.1. Listeria in cells

Somewhat surprisingly, most modern approaches to studying actin networks *in vitro* can trace their inspiration back to the food-borne pathogen *Listeria monocytogenes* (Fig. 1). This bacterium propels itself in the host cell cytosol not by swimming with a flagellum, but by building a network of filamentous actin behind itself, dubbed an actin tail or actin comet due to its appearance by electron and light microscopy (reviewed in [8]). What made this motility mode interesting to the general cell biology community was the discovery that the bacteria produced a single factor necessary for its motility, the ActA protein, which was displayed on its surface and was responsible for forming the actin comet from host cell components (reviewed in [9]). In addition landmarking experiments in the actin network of moving cells and in *Listeria* tails showed that both processes involved insertion of newly polymerized actin at the cell membrane or bacterial surface, and this was

☆ This article is part of a Special Issue entitled: Mechanobiology.
* Corresponding author at: Institut Curie, Centre de Recherche, Paris F-75248 France.
E-mail address: julie.plastino@curie.fr (J. Plastino).

http://dx.doi.org/10.1016/j.bbamcr.2015.07.021
0167-4889/

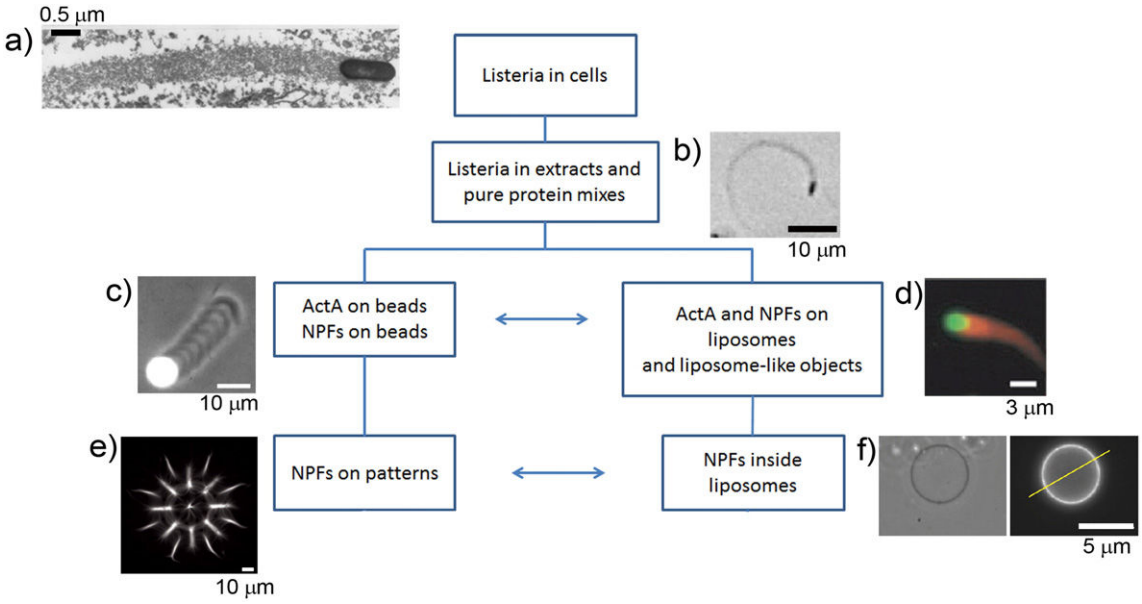

Fig. 1. The family tree of biomimetic systems of actin motility and dynamics. The original inspiration came from *Listeria* motility in cells a), which led to studies of *Listeria* in cell extracts and pure protein mixes b). The next generation of *in vitro* systems can be split into two groups, one involving reconstitution on solid supports such as beads c) and the other involving the use of fluid, deformable substrates such as liposomes d). ActA from *Listeria* was used to coat the beads and liposomes, but also mammalian nucleation promoting factors (NPFs) of the WASP/WAVE/Scar family. The recent innovations in each branch of the family consist of reconstitution of actin dynamics on micropatterns on one hand e), and reconstitution of actin cortices inside liposomes on the other hand f). The lateral double-headed arrows indicate cross-talk between the different systems. a) Reprinted from [114]: *Cell*, vol. 68, C. Kocks, E. Gouin, M. Tabouret, P. Berche, H. Ohayon, P. Cossart, *L. monocytogenes*-induced actin assembly requires the *actA* gene product, a surface protein, 521–531 (1992), with permission from Elsevier. b) Adapted by permission from Macmillan Publishers Ltd: *Nature* [28], 1999. c) Adapted by permission from Macmillan Publishers Ltd: *Nature* [68], 2002. d) Adapted by permission from the National Academy of Sciences: *PNAS* [74], 2003. e) Adapted by permission from Macmillan Publishers Ltd: *Nature Materials* [101], 2010. f) Reprinted from [95]: *Biophysical Journal*, vol. 96, L.-L. Pontani, J. Van der Gucht, G. Salbreaux, J. Heuvingh, J.-F. Joanny, C. Sykes, Reconstitution of an actin cortex inside a liposome, 192–198 (2009), with permission from Elsevier.

hypothesized to be the driving force for propulsion in both cases [10,11]. It was quickly realized by pioneers in the field that the *Listeria* actin network could be a powerful tool to study the biochemical basis of mammalian actin assembly, in isolation from cell signaling and adhesion. This discovery also opened up new avenues for studying how actin assembly created movement from a physical perspective since bacterial movement was a more tractable object to manipulate and model than an entire cell [12,13]. We will discuss here *Listeria* motility, but other pathogens with similar motility mechanisms have also been useful in the study of actin-based motility [14].

Initial experiments involved observation of *Listeria* movement in living cells. Such studies revealed that many host cell actin-binding proteins were present in the *Listeria* comet tail ([15] and references therein). Further this type of experiment led to more unexpected results, such as the fact that the actin tail composition changed depending on the intracellular location: in the cell body, comets contained α-actinin, while in cell protrusions, comets shed α-actinin concomitant with an evolution of the comet structure toward an aligned unbranched array of long filaments [16]. Information about how the actin network was constructed was also gleaned from altering the ActA protein itself and observing how this changed *Listeria* motility in cells, notably identifying the Arp2/3 complex and Ena/VASP binding domains as important motility motifs [17,18]. However the limitations of this approach quickly became apparent. For example, a back-to-back study of *Listeria* motility in cells expressing different forms of Ena/VASP proteins as compared to the movement of the cells themselves showed that cell movement and *Listeria* movement required different domains of Ena/VASP [19,20]. This perplexing result could have resulted from off-target effects, including mislocalization of the mutant proteins in the host cells, and changes in the internal structure of the host cell that could have decreased or enhanced *Listeria* motility. Indeed other studies showed that the mechanical inhomogeneity of the cell interior altered the motile behavior of *Listeria* [21].

2.2. Listeria in cell extracts and pure protein mixes

The cell interior was too complex of a place to conduct controlled biochemical motility assays, and physical manipulations were rendered difficult. The solution to the confounding effects of the biochemical and mechanical heterogeneity of the cell interior was the use of cell extracts, homogenous cytosolic preparations lacking organelles and cell membrane. Although not without its own challenges, mostly associated with obtaining cell extracts sufficiently concentrated in cytoskeleton factors that were not even entirely known at the time, cell extracts were successfully used to perform some first quantitative physical and biochemical characterizations. For example *Listeria* actin tail elasticity was measured using optical tweezers, and the roles of profilin and Ena/VASP proteins in *Listeria* movement were examined [22–24]. At about the same time, great advances were being made in the understanding of how actin assembly was catalyzed in cells. A major step was the discovery of the Arp2/3 complex as a weak catalyzer or "nucleator" of actin assembly that made branches from the sides of existing filaments, and the subsequent finding that the *Listeria* ActA protein and the mammalian nucleation promoting factors (NPFs) WASp and Scar activated the activity of the Arp2/3 complex [25–27]. All together these findings paved the way for the next great advance: the reconstitution of *Listeria* motility in a mix of pure proteins [28]. The purified protein mix provided tight control of biochemical parameters, and is still today the method of choice for studying actin-based motility, especially for attaining the reproducibility needed for quantitative measurements.

However cell extracts should not be neglected. The study of a pure protein can reveal its mechanism in isolation, but not necessarily its mode of action *in vivo* in association with other proteins. A case in point is ADF/cofilin, an actin filament fragmenting protein. When pure ADF/cofilin was mixed with pure actin filaments in conditions where ADF/cofilin fully decorated the filaments, ADF/cofilin lost its ability to

sever [29]. This was perplexing since high ratios of ADF/cofilin to actin are in fact physiological in some cell types. Recent results using cell extracts showed that an additional factor, Aip1, was present in cytosol that permitted ADF/cofilin to efficiently sever and disassemble actin at high ratios [30], although the exact mode of action of Aip1 is the subject of some controversy [31–33]. The use of cell extracts also permitted other exciting developments such as the reconstruction of complex actin structures like the cleavage furrow in cytokinesis [34]. Recent advances make possible the production of mutant extracts to study individual proteins while retaining the complexity of the cell cytosol and the preparation of staged extracts to examine how actin assembly varies with the cell cycle [35,36].

3. The next generation

3.1. Replacing Listeria with beads

The first reconstituted motility systems using *Listeria* set the stage for the next generation of *in vitro* systems where the pathogen was replaced by a bead or other particle coated with the ActA protein (Fig. 1). This allowed for control of the size and properties of the cargo and the density and nature of the activating protein on the surface, including, importantly, the use of mammalian factors (next section).

The first successful bead systems were performed with ActA-coated particles in cell extracts [37]. This study brought to light one of the stumbling blocks of working with particles in the place of *Listeria*: homogenous distribution of the ActA protein on the bead surface led to homogenous actin growth, which had to undergo "symmetry breaking" to form a polarized actin network and directional motility. Symmetry breaking was shown to depend on particle size, coating density and the concentration of the cell extract, and could be circumvented by preparing artificially asymmetric beads *via* silicon monoxide shadowing [37,38]. Studies of such comets allowed for the important demonstration that actin comet tails observed by electron microscopy had a similar dendritic organization to that found in the lamellipodia of moving cells, thus further validating the use of the bead system as a mini-lamellipodium mimic [39].

Although an impediment to forming actin comets, symmetry breaking was an interesting topic in and of itself, and much was learned about actin network mechanics by observing the growth and rupture of actin networks on spherical beads. In particular it was demonstrated that the network had elastic properties, due to its entangled nature, and stresses could develop in the network and affect growth dynamics [40,41]. Later with the purified protein mix, symmetry breaking on beads was thoroughly characterized and it was shown that stress build-up drove the polarization of the actin network and that stress development depended in predictable ways on the biochemical components of the protein mixture and the balance between nucleation of new filaments, capping and crosslinking [42–44].

3.2. What to coat the beads with?

ActA-coated beads are less employed today, but these original studies opened the door to grafting beads with the mammalian equivalent of ActA, the WASP/WAVE/Scar proteins. Reconstitution of actin comet tails and motility of beads coated with the NPF WASP in bovine brain extracts was the first entirely mammalian reconstitution of actin-based motility [45]. Subsequently the WASP proteins and the related Scar/WAVE molecules were picked apart by absorbing different protein fragments to bead surfaces and observing which domains gave optimal actin network growth and optimal motility in cell extracts and pure protein mixes [46–48]. Different domains from different actin-binding proteins were also absorbed simultaneously and in different proportions to bead surfaces, for example to recruit and activate the Arp2/3 complex in varying proportions with Ena/VASP proteins [49]. When formin proteins were identified as actin polymerization nucleators that produced unbranched networks, in contrast to the Arp2/3 complex-based branched networks, formin-based actin assembly and movement were also reproduced on bead surfaces [50,51]. Given this history, it is remarkable that no one has yet recreated Arp2/3 complex-based and formin-based nucleation together on a bead surface, despite the biological relevance to the lamellipodium where both nucleation systems co-exist and actin networks are generally mixes of branched and unbranched filaments [52,53]. This is particularly pertinent given a recent study that showed that the Arp2/3 complex and formin worked together in a mechanism where the new filament ends created by the Arp2/3 complex were captured and elongated by the formin FMNL2 [54]. However other studies showed that formin and the Arp2/3 complex compete for actin monomers in cells [55], and are not favored by the same conditions in profilin *in vitro* [56], so reconstitution of the two activities together may be a challenge.

In general exotic surface coatings remain rare in the biomimetic field, and the predominant activating proteins used today in *in vitro* systems are human WASP protein fragments, in particular the VCA domain that binds and activates the Arp2/3 complex or its variant pVCA that additionally encompasses the proline-rich portion of WASP that binds profilin actin. VCA is also called WA, due to vocabulary created simultaneously by different labs [57–59]. The pVCA construct is more effective for Arp2/3 complex activation than VCA when monomeric actin is bound with profilin [27]. Indeed most modern reconstitution studies use high concentrations of globular actin bound with profilin to prevent spontaneous nucleation, a closer mimic of actual conditions in cell cytosol and a departure from the original pure protein reconstitution system which used a reservoir of prepolymerized filamentous actin to maintain a low but stable concentration of actin monomers *via* depolymerization [28,60].

The choice of pVCA from WASP as the most-used NPF is more motivated by history than by physiology. WASP is in fact a protein that is only found in hematopoietic cells, while the closely-related N-WASP protein is ubiquitous, but was discovered later (reviewed in [61]). N-WASP-coated beads were used in some studies [62,63], and it is the VCA domain of human N-WASP that is currently commercially available. N-WASP is a more effective Arp2/3 complex activator than either WASP or WAVE/Scar due to the enhanced acidity of the A domain in the case of N-WASP, not as originally believed due to the extra V domain that N-WASP proteins contain [64]. WAVE/Scar-derived bead coatings have been used for some studies, but less extensively than the other NPFs [46,65]. WAVE proteins exist in regulatory complexes, which are impossible to mimic in pure protein mixtures although the WAVE regulatory complex has been successfully recruited to membrane-coated glass beads to form actin comets in cell extracts [66]. In the cell, NPFs have very different roles downstream of signaling cascades: WAVE/Scar proteins are involved in lamellopodial protrusion, while WASP proteins are implicated in filopodia formation and endocytosis (for review [67]). However, as far as biomimetics are concerned, where the regulatory portions of the NPFs are removed, the different NPFs can be used interchangeably since the VCA portion of the different NPFs give the same end product: an Arp2/3 complex-branched network.

3.3. The power of the bead system in the pure protein mix

The combination of the bead system with the pure protein mix changed the face of how actin polymerization was studied. Most importantly it made possible a type of biophysical experiment that had been impossible before, namely varying biochemical and physical parameters and observing how that changed actin assembly and motility. For example it was observed that simply changing particle size or bead-coating density could completely change how the actin comet created movement, switching between continuous and periodic, even though biochemical conditions were identical [68]. Controlled force measurements also became possible in a variety of different experimental set-ups [62,69]. Bead/pure protein mixes were also used to

study the role of the important actin factor, capping protein, showing that capping protein restricted polymerization to the surface *via* promotion of Arp2/3 complex activity [70,71].

Bead speeds were a particularly easy parameter to measure while changing the biochemistry of the mix. As one example, this approach was used to resolve the confusion concerning Ena/VASP proteins and *Listeria* motility mentioned previously. When recruited to the bead surface, Ena/VASP proteins were shown to indeed increase bead speed and different mutants of Ena/VASP showed concordant effects on beads and on an *in vivo* cell motility event [49,65,72]. However the relation between actin polymerization and particle speed is a complex one. It has been observed since the conception of the pure protein mix that movement velocity has a bell-curve dependence on the concentration of polymerization factors: both too much and too little of a given component can reduce speed [28]. In the case of Ena/VASP for example, under different conditions than the study cited above, it was observed that a bead that was already moving very efficiently displayed drastically reduced motility when treated with Ena/VASP, concomitant with the production of a much denser comet tail (Fig. 2). So it seems that when motility is optimal, adding factors that increase polymerization (like Ena/VASP or even the Arp2/3 complex) can slow bead motility and this is something to keep in mind when using bead velocity as a readout of protein function.

4. Polymerization from soft, fluid and deformable substrates

The work on beads spawned a whole other branch of the reconstitution family (Fig. 1) involving polymerization on an assortment of fluid and sometimes deformable substrates like oil droplets, liposomes, lipid-coated beads or supported bilayers, moving one step closer to the real conditions for actin polymerization at a cell membrane bilayer.

The first of such studies involved the absorption of a His-tagged form of ActA to liposomes containing nickel lipids and incubation in cell extracts or cell extracts supplemented in the Arp2/3 complex to form actin comets [73,74]. Several interesting observations came out of these studies, observations that were corroborated subsequently

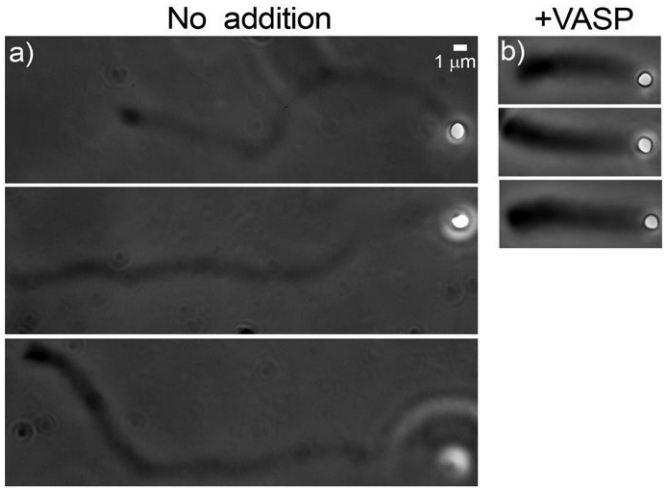

Fig. 2. Enhancing polymerization does not always increase bead motility. a) When motility is very fast (2–3 μm/min), the addition of VASP b) slows the beads down (below 1 μm/min) even though the comet is denser. So the effect of VASP on motility seems to depend on the initial state of the system, and when speed is already optimal, adding an enhancing molecule like VASP does not have the expected effect. Images taken at about 10–15 min reaction time of PRD-VCA-WAVE-coated beads in reconstituted motility mix as described in [65], but with commercial Arp2/3 complex. Phase contrast microscopy. Comet appears as a dark streak behind the white bead. Since there is no depolymerization in this system, comet length is proportional to bead velocity. Images M. Abou-Ghali, 2014.

under different conditions: using the mammalian NPFs VCA-WASP and N-WASP absorbed to liposomes or non-specifically to oil droplets and incubated in either cell extracts or purified protein mixes [75–77]. Although liposomes were more physiological, the advantage of oil droplets was that the surface tension was known so the curvature of the droplet surface could be used to calculate stresses exerted by the growing actin cytoskeleton. One of the main findings from such studies was, first of all, a direct visual proof of the elastic squeezing effect evoked to explain symmetry breaking, mentioned previously. The growth of an actin gel on a convex surface created compressive or squeezing stresses, and this could be clearly seen with both liposomes and oil droplets as a deformation from spherical shape (Fig. 3a, b). Furthermore it was shown that the actin comet exerted retarding or pulling forces on its substrate, presumably due to transient attachments between the actin network and the surface-bound NPFs mediated by the Arp2/3 complex. As a result, the NPFs on the fluid surface were convected under the comet (Fig. 3c). In line with this, another study using the bead system showed that cortactin enhanced motility by releasing NPF molecules from new branches [78]. Another proposed mechanism for transient network-surface attachment was the binding of the WH2 (or V) domain of NPFs to filament barbed ends, an interaction that was mediated by monomeric actin, giving convection of NPFs on lipid-coated glass beads [79]. WASP/WAVE WH2 domains do not bind profilin–actin [80], the predominant form of actin *in vivo* so, in the cell, a combination of attachment *via* the Arp2/3 complex and WH2 domains may be occurring. From all this, it is clear that actin growth exerts both protrusive and braking forces on the objects it acts upon.

However much was also gleaned from biomimetic membrane systems in conjunction with actin polymerization in the absence of motility (for review [7]). For example actin polymerization was shown to induce phase separation of lipids in giant vesicles grafted with N-WASP, incubated in actin and the Arp2/3 complex [81]. In a similar experiment, the branched actin network produced by Arp2/3 complex-based polymerization was observed to be reorganized into bundled filopodia-type structures by the deformable lipid bilayer [82]. Even simpler, and in a continuum with approaches using lipid-coated glass beads, actin polymerization was reproduced on supported lipid bilayers. In particular filopodia formation was recreated on such bilayers, showing that recruitment of biochemical factors from the cell extract gave spontaneous self-assembly of the bundled structure in the absence of membrane deformation [83].

Overall the actin network-on-liposome/droplet systems were a great advance in the field because they brought information as to the interplay between actin assembly and lipid bilayer properties and also opened the door to looking at actin-based deformations. Supported bilayers as a subset of this family have the advantage that they are easier to manipulate physically and image by techniques such as Total Internal Reflection Microscopy (TIRF), but give up the deformability of the liposome system and reduce the mobility of factors in the membrane *via* friction with the support [7].

5. Expanding the biomimetic repertoire

5.1. Confining physiologically nucleated dynamic actin networks

There is nothing new about encapsulating actin polymerization. For decades people have been incorporating monomeric actin into liposomes, triggering polymerization and then observing shape changes. A non-exhaustive list of such studies includes [84–88]. Some studies included non-physiological bonds between the encapsulated actin network and the liposome inner leaflet, such as the linking of biotin actin to biotin lipids *via* streptavidin [89]. Similar experiments have been performed with pure actin and actin-binding proteins or with cell extracts confined in stabilized aqueous-in-oil emulsions, two examples of which are [90,91]. More recently actin polymerization has been confined in

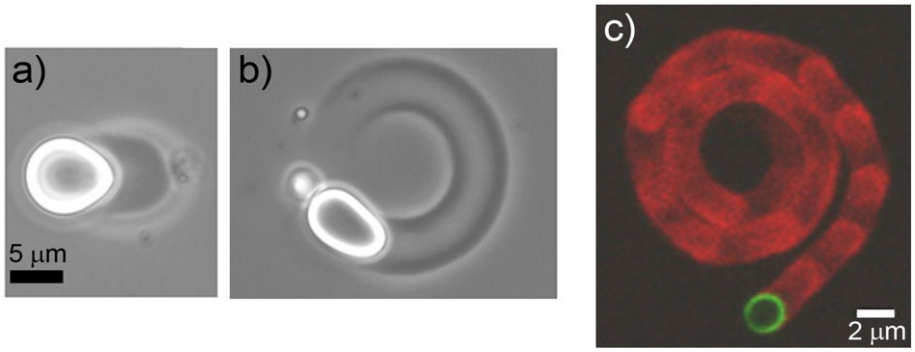

Fig. 3. Actin polymerization on deformable, fluid supports. a) and b) Oil droplets are deformed by the actin comet, depending on how the comet is organized. When the oil droplet is grafted with VCA a), motility is slow, comets are uniform and dense and the droplet is deformed in a pear shape. When the droplet is coated with a mix of VCA and PRO b), a fragment of the ActA protein that recruits VASP, movement is rapid, the comet is partially hollow and the droplet is therefore deformed differently than in a) into a kiwi shape. See also [77]. Phase contrast microscopy. c) On the fluid surface of the oil droplet, VCA (green) is enriched under the comet (actin in red), as observed by the dimmer intensity of VCA at the front of the droplet. The droplet is undergoing jumping movement. For more details see [77]. Confocal fluorescence microscopy. All images Léa Trichet, 2004–2005.

microchambers [92]. In all cases restricting actin polymerization led to interesting phenomena including self-organization, which were not seen in unconfined solutions. This can be understood in the larger framework of how confinement changes biological processes, including cytoskeleton dynamics [93].

A new development concerning confined actin polymerization builds on these experiments, but with several additional characteristics that were previously absent. Namely, to truly reproduce cellular dynamics, the actin network should be growing from the surface *via* localized actin polymerization nucleation. This means that there are transient attachments between the network and the surface, and the barbed ends are growing mostly toward or near the surface. The actin network should also be depolymerizing, and monomers continually recharging with ATP and repolymerizing to make a dynamic network. These aspects are important for mimicking not only lamellipodia-type protrusions, but also for reconstituting other cytoskeletal organelles as we will see in the next section.

Advances have been made in this direction over the last few years. Liposomes were made from native membranes and swelled in the presence of actin, with or without the membrane-actin crosslinking proteins ankyrin/spectrin. In the presence of ankyrin/spectrin, polymerized actin was anchored and bundled at the membrane [94]. This was a physiological link, however the filaments were not dynamic. At about the same time, liposomes were made by a different technique, the inverted emulsion technique, whereby the reconstituted motility mix of pure proteins described earlier was encapsulated in low salt conditions that prevented polymerization and then polymerization was triggered by inserting pores in the membrane to allow passage of salts [95]. Importantly polymerization occurred preferentially at the membrane because a VCA protein was specifically bound there by interaction of its histidine tag with nickel lipids in the membrane, and additionally this actin layer was shown to be actively turning over due to the presence of actin depolymerizing and recycling factors in the liposome interior. This study produced for the first time a dynamic membrane-associated actin structure in a liposome, polymerized in a physiological manner. Subsequently the inverted emulsion technique was used for actin/actin-binding protein encapsulation and micropipette aspiration experiments to show that the membrane-associated actin layer was determinant for the mechanical properties of the liposome [96,97]. Additionally membrane-bound actin layers have since been formed in aqueous-in-oil emulsions, using interface-targeted ActA protein and cell extracts [98]. These actin networks were shown to not only be actively turning over, but also were capable of auto-organization to break symmetry. An added motivation to use liposome-type biomimetic systems is to study proteins that recognize or impose membrane curvature and also interface with the actin cytoskeleton, such as BAR domain proteins [99].

5.2. Patterning actin assembly

Another innovation in the actin biomimetics field is that of making defined actin structures *via* micropatterning of nucleation sites [100]. In some ways this is similar to the previous challenge, but the confinement is imposed by the filament source instead of being created by the envelope. A pioneering study showed that the angle and distance between nucleation sites for actin assembly determined the proportion of parallel bundles *versus* anti-parallel structures within a given actin network although the biochemistry of the networks was identical [101]. This showed that the geometry of filament growth could determine macroscopic structure formation, something that had previously been ascribed to actin-binding proteins. However in cells there is surely a mixture of both geometrical and biochemical control, for when the anti-parallel actin bundler α-actinin was added in high concentrations into the actin polymerization mix, antiparallel filament structures were favored even though the geometry dictated predominant parallel bundle formation [101].

6. Reconstituting acto-myosin contractility *in vitro* in cell-like systems

The stage is now set for one of the next big challenges in actin biomimetics: reproducing the acto-myosin contractile structure found in non-muscle cells juxtaposed to the plasma membrane, an organelle commonly called the cell cortex. This mixed network of actin filaments and myosin motors dynamically polymerizes, depolymerizes and contracts, while at the same time being transiently linked to the plasma membrane that it deforms to produce cell shape changes. In the well-studied contractile system of the muscle sarcomere, unbranched actin filaments are arranged in an anti-parallel manner so as to enable myosin-based contraction. In non-muscle cells, the actin network in the cell cortex is a random array of branched and unbranched actin filaments, not organized like in a muscle sarcomere [52,53]. The question then is: how does the cortex contract efficiently? To answer this, the previously-described techniques are being used to produce cell-like dynamic actin networks, but now containing myosin.

6.1. Interplay between actin organization and myosin contractility

As would be predicted from consideration of how myosin functions, it has been shown experimentally that the overall actin architecture can modify where and how effectively myosin contracts the actin network. The micropatterning approach described above was used to create different network geometries, mixed parallel bundles and anti-parallel structures. When myosin was added to this network, it preferentially contracted anti-parallel structures although it decorated parallel

bundles as well [102]. Myosin was capable of contracting entangled branched networks, albeit much more slowly. However this appeared to be due to the spontaneous occurrence of anti-parallel structures within such networks that were the real substrate for myosin function [102]. A very different experimental approach involving acto-myosin layers near but not attached to supported lipid bilayers also showed that a disordered actin network was efficiently contracted by myosin, but only above a critical myosin concentration [103].

When a static disordered acto-myosin network was attached to the outside or the inside of a lipsome, the outcome of contraction was modulated by the attachment to the bilayer [104]. In the "outside geometry", the balance between contraction and membrane attachment determined whether the acto-myosin network compacted and peeled off the exterior of the lipsome or whether the network contracted and crushed the liposome. In the "inside geometry", contraction either occurred on the bilayer or pulled off the bilayer depending on attachment strength. Taking this experiment one step further, actin was polymerized in the outside geometry with a physiological attachment to the bilayer *via* a membrane-bound VCA molecules, with the Arp2/3 complex, capping protein and profilin to mimic cellular actin polymerization [105]. It was observed that both myosin contraction and actin polymerization contributed to stress build-up in this system, and importantly, that the cocktail of actin-binding proteins determined the window where myosin produced contraction. All together, these results emphasize the importance of the geometry of the network, its attachment to the bilayer and the biochemistry of network formation for determining myosin contractility. This is why there is much to be learned by performing biomimetic experiments, which could give very different behavior from pure acto-myosin networks in the absence of constraints, attachments and physiological polymerization.

Another aspect of actin architecture that could affect myosin contractility efficiency is the presence of crosslinkers. The contraction of the anti-parallel regions of the actin network grown from micropatterns was slower in the presence of the anti-parallel cross-linking protein α-actinin, presumably due to resistance to filament sliding imposed by the cross-links [102]. However a macroscopic contraction assay using suspended actin layers showed that the connectivity conferred by actin cross-linking proteins was necessary for a global contraction [106]. These biomimetic studies show that cross-linking may play a role in controlling how the network contracts. Indeed cross-linking proteins are abundant in the acto-myosin cell cortex [107], and myosin-regulatory roles for the actin-binding proteins fascin and ADF/cofilin, sometimes contradictory in the latter case, have been recently reported in cells [31,108–110]. These issues will be one of the many questions to address in the future with biomimetics.

6.2. Myosin contractility as a disassembly agent

Contraction was expected to change the organization of the actin network by compacting it. What was somewhat unexpected was the observation that motor activity also severed and dismantled the network. This had been observed with actin bundles in bulk assays [111]. However as concerns biomimetic networks, this depolymerization effect was most clearly demonstrated with the micropatterning experiments where contraction of the anti-parallel portions of the network led to their disappearance, and seemingly liberated monomeric actin,

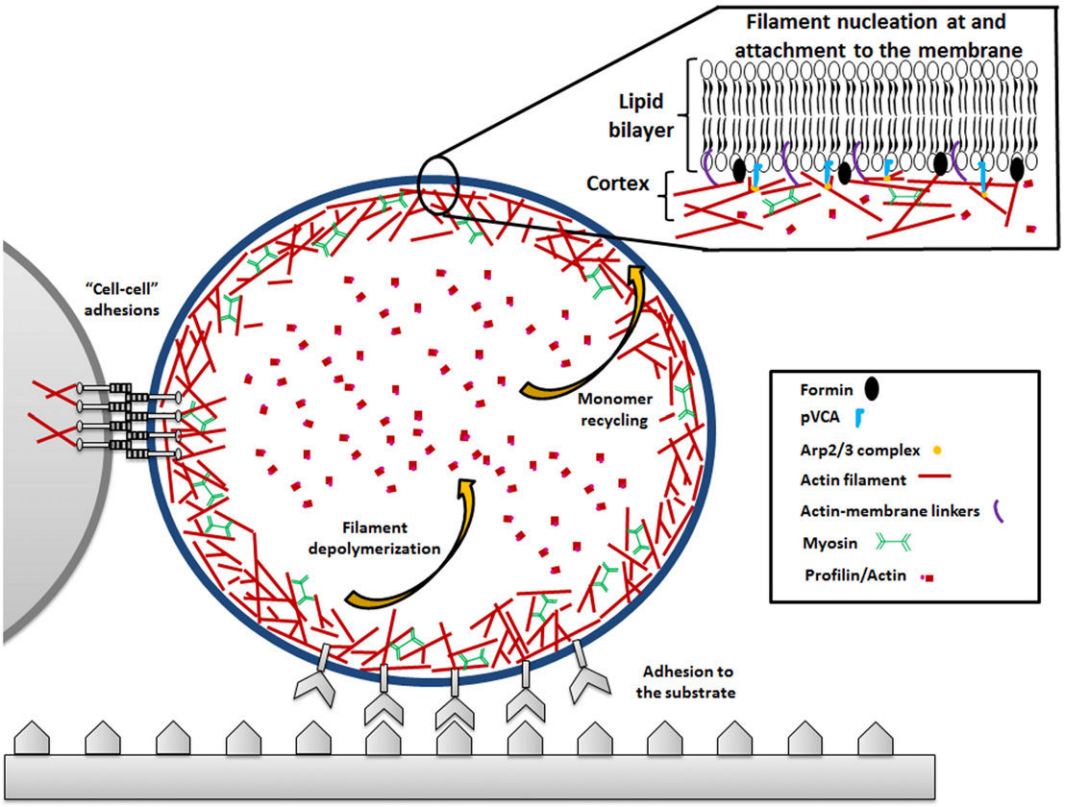

Fig. 4. The ideal artificial acto-myosin *in vitro* system. The main characteristics include: 1) the system has a cell-like geometry confined by a lipid bilayer to mimic the cell membrane, 2) actin filament nucleation occurs at the membrane by physiological factors such as the Arp2/3 complex or another nucleator such as formin, 3) attachment to the membrane is ensured by transient links *via* the Arp2/3 complex and physiological actin filament-membrane linkers such as ezrin, 4) non-muscle myosins are included in the artificial cell interior, 5) actin filaments disassemble either due to the activity of proteins such as ADF/cofilin or to the buckling/severing action that results from myosin contraction and 6) the actin monomers thus liberated are recycled to the cell membrane for subsequent rounds of nucleation. Like in cells, spontaneous formation of filaments in the "cell" interior is inhibited by maintaining free actin in its profilin-bound form. In gray are depicted the future of such systems where, in addition to all the characteristics listed above, the artificial cell is also capable of adhering to its substrate and to its neighboring "cells" *via* its cytoskeleton and transmembrane proteins, thus mimicking epithelial tissues.

as evidenced by an enhanced growth of the parallel bundles in the assay [102]. This macroscopic effect reflected what was happening on the single filament level, where myosin activity was observed to buckle and fragment filaments that were attached to a lipid bilayer [112,113].

7. Conclusion

One of the next challenges for biomimetics is to put together all that we have learned over the last 15 years in order to produce the ideal artificial acto-myosin *in vitro* system (Fig. 4). The goal is to reconstitute inside a cell-like confinement the acto-myosin network, while preserving the architecture of the network as found in living cells, its attachment to the bilayer and the biochemistry of network formation, all of which appear to be important for determining myosin contractility. Such systems should allow for the *in vitro* study of shape changes and spontaneous oscillations. Down the road, the next step will be to include adhesion to the substrate to make motile biomimetic cells, and adhesion to adjacent "cells" to build up artificial tissues in order to mimic and study collective shape changes.

Transparency document

The Transparency document associated with this article can be found, in the online version.

Acknowledgments

We thank Cécile Sykes for discussions and reading of the manuscript. This work was funded by the Fondation pour la Recherche Médicale (Grant DEQ20120323737). R.C. was funded by a PhD fellowship from ITMO Cancer.

References

[1] T.D. Pollard, Rate constants for the reactions of ATP- and ADP-actin with the ends of actin filaments, J. Cell Biol. 103 (1986) 2747–2754.
[2] T.D. Pollard, L. Blanchoin, R.D. Mullins, Molecular mechanisms controlling actin filament dynamics in nonmuscle cells, Annu. Rev. Biophys. Biomol. Struct. 29 (2000) 545–576.
[3] D. Brüggemann, J.P. Frohnmayer, J.P. Spatz, Model systems for studying cell adhesion and biomimetic actin networks, Beilstein J. Nanotechnol. 5 (2014) 1193–1202.
[4] S.K. Vogel, P. Schwille, Minimal systems to study membrane–cytoskeleton interactions, Curr. Opin. Biotechnol. 23 (2012) 758–765.
[5] R.D. Mullins, S.D. Hansen, In vitro studies of actin filament and network dynamics, Curr. Opin. Cell Biol. 25 (2013) 6–13.
[6] A.P. Liu, D.A. Fletcher, Biology under construction: in vitro reconstitution of cellular function, Nat. Rev. Mol. Cell Biol. 10 (2009) 644–650.
[7] M. Loose, P. Schwille, Biomimetic membrane systems to study cellular organization, J. Struct. Biol. 168 (2009) 143–151.
[8] L.G. Tilney, M.S. Tilney, The wily ways of a parasite: induction of actin assembly by *Listeria*, Trends Microbiol. 1 (1993) 25–31.
[9] P. Cossart, Actin-based bacterial motility, Curr. Opin. Cell Biol. 7 (1995) 94–101.
[10] J.A. Theriot, T.J. Mitchison, Actin microfilament dynamics in locomoting cells, Nature 352 (1991) 126–131.
[11] J.A. Theriot, T.J. Mitchison, L.G. Tilney, D.A. Portnoy, The rate of actin-based motility of intracellular *Listeria monocytogenes* equals the rate of actin polymerization, Nature 357 (1992) 257–260.
[12] C.S. Peskin, G.M. Odell, G.F. Oster, Cellular motions and thermal fluctuations: the Brownian ratchet, Biophys. J. 65 (1993) 316–324.
[13] A. Mogilner, G. Oster, Cell motility driven by actin polymerization, Biophys. J. 71 (1996) 3030–3045.
[14] E. Gouin, H. Gantelet, C. Egile, I. Lasa, H. Ohayon, V. Villiers, P. Gounon, P.J. Sansonetti, P. Cossart, A comparative study of the actin-based motilities of the pathogenic bacteria Listeria monocytogenes, *Shigella flexneri* and *Rickettsia conorii*, J. Cell Sci. 112 (1999) 1697–1708.
[15] S. Pistor, T. Chakraborty, U. Walter, J. Wehland, The bacterial actin nucleator protein ActA of Listeria monocytogenes contains multiple binding sites for host microfilament proteins, Curr. Biol. 5 (1995) 517–525.
[16] A. Sechi, J. Wehland, J.V. Small, The isolated comet tail pseudopodium of Listeria monocytogenes: a tail of two actin filament populations, long and axial and short and random, J. Cell Biol. 137 (1997) 155–167.
[17] J. Skoble, D.A. Portnoy, M.D. Welch, Three regions within ActA promote Arp2/3 complex-mediated actin nucleation and *Listeria monocytogenes* motility, J. Cell Biol. 150 (2000) 527–537.
[18] J. Skoble, V. Auerbuch, E.D. Goley, M.D. Welch, D.A. Portnoy, Pivotal role of VASP in Arp2/3 complex-mediated actin nucleation, actin branch-formation, and *Listeria monocytogenes* motility, J. Cell Biol. 155 (2001) 89–100.
[19] J.J. Loureiro, D.A. Rubinson, J.E. Bear, G.A. Baltus, A.V. Kwiatkowski, F.B. Gertler, Critical roles of phosphorylation and actin binding motifs, but not the central proline-rich region, for Ena/Vasodilator-stimulated Phosphoprotein (VASP) function during cell migration, Mol. Biol. Cell 13 (2002) 2533–2546.
[20] M. Geese, J.J. Loureiro, J.E. Bear, J. Wehland, F.B. Gertler, A.S. Sechi, Contribution of Ena/VASP proteins to intracellular motility of *Listeria* requires phosphorylation and proline-rich core but not F-actin binding or multimerization, Mol. Biol. Cell 13 (2002) 2383–2396.
[21] P.A. Giardini, J.A. Theriot, Effects of intermediate filaments on actin-based motility of *Listeria monocytogenes*, Biophys. J. 81 (2001) 3193–3203.
[22] F. Gerbal, V. Laurent, A. Ott, M.-F. Carlier, P. Chaikin, J. Prost, Measurement of the elasticity of the actin tail of *Listeria monocytogenes*, Eur. Biophys. J. 29 (2000) 134–140.
[23] J.A. Theriot, J. Rosenblatt, D.A. Portnoy, P.J. Goldschimdt-Clermont, T.J. Mitchison, Involvement of profilin in the actin-based motility of *L. monocytogenes* in cells and cell-free extracts, Cell 76 (1994) 505–517.
[24] V. Laurent, T.P. Loisel, B. Harbeck, A. Wehman, L. Gröbe, B.M. Jockusch, J. Wehland, F.B. Gertler, M.-F. Carlier, Role of proteins of the Ena-VASP family in actin-based motility of *Listeria monocytogenes*, J. Cell Biol. 144 (1999) 1245–1258.
[25] R.D. Mullins, J.A. Heuser, T.D. Pollard, The interaction of Arp2/3 complex with actin: nucleation, high affinity pointed end capping, and formation of branching networks of filaments, Proc. Natl. Acad. Sci. 95 (1998) 6181–6186.
[26] M.D. Welch, J. Rosenblatt, J. Skoble, D.A. Portnoy, T.J. Mitchison, Interaction of human Arp2/3 complex and the Listeria monocytogenes ActA protein in actin filament nucleation, Science 281 (1998) 105–108.
[27] L.M. Machesky, R.D. Mullins, H.N. Higgs, D.A. Kaiser, L. Blanchoin, R.C. May, M.E. Hall, T.D. Pollard, Scar, a WASp-related protein, activates nucleation of actin filaments by the Arp2/3 complex, Proc. Natl. Acad. Sci. 96 (1999) 3739–3744.
[28] T.P. Loisel, R. Boujemaa, D. Pantaloni, M.F. Carlier, Reconstitution of actin-based motility of *Listeria* and *Shigella* using pure proteins, Nature 401 (1999) 613–616.
[29] E. Andrianantoandro, T.D. Pollard, Mechanism of actin filament turnover by severing and nucleation at different concentrations of ADF/Cofilin, Mol. Cell 24 (2006) 13–23.
[30] A.V. Nadkarni, W.M. Brieher, Aip1 destabilizes cofilin-saturated actin filaments by severing and accelerating monomer dissociation from ends, Curr. Biol. 24 (2014) 2749–2757.
[31] Q. Chen, N. Courtemanche, T.D. Pollard, Aip1 promotes actin filament severing by cofilin and regulates constriction of the cytokinetic contractile ring, J. Biol. Chem. 290 (2015) 2289–2300.
[32] L. Gressin, A. Guillotin, C. Guérin, L. Blanchoin, A. Michelot, Architecture dependence of actin filament network disassembly, Curr. Biol. 25 (2015) 1437–1447.
[33] S. Jansen, A. Collins, S.M. Chin, C.A. Ydenberg, J. Gelles, B.L. Goode, Single-molecule imaging of a three-component ordered actin disassembly mechanism, Nat. Commun. 6 (2015) 7202.
[34] P.A. Nguyen, A.C. Groen, M. Loose, K. Ishihara, M. Wühr, C.M. Field, T.J. Mitchison, Spatial organization of cytokinesis signaling reconstituted in a cell-free system, Science 346 (2014) 244–247.
[35] Y. Miao, C.C.L. Wong, V. Mennella, A. Michelot, D.A. Agard, L.J. Holt, J.R.I. Yates, D.G. Drubin, Cell-cycle regulation of formin-mediated actin cable assembly, Proc. Natl. Acad. Sci. U. S. A. 110 (2013) E4446–E4455.
[36] A. Michelot, A. Grassart, V. Okreglak, M. Costanzo, C. Boone, D.G. Drubin, Actin filament elongation in Arp2/3-derived networks is controlled by three distinct mechanisms, Dev. Cell 24 (2013) 182–195.
[37] L.A. Cameron, M.J. Footer, A. Van Oudenaarden, J.A. Theriot, Motility of ActA protein-coated microspheres driven by actin polymerization, Proc. Natl. Acad. Sci. 96 (1999) 4908–4913.
[38] L.A. Cameron, T.M. Svitkina, D. Vignjevic, J.A. Theriot, G.G. Borisy, Dendritic organization of actin comet tails, Curr. Biol. 11 (2001) 130–135.
[39] T.M. Svitkina, G.C. Borisy, Arp2/3 complex and actin depolymerizing factor/cofilin in dendritic organization and treadmilling of actin filament array in lamellipodia, J. Cell Biol. 145 (1999) 1009–1026.
[40] V. Noireaux, R.M. Golsteyn, E. Friederich, J. Prost, C. Antony, D. Louvard, C. Sykes, Growing an actin gel on spherical surfaces, Biophys. J. 278 (2000) 1643–1654.
[41] J. Plastino, I. Lelidis, J. Prost, C. Sykes, The effect of diffusion, depolymerization and nucleation promoting factors on actin gel growth, Eur. Biophys. J. 33 (2004) 310–320.
[42] J. van der Gucht, E. Paluch, J. Plastino, C. Sykes, Stress release drives symmetry breaking for actin-based movement, Proc. Natl. Acad. Sci. U. S. A. 102 (2005) 7847–7852.
[43] M.J. Dayel, O. Akin, M. Landeryou, V. Risca, A. Mogilner, R.D. Mullins, In silico reconstitution of actin-based symmetry breaking and motility, PLoS Biol. 7 (2009) 1000201.
[44] A. Kawska, K. Carvalho, J. Manzi, R. Boujemaa-Paterski, L. Blanchoin, J.-L. Martiel, C. Sykes, How actin network dynamics control the onset of actin-based motility, Proc. Natl. Acad. Sci. U. S. A. 109 (2012) 14440–14445.
[45] D. Yarar, W. To, A. Abo, M.D. Welch, The Wiskott–Aldrich syndrome protein directs actin-based motility by stimulating actin nucleation with the Arp2/3 complex, Curr. Biol. 9 (1999) 555–558.
[46] D. Yarar, J.A. D'Alessio, R.L. Jeng, M.D. Welch, Motility determinants in WASP family proteins, Mol. Biol. Cell 13 (2002) 4045–4059.
[47] F. Castellano, C. Le Clainche, D. Patin, M.-F. Carlier, P. Chavrier, A WASP–VASP complex regulates actin polymerization at the plasma membrane, EMBO J. 20 (2001) 5603–5614.

[48] J. Fradelizi, V. Noireaux, J. Plastino, B. Menichi, D. Louvard, C. Sykes, R.M. Golsteyn, E. Friederich, ActA and human zyxin harbour Arp2/3-independent actin-polymerization activity, Nat. Cell Biol. 3 (2001) 699–707.
[49] J. Plastino, S. Olivier, C. Sykes, Actin filaments align into hollow comets for rapid VASP-mediated propulsion, Curr. Biol. 14 (2004) 1766–1771.
[50] S. Romero, C. Le Clainche, D. Didry, C. Egile, D. Pantaloni, M.-F. Carlier, Formin is a processive motor that requires profilin to accelerate actin assembly and associated ATP hydrolysis, Cell 119 (2004) 419–429.
[51] A. Michelot, J. Berro, C. Guérin, R. Boujemaa-Paterski, C.J. Staiger, J.-L. Martiel, L. Blanchoin, Actin-filament stochastic dynamics mediated by ADF/Cofilin, Curr. Biol. 17 (2007) 825–833.
[52] M. Bovellan, Y. Romeo, M. Biro, A. Boden, P. Chugh, A. Yonis, M. Vaghela, M. Fritzsche, D. Moulding, R. Thorogate, A. Jégou, A.J. Thrasher, G. Romet-Lemonne, P.P. Roux, E. Paluch, G. Charras, Cellular control of cortical actin nucleation, Curr. Biol. 24 (2014) 1628–1635.
[53] N. Morone, T. Fujiwara, K. Murase, R.S. Kasai, H. Ike, S. Yuasa, J. Usukura, A. Kusumi, Three-dimensional reconstruction of the membrane skeleton at the plasma membrane interface by electron tomography, J. Cell Biol. 174 (2006) 851–862.
[54] J. Block, D. Breitsprecher, S. Kühn, M. Winterhoff, F. Kage, R. Geffers, P. Duwe, J.L. Rohn, B. Baum, C. Brakebusch, M. Geyer, T.E.B. Stradal, J. Faix, K. Rottner, FMNL2 drives actin-based protrusion and migration downstream of Cdc42, Curr. Biol. 22 (2012) 1005–1012.
[55] T.A. Burke, J.R. Christensen, E. Barone, C. Suarez, V. Sirotkin, D.R. Kovar, Homeostatic actin cytoskeleton networks are regulated by assembly factor competition for monomers, Curr. Biol. 24 (2014) 579–585.
[56] C. Suarez, R.T. Carroll, T.A. Burke, J.R. Christensen, A.J. Bestul, J.A. Sees, M.L. James, V. Sirotkin, D.R. Kovar, Profilin regulates F-actin network homeostasis by favoring formin over Arp2/3 complex, Dev. Cell 32 (2015) 43–53.
[57] R. Rohatgi, L. Ma, H. Miki, M. Lopez, H. Kirchausen, T. Takenawa, M. Kirschner, The interaction between N-Wasp and the Arp2/3 complex links Cdc42-dependent signals to actin assembly, Cell 97 (1999) 221–231.
[58] L.M. Machesky, R.H. Insall, Scar1 and the related Wiskott–Aldrich syndrome protein, WASP, regulate the actin cytoskeleton through the Arp2/3 complex, Curr. Biol. 8 (1998) 1347–1356.
[59] H. Miki, S. Suetsugu, T. Takenawa, WAVE, a novel WASP-family protein involved in actin reorganization induced by Rac, EMBO J. 17 (1998) 6932–6941.
[60] L. Blanchoin, R. Boujemaa-Paterski, C. Sykes, J. Plastino, Actin dynamics, architecture and mechanics in cell motility, Physiol. Rev. 94 (2014) 235–263.
[61] H. Miki, T. Takenawa, Regulation of actin dynamics by WASP family proteins, J. Biochem. 134 (2003) 309–313.
[62] Y. Marcy, J. Prost, M.-F. Carlier, C. Sykes, Forces generated during actin-based propulsion: a direct measurement by micromanipulation, Proc. Natl. Acad. Sci. U. S. A. (2004) 5992–5997.
[63] S. Wiesner, E. Helfer, D. Didry, G. Ducouret, F. Lafuma, M.-F. Carlier, D. Pantaloni, A biomimetic motility assay provides insight into the mechanism of actin-based motility, J. Cell Biol. 160 (2003) 387–398.
[64] J. Zalevsky, L. Lempert, H. Kranitz, R.D. Mullins, Different WASP family proteins stimulate different Arp2/3 complex-dependent actin-nucleating activities, Curr. Biol. 11 (2001) 1903–1913.
[65] S. Havrylenko, P. Noguera, M. Abou-Ghali, J. Manzi, F. Faqir, A. Lamora, C. Guérin, L. Blanchoin, J. Plastino, WAVE binds Ena/VASP for enhanced Arp2/3 complex-based actin assembly, Mol. Biol. Cell 26 (2015) 55–65.
[66] V. Koronakis, P.J. Hume, D. Humphreys, T. Liu, O. Horning, O.N. Jensen, E.J. McGhie, WAVE regulatory complex activation by cooperating GTPases Arf and Rac1, Proc. Natl. Acad. Sci. U. S. A. 108 (2011) 14449–14454.
[67] K.G. Campellone, M.D. Welch, A nucleator arms race: cellular control of actin assembly, Nat. Rev. Mol. Cell Biol. 11 (2010) 237–251.
[68] A. Bernheim-Groswasser, S. Wiesner, R.M. Golsteyn, M.-F. Carlier, C. Sykes, The dynamics of actin-based motility depend on surface parameters, Nature 417 (2002) 308–311.
[69] T. Pujol, O. du Roure, M. Fermigier, J. Heuvingh, Impact of branching on the elasticity of actin networks, Proc. Natl. Acad. Sci. U. S. A. 109 (2012) 10364–10369.
[70] O. Akin, R.D. Mullins, Capping protein increases the rate of actin-based motility by promoting filament nucleation by the Arp2/3 complex, Cell 133 (2008) 841–851.
[71] V. Achard, J.-L. Martiel, A. Michelot, C. Guérin, A.-C. Reymann, L. Blanchoin, R. Boujemaa-Paterski, A "primer"-based mechanism underlies branched actin filament network formation and motility, Curr. Biol. 20 (2010) 423–428.
[72] S. Samarin, S. Romero, C. Kocks, D. Didry, D. Pantaloni, M.-F. Carlier, How VASP enhances actin-based motility, J. Cell Biol. 163 (2003) 131–142.
[73] A. Upadhyaya, J.R. Chabot, A. Andreeva, A. Samadani, A. van Oudenaarden, Probing polymerization forces by using actin-propelled lipid vesicles, Proc. Natl. Acad. Sci. 100 (2003) 4521–4526.
[74] P.A. Giardini, D.A. Fletcher, J.A. Theriot, Compression forces generated by actin comet tails on lipid vesicles, Proc. Natl. Acad. Sci. 100 (2003) 6493–6498.
[75] H. Boukellal, O. Campas, J.-F. Joanny, J. Prost, C. Sykes, Soft *Listeria*: actin-based propulsion of liquid drops, Phys. Rev. E 69 (2004) (061906/061901-061906/061904).
[76] V. Delatour, E. Helfer, D. Didry, K.H.D. Lê, J.-F. Gaucher, M.-F. Carlier, G. Romet-Lemonne, Arp2/3 controls the motile behavior of N-WASP-functionalized GUVs and modulates N-WASP surface distribution by mediating transient links with actin filaments, Biophys. J. 94 (2008) 4890–4905.
[77] L. Trichet, O. Campas, C. Sykes, J. Plastino, VASP governs actin dynamics by modulating filament anchoring, Biophys. J. 92 (2007) 1081–1089.
[78] O. Siton, Y. Ideses, S. Albeck, T. Unger, A.D. Bershadsky, N.S. Gov, A. Bernheim-Groswasser, Cortactin releases the brakes in actin-based motility by enhancing WASP-VCA detachment from Arp2/3 branches, Curr. Biol. 21 (2011) 2092–2097.
[79] C. Co, D.T. Wong, S. Gierke, V. Change, J. Taunton, Mechanism of actin network attachment to moving membranes: barbed end capture by N-WASP WH2 domains, Cell 128 (2007) 901–913.
[80] F. Ferron, G. Rebowski, S.H. Lee, R. Dominguez, Structural basis for the recruitment of profilin–actin complexes during filament elongation by Ena/VASP, EMBO J. 26 (2007) 4597–4606.
[81] A.P. Liu, D.A. Fletcher, Actin polymerization serves as a membrane domain switch in model lipid bilayers, Biophys. J. 91 (2006) 4064–4070.
[82] A.P. Liu, D.L. Richmond, L. Maibaum, S. Pronk, P.L. Geissler, D.A. Fletcher, Membrane-induced bundling of actin filaments, Nat. Phys. 4 (2008) 789–793.
[83] K. Lee, J.L. Gallop, K. Rambani, M.W. Kirschner, Self-assembly of filopodia-like structures on supported lipid bilayers, Science 329 (2010) 1341–1345.
[84] J.D. Cortese, B. Schwab III, C. Frieden, E.L. Elson, Actin polymerization induces a shape change in actin-containing vesicles, Proc. Natl. Acad. Sci. U. S. A. 86 (1989) 5773–5777.
[85] L. Limozin, M. Bärmann, E. Sackmann, On the organization of self-assembled actin networks in giant vesicles, Eur. Phys. J. E 10 (2003) 319–330.
[86] L. Limozin, E. Sackmann, Polymorphism of cross-linked actin networks in giant vesicles, Phys. Rev. Lett. 89 (2002) 168103.
[87] H. Miyata, H. Hotani, Morphological changes in liposomes caused by polymerization of encapsulated actin and spontaneous formation of actin bundles, Proc. Natl. Acad. Sci. U. S. A. 89 (1992) 11547–11551.
[88] H. Miyata, S. Nishiyama, K.-I. Akashi, K. Kinosita Jr., Protrusive growth from giant liposomes driven by actin polymerization, Proc. Natl. Acad. Sci. U. S. A. 96 (1999) 2048–2053.
[89] F.-C. Tsai, B. Stuhrmann, G. Koenderink, Encapsulation of active cytoskeletal protein networks in cell-sized liposomes, Langmuir 27 (2011) 10061–10071.
[90] M. Pinot, V. Steiner, B. Dehapiot, B.-K. Yoo, F. Chesnel, L. Blanchoin, C. Kervrann, Z. Gueroui, Confinement induces actin flow in a meiotic cytoplasm, Proc. Natl. Acad. Sci. U. S. A. 109 (2012) 11705–11710.
[91] M.M.A.E. Claessens, M. Bathe, E. Frey, A.R. Bausch, Actin-binding proteins sensitively mediate F-actin bundle stiffness, Nat. Mater. 5 (2006) 748–753.
[92] J. Alvarado, B.M. Mulder, G.H. Koenderink, Alignment of nematic and bundled semiflexible polymers in cell-sized confinement, Soft Matter 10 (2014) 2354–2364.
[93] M.D. Vahey, D.A. Fletcher, The biology of boundary conditions: cellular reconstitution in one, two, and three dimensions, Curr. Opin. Cell Biol. 26 (2014) 60–68.
[94] D. Merkle, N. Kahya, P. Schwille, Reconstitution and anchoring of cytoskeleton inside giant unilamellar vesicles, ChemBioChem 9 (2008) 2673–2681.
[95] L.-L. Pontani, J. Van der Gucht, G. Salbreaux, J. Heuvingh, J.-F. Joanny, C. Sykes, Reconstitution of an actin cortex inside a liposome, Biophys. J. 96 (2009) 192–198.
[96] T. Luo, V. Srivastava, Y. Ren, D.N. Robinson, Mimicking the mechanical properties of the cell cortex by the self-assembly of an actin cortex in vesicles, Appl. Phys. Lett. 104 (2014) 153701.
[97] C. Campillo, P. Sens, D. Köster, L.-L. Pontani, D. Lévy, P. Bassereau, P. Nassoy, C. Sykes, Unexpected membrane dynamics unveiled by membrane nanotube extrusion, Biophys. J. 104 (2013) 1248–1256.
[98] E.A. Shah, K. Keren, Symmetry breaking in reconstituted actin cortices, eLife 3 (2014) e01433.
[99] S. Suetsugu, S. Kurisu, T. Takenawa, Dynamic shaping of cellular membranes by phospholipids and membrane-deforming proteins, Physiol. Rev. 94 (2014) 1219–1248.
[100] A.-C. Reymann, C. Guérin, M. Théry, L. Blanchoin, R. Boujemaa-Paterski, Geometrical control of actin assembly and contractility, Methods Cell Biol. 120 (2014) 19–38.
[101] A.-C. Reymann, J.-L. Martiel, T. Cambier, L. Blanchoin, R. Boujemaa-Paterski, M. Théry, Nucleation geometry governs ordered actin networks structures, Nat. Mater. 9 (2010) 827–832.
[102] A.-C. Reymann, R. Boujemaa-Paterski, J.-L. Martiel, C. Guérin, W. Cao, H.F. Chin, E.M. De La Cruz, M. Théry, L. Blanchoin, Actin network architecture can determine myosin motor activity, Science 336 (2012) 1310–1314.
[103] M. Murrell, M.L. Gardel, Actomyosin sliding is attenuated in contractile biomimetic cortices, Mol. Biol. Cell 25 (2014) 1845–1853.
[104] K. Carvalho, F.-C. Tsai, E. Lees, R. Voituriez, G. Koenderink, C. Sykes, Cell-sized liposomes reveal how actomyosin cortical tension drives shape change, Proc. Natl. Acad. Sci. U. S. A. 110 (2013) 16456–16461.
[105] K. Carvalho, J. Lemière, F. Faqir, J. Manzi, L. Blanchoin, J. Plastino, T. Betz, C. Sykes, Actin polymerization or myosin contraction: two ways to build up cortical tension for symmetry breaking, Philos. Trans. R. Soc. B 368 (2013) 20130005.
[106] J. Alvarado, M. Sheinman, A. Sharma, F.C. MacKintosh, G.H. Koenderink, Molecular motors robustly drive active gels to a critically connected state, Nat. Phys. 9 (2013) 591–597.
[107] G.T. Charras, C.-K. Hu, M. Coughlin, T.J. Mitchison, Reassembly of contractile actin cortex in cell blebs, J. Cell Biol. 175 (2006) 477–490.
[108] N. Elkhatib, M.B. Neu, C. Zensen, K.M. Schmoller, D. Louvard, A.R. Bausch, T. Betz, D.M. Vignjevic, Fascin plays a role in stress fiber organization and focal adhesion disassembly, Curr. Biol. 24 (2014) 1492–1499.
[109] O. Wiggan, A.E. Shaw, J.G. DeLuca, J.R. Bamburg, ADF/Cofilin regulates actomyosin assembly through competitive inhibition of Myosin II binding to F-actin, Dev. Cell 22 (2012) 530–543.
[110] I. Mendes Pinto, B. Rubinstein, A. Kucharavy, J.R. Unruh, R. Li, Actin depolymerization drives actomyosin ring contraction during budding yeast cytokinesis, Dev. Cell 22 (2012) 1247–1260.

[111] L. Haviv, D. Gillo, F. Backouche, A. Bernheim-Groswasser, A cytoskeletal demolition worker: myosin II acts as an actin depolymerization agent, J. Mol. Biol. 375 (2008) 325–330.
[112] M.P. Murrell, M.L. Gardel, F-actin buckling coordinates contractility and severing in a biomimetic actomyosin cortex, Proc. Natl. Acad. Sci. 109 (2012) 20820–20825.
[113] S.K. Vogel, Z. Petrasek, F. Heinemann, P. Schwille, Myosin motors fragment and compact membrane-bound actin filaments, eLife 2 (2013) e00116.
[114] C. Kocks, E. Gouin, M. Tabouret, P. Berche, H. Ohayon, P. Cossart, *L. monocytogenes*-induced actin assembly requires the *actA* gene product, a surface protein, Cell 68 (1992) 521–531.

Summary:

Basement membrane (BM) is a dense sheet of specialized extracellular matrix that separates epithelia from underlying tissue. The penetration of cells through BM barriers, called "invasion", is an important process during normal tissue development and in cancer metastasis. Much has been understood concerning the genetics and signaling of how holes are formed in the BM during invasion. However less is clear about the physical forces involved: how myosin contractility participates in BM removal and how different actin polymerization factors and crosslinkers contribute to the invasive process. To address these questions, we studied an invasion event in a developmental process, anchor cell (AC) invasion in *Caenorhabditis elegans*. AC breaching of the BM is known to depend on an actin-rich protrusion and the activity of matrix metalloproteases (MMPs), similar to cancer cell invasion.

RNAi knockdown of different actin polymerization activators and nucleators, and expression of a dominant negative form of an Arp2/3 complex activator specifically in the AC showed that AC invasion depended strongly on branched filaments formed via WASP/WSP-1 activation of the Arp2/3 complex. Super-resolution microscopy indicated that the AC invasive protrusion was densely packed with filaments, in keeping with the idea that the invasive protrusion was highly branched. We further showed that another Arp2/3 complex activator, WAVE/WVE-1, could enable invasion when WASP/WSP-1 was absent. Formins appeared not to play a major role and actin cross-linking proteins were likewise dispensable for AC invasion.

In wild type worms, we observed that myosin activity was not needed for invasion. However it has been reported that cancer cells upregulate myosin contractility to invade in the absence of proteases, so we used a worm deleted for the five main MMPs of the worm genome to test the role of myosin in this context. AC invasion took place in MMP- worms, but with a time delay. RNAi knockdown of different components of the myosin machinery gave no enhancement of the invasion defect. In addition visualization of the actin cytoskeleton in MMP- worms revealed that actin was concentrated in the AC protrusion and barely detectable in the cortex, making it unlikely that myosin contraction of the cortex was helping the cell squeeze through the BM as reported in cancer cells in the absence of proteases.

All together these results showed that the invasive cell adapted its branched actin filament polymerization to maintain invasion in different biochemical and environmental contexts. This plasticity is a crucial point that needs to be better understood in order to develop future treatments targeting cancer cell invasion.